REGULATION OF IN VITRO AND IN VIVO HEPATIC STELLATE CELL ACTIVATION BY THE ARYL HYDROCARBON RECEPTOR

by

Shivakumar Rayavara Veerabhadraiah

A dissertation

submitted in partial fulfillment

of the requirements for the degree of

Doctor of Philosophy in Biomolecular Sciences

Boise State University

December 2020

BOISE STATE UNIVERSITY GRADUATE COLLEGE

DEFENSE COMMITTEE AND FINAL READING APPROVALS

of the dissertation submitted by

Shivakumar Rayavara Veerabhadraiah

Dissertation Title: Regulation of In Vitro and In Vivo Hepatic Stellate Cell Activation by the Aryl Hydrocarbon Receptor

Date of Final Oral Examination: 08 October 2020

The following individuals read and discussed the dissertation submitted by student Shivakumar Rayavara Veerabhadraiah, and they evaluated the presentation and response to questions during the final oral examination. They found that the student passed the final oral examination.

Kristen A. Mitchell, Ph.D.	Chair, Supervisory Committee
Kenneth A. Cornell, Ph.D.	Member, Supervisory Committee
Allan R. Albig, Ph.D.	Member, Supervisory Committee
Eric J. Hayden, Ph.D.	Member, Supervisory Committee
Matthew L. Ferguson, Ph.D.	Member, Supervisory Committee

The final reading approval of the dissertation was granted by Kristen A. Mitchell, Ph.D., Chair of the Supervisory Committee. The dissertation was approved by the Graduate College.

DEDICATION

This dissertation is dedicated to my mother, Narasamma Kodegenahalli Venkatappa (Nagamma), and my father, Veerabhadraiah Rayavara Veeranna. Their unconditional love, support, and encouragement made me dream big and believe in my abilities. My special thanks to all my sisters, Vijayalakshmi, Padmavathi, Sowbhagya, Yashodha, and my grandmothers Thimakka and Lakshmamma, who always thought my accomplishment is their victory.

ACKNOWLEDGMENTS

First, and most of all, I would like to express my sincere gratitude to my advisor Dr. Kristen Mitchell for her understanding, continuous support, motivation, guidance, assistance, and patience that made me complete my Ph.D.

Besides my advisor, I owe many thanks to Dr. Kenneth Cornell for his insightful comments, scientific support, encouragement, inspiration, and the opportunity to work in his lab. Many thanks also to my other committee members Dr. Allan Albig, Dr. Eric Hayden, and Dr. Matthew Ferguson, for their scientific support and even letting me use their lab resources.

I also extend my sincere thanks to the Biomolecular Sciences Graduate Programs for the funding support towards my Ph.D. I gratefully acknowledge the program director, Dr. Denise Wingett, and program coordinator, Beth Gee, for their kindness, endless support, and encouragement.

I greatly appreciate the support from the Biomolecular Research Center at Boise State University for providing me with the opportunity to apply for pilot training grants and for letting me use their facility and resources when required. In particular, I sincerely thank Dr. Julia Oxford, Dr. Cindy Keller-Peck, and Dr. Richard Beard for their scientific discussions and technical assistance.

I am also grateful to the staff at the Biomedical Research Vivarium Core, especially Sarah McCusker and Dr. Jared Romero, who provided scientific support and technical assistance.

I also extend very special thanks to Dr. Daniel Fologea for providing me with the opportunity to work in his lab and for helping me optimize the transfection experiments.

This project was supported by the Institutional Development Awards (IDeA) from the National Institute of General Medical Sciences of the National Institutes of Health. I also acknowledge support from the Biomolecular Research Center at Boise State with funding from the National Science Foundation, the M.J. Murdock Charitable Trust, and the Idaho State Board of Education.

I also thank my colleagues and my fellow lab mates for stimulating discussions, scientific input, and technical assistance over the last five years. I would like to thank Angela Fairbanks for assistance with preparing my manuscripts and dissertation. Finally, I would like to thank all of my friends, in particular, Mr. Dhanush Kumar Ratakonda, Dr. Giovan Cholico, and Mrs. Jessica Roberts.

ABSTRACT

Liver fibrosis is a pathological condition characterized by the excessive deposition of extracellular matrix material by activated hepatic stellate cells (HSCs). We recently reported that activation of the aryl hydrocarbon receptor (AhR), a ligand-activated transcription factor, with 2,3,7,8-tetrachlorodibenzo-*p*-dioxin (TCDD) increases HSC activation *in vitro* and in mouse models of experimental liver fibrosis. The goal of this project was to determine the mechanism by which AhR activation impacts HSC activation and the subsequent development of liver fibrosis. It is possible that HSCs are direct cellular targets for TCDD. Alternatively, TCDD could increase HSC activation indirectly by exacerbating hepatocyte damage and inflammation. To investigate this, we generated mice in which the AhR was selectively removed from either hepatocytes or HSCs to determine the ramifications on liver injury, inflammation, and HSC activation in an experimental model of liver fibrosis elicited by chronic administration of TCDD. Results from these studies indicate that TCDD does not directly activate HSCs in the mouse liver to produce fibrosis. Instead, it appears that TCDD-induced changes in hepatocytes, such as the development of steatosis, are what ultimately stimulate HSC activation and produce fibrosis. A second focus of this project was to investigate an endogenous role for AhR signaling in the regulation of HSC activation in the absence of liver injury and inflammation. To this end, I used CRISPR/Cas9 technology to knock down the AhR in the human HSC cell line, LX-2. I discovered that a functional AhR is required for optimal proliferation of activated HSCs. However, other endpoints of HSC

activation, such as the production of collagen type I, were not impacted by the removal of AhR signaling. These findings are important because the AhR has been shown to be a druggable target, and there is growing interest in therapeutically modulating AhR activity to prevent or reverse HSC activation. Collectively, results from this project indicate that therapeutically targeting AhR signaling in hepatocytes, instead of AhR signaling in HSCs, might be a preferred approach for limiting HSC activation and preventing or diminishing liver fibrosis.

TABLE OF CONTENTS

LIST OF TABLES

LIST OF FIGURES

LIST OF ABBREVIATIONS

αSMA	Alpha Smooth Muscle Actin
AhR	Aryl Hydrocarbon Receptor
ARNT	AhR Nuclear Translocator
Cas9	CRISPR-Associated Protein 9
CCl_4	Carbon Tetrachloride
CRISPR	Clustered Regularly Interspaced Short Palindromic Repeats
ECM	Extracellular Matrix
HAH	Halogenated Aromatic Hydrocarbon
HSC	Hepatic Stellate Cell
IL	Interleukin
KO	Knockout
MMP	Matrix Metalloproteinase
PAHs	Polycyclic Aromatic Hydrocarbons
PAS	Per-ARNT-Sim
PCR	Polymerase Chain Reaction
POPs	Persistent Organic Pollutants
PCBs	Polychlorinated Biphenyls
PCDDs	Polychlorinated Dibenzo-*p*-dioxins
PCDFs	Polychlorinated Dibenzofurans
TCDD	2,3,7,8-Tetrachlorodibenzo-*p*-dioxin

TIMP	Tissue Inhibitor of Matrix Metalloproteinase
WT	Wildtype
XRE	Xenobiotic Response Element

CHAPTER ONE: INTRODUCTION

Halogenated Aromatic Hydrocarbons

Halogenated aromatic hydrocarbons (HAHs) are widespread and persistent environmental pollutants that include dioxins, furans, and biphenyls (Poland and Knutson, 1982). These chemicals share a similar chemical structure, which includes a benzene ring and one or more atoms of a halogen (Figure 1.1). Because HAHs are lipophilic, they partition into the fatty tissue of living organisms, where they bioaccumulate (Birnbaum, 1985). Most humans accumulate these chemicals over a lifetime through the consumption of fish, meat, poultry, and dairy products.

Within the HAH family of chemicals, the polychlorinated biphenyls (PCBs), dioxins, and furans are of particular concern because they are further classified as persistent organic pollutants (POPs). POPs are a global concern because of their ability to persist in the environment, be transported long distances, bioaccumulate in the food chain, and adversely affect human health and the environment. In 2001, an international environmental treaty was signed to eliminate or restrict the production and use of POPs. This treaty, which was called the Stockholm Convention on Persistent Organic Pollutants, originally identified twelve POPs of particular concern, and these chemicals are referred to as the "Dirty Dozen." Three of the 12 chemicals on this list are members of the HAH family: PCBs, polychlorinated dibenzo-*p*-dioxins (PCDDs), and polychlorinated dibenzofurans (PCDFs).

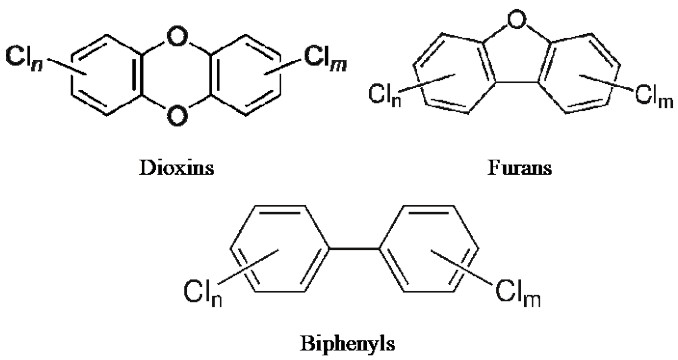

Figure 1.1 Structures of HAHs

PCBs

PCBs were once widely produced for industrial use as heat exchange fluids, in electric transformers and capacitors, and as additives in paint, carbonless copy paper, and plastics (Erickson and Kaley, 2011). These chemicals were heavily manufactured until being banned in the U.S. in 1979, and the use of PCBs in equipment is scheduled to be phased out by 2025 (Robertson *et al.*, 2018). However, PCBs are still released into the environment from the disposal of large-scale electrical equipment and waste, and these chemicals continue to pose a human health concern due to their persistence in the environment.

There are 209 different possible congeners within the PCB family, and the degree of toxicity of each congener depends on its chlorination pattern. The most toxic PCB congeners have their two phenyl rings in the same plane with no chlorine atoms in the ortho position. Compared to non-coplanar PCBs, these coplanar (or "non-ortho") PCBs are more stable in the environment, more resistant to degradation, and capable of producing greater toxicity. Coplanar PCBs are also called "dioxin-like" PCBs because they are structurally similar to dioxins and share a common mechanism of action, which involves binding to the aryl hydrocarbon receptor (AhR). Of the 209 PCB congeners, 12

have been classified as dioxin-like compounds and are the focus of concern from an environmental and public health standpoint.

PCDDs and PCDFs

The other two HAHs on the Dirty Dozen list are the PCDDs and PCDFs. Both of these compounds have never been intentionally produced. Instead, they are typically produced unintentionally, either through incomplete combustion or during the manufacturing of chlorine-based herbicides and pesticides. Dioxins, in particular, have been associated with numerous adverse effects in humans and laboratory animals. Furans are produced through the same processes that produce dioxins, and also during the production of PCBs.

The basic chemical structure of all dioxins consists of two benzene rings, which are connected by one or two oxygen atoms, and 4-8 chlorine atoms as substituents. Based on the position of the chlorine atoms, there are 75 possible dioxin congeners (reviewed in Schecter et al., 2006). The World Health Organization classified 7 PCDDs as dioxins that are of concern to the environment (WHO, 2010). This classification was performed based on the toxic potency of each chemical relative to 2,3,7,8-tetrachlorodibenzo-*p*-dioxin (TCDD) (Berg *et al.*, 2006). TCDD is the most toxic dioxin due to the pattern of chlorine substitutions at positions 2, 3, 7, and 8 on the benzene rings (Figure 1.2).

2,3,7,8-Tetrachlorodibenzo-*p*-dioxin (TCDD)

TCDD is a persistent environmental pollutant with a half-life of 10-100 years in soil (Seike et al., 2007). Degradation of TCDD occurs primarily by photolysis via ultraviolet exposure, which splits the chlorine atoms off of TCDD. The half-life of TCDD is 11 days in mice and 23.7 days in rats and rabbits (Ryan et al., 1990). In humans, the half-life of TCDD is reported to be 1-2 years (Sorg *et al.*, 2009). TCDD is a potent inducer of the gene encoding the xenobiotic metabolizing enzyme, cytochrome P4501A1, as well as several other enzymes involved in phase I and phase II metabolism (Nebert, Puga and Vasiliou, 1993). However, TCDD itself is not a substrate for cytochrome P4501A1, due to steric hindrance at the enzyme active site (Dutkiewicz and Mikstacka, 2018). As a result, TCDD is not metabolized, which contributes to its long half-life compared to other environmental contaminants, including other HAHs (Ryan et al.,1990).

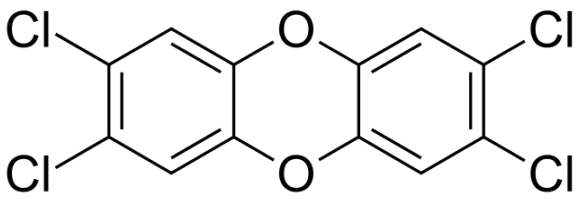

Figure 1.2 Structure of 2, 3, 7,8-Tetrachlorodibenzo-*p*-dioxin (TCDD)

TCDD Sources and Exposure

There are both natural and human-made sources of TCDD. Natural sources of TCDD include volcanoes and forest fires. TCDD is also produced as an unintentional byproduct of herbicide manufacturing and the chlorine bleaching of paper. TCDD gained notoriety when it was found to have been released as an unintended contaminant of Agent Orange, which was an herbicide that was sprayed during the Vietnam War from the early

1960s to the early 1970s. Currently, the most prominent source of TCDD in the environment is the burning of waste products such as chlorine-based plastics, and household and municipal waste, which primarily results in dioxin formation within the temperature range of 200-450°C (Z, 2018). Once formed, TCDD is released into the environment either in an aerosol state, which is adsorbed onto dust particles, or liquid state, which deposits into water or onto land. From any of these sources, TCDD may then reach plants and animals and bioaccumulate. The primary source of human exposure to TCDD is through dietary consumption. For example, TCDD- contaminated animal feed led to the contamination of pork products from Ireland in 2008 (Tlustos *et. al.*, 2011). Another example is the disposal of TCDD-contaminated industrial oil, which resulted in contamination of animal feed and animal-based food products from Belgium in 1999 (Bernard and Fierens 2002). However, human exposure can also occur through accidental and occupational exposures (Pelclova *et al.*, 2006). In fact, one of the worst industrial accidents in the world occurred in 1976, when a chemical plant explosion exposed residents in Seveso, Italy, to high levels of TCDD (Eskenazi *et al.*, 2018). Hence, TCDD and related dioxins pose a public health issue, as humans can potentially be exposed to these chemicals through environmental and accidental exposure.

TCDD Toxicity in Humans

The consequences of TCDD exposure in humans have largely been identified based on analyzing longitudinal health data of people exposed accidentally to TCDD. In humans that were exposed during the chemical plant explosion in Seveso, Italy, one of the most prevalent toxic effects of TCDD was chloracne, which is characterized by skin eruption of blackheads, cysts, and nodules (Reggiani, 1980). Several studies also revealed

an increased risk for type 2 diabetes with dioxin exposure (Kim et al. 2003; Kogevinas 2001; Remillard and Bunce, 2002). Additional toxic effects of TCDD that have been reported include atherosclerosis, neuropsychological impairment, and ocular vascular changes after decades of exposure (Kim *et al.*, 2003; Pelclova *et al.*, 2006). In addition, railroad workers exposed to TCDD showed dystonia and peripheral neuropathy (Klawans, 1987).

TCDD is classified as a "known human carcinogen" by the International Agency for Research on Cancer (Cole *et al.*, 2003). Available data from workers at Dow Chemical, where TCDD was produced, indicate that chronic exposure to TCDD increased the risk for cancer (Kogevinas, 2001). Furthermore, increased risk of prostate cancer was identified in U.S. Air Force veterans who served in the Vietnam War in Operation Ranch Hand, which was the operation in which Agent Orange was sprayed (Pavuk, Michalek and Ketchum, 2006).

The Aryl Hydrocarbon Receptor (AhR)

TCDD and other HAHs exert their toxic effects through interaction with a soluble, cytoplasmic protein called the aryl hydrocarbon receptor (AhR) (Fernandez-Salguero *et al.*, 1996). The AhR is a transcription factor that belongs to the basic helix-loop-helix-Per-ARNT-Sim family (bHLH-PAS). As shown in Figure 1.3, the amino terminus of the AhR protein contains bHLH motifs that function in DNA binding (Fukunaga and Hankinson, 1996). Next to the bHLH domain is the PAS domain, which contains a conserved domain of 250-300 amino acids. The PAS domain shares sequence similarity with three eukaryotic proteins: the *period* circadian protein (Per), the vertebrate AhR nuclear translocator (ARNT), and a Drosophila protein involved in embryonic

development called single-minded (Sim) (Burbach *et al.*, 1992). The PAS domain also contains binding sites for two molecules of heat shock 90 (Hsp90) protein, which are molecular chaperones (Antonsson et al. 1995; Fukunaga et al. 1995). The PAS domain is comprised of two subdomains, PAS-A and PAS-B, each of which contains about 50 amino acids. The PAS-B subdomain contains a ligand-binding domain that allows the AhR to interact with ligands (Coumailleau et al. 1995). In fact, the AhR is the only protein in the bHLH/PAS family that functions as a receptor (Coumailleau *et al.*, 1995). The carboxy-terminus contains highly variable amino acids that make up a transcription activation domain and determines the cellular localization of the AhR (Coumailleau *et al.*, 1995).

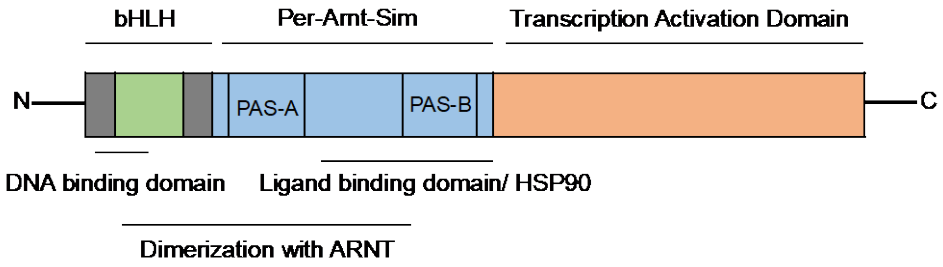

Figure 1.3 Functional Domains of the AhR

The domains that are common to proteins in the bHLH/PAS family are represented. Hsp90, heat shock protein-90.

Mechanism of AhR Activation

Vertebrates have evolved to defend against exposure to toxic compounds encountered in the environment and produced within the body as byproducts of enzymatic reactions. The AhR appears to mediate dynamic responses to both environmentally and endogenously generated toxins, and this led researchers to consider

the wide-ranging roles of AhR. Understanding the molecular mechanisms of AhR activation is crucial for elucidating the broad functions of this protein.

In the absence of ligand, the AhR is found in the cytoplasm, where it forms a complex with Hsp90 (Denis *et al.*, 1988), AhR interacting protein (AIP; also called X-associated protein-2) (Ma and Whitlock, 1997; Meyer *et al.*, 1998), and a 23-kDa protein (p23) (Cox and Miller, 2004). Also, the tyrosine kinase c-src has been reported as an integral component of the cytosolic AhR complex (Enan and Matsumura, 1996). Hsp90 has roles in localizing AhR in the cytoplasm and preventing its degradation (Pongratz, Mason and Poellinger, 1992; Bell and Poland, 2000). AIP protects the AhR from ubiquitination-mediated degradation (Kazlauskas, Poellinger and Pongratz, 2000), and p23 helps stabilize the AhR-Hsp90 interaction (Cox and Miller, 2004). Hsp90 masks the ligand-binding site and nuclear localization sequence (NLS) in the bHLH domain of the AhR (Pongratz, Mason and Poellinger, 1992). Upon ligand binding at the PAS-B domain, the AhR undergoes a conformational change that releases these cofactors (Wilhelmsson *et al.*, 1990; Ikuta *et al.*, 1998). As a result, the NLS and DNA-binding domains are revealed, and the AhR translocates to the nucleus (Pollenz, Sattler and Poland, 1994). This “classical” mechanism of AhR activation is shown in Figure 1.4.

Once inside the nucleus, the AhR binds with ARNT and forms a heterodimeric transcriptional complex. The heterodimerization happens through the interaction of the bHLH and PAS domains of both proteins (Probst *et al.*, 1993). The AhR/ARNT complex then binds to cognate DNA sequences termed xenobiotic response elements (XREs), also known as dioxin-responsive elements (DRE), through the bHLH domain (Ko *et al.*, 1997). The XRE motif contains the core bases 5'-GCGTG-3'. Gene that contain XREs in

the promoter and/or enhancer regions and are responsive to AhR activation are said to be AhR-regulated genes.

Binding of the AhR/ARNT complex to DNA leads to the physical interaction of the complex with several co-activator proteins that relax the chromatin structure and recruit the transcription machinery. The AhR contains several modular domains: an acidic region, a glutamine-rich region, and a region rich in proline/serine/threonine residues. The ARNT protein possesses domains of glutamine-rich region and proline/serine/threonine residues (Jain *et al.*, 1994). These domains interact with different cofactors to serve different functions. Upon DNA binding, the AhR/ARNT complex recruits several transcriptional co-activator proteins, including CBP/p300 (Kobayashi *et al.*, 1997), SRC-1 (Kumar and Perdew, 1999), NCoA2/GRIP1/TIF2, p/CIP, RIP140 (Beischlag *et al.*, 2002), and Brg-1 (Wang and Hankinson, 2002). The AhR/ARNT complex can also directly interact with transcription factors, such as TFIIB, TFIID/TBP, and TFIIF (Rowlands, Mcewan and Gustafsson, 1996; Swanson and Yang, 1998). This interaction occurred through the AhR/ARNT complex, while either AhR or ARNT alone were insufficient for this the interaction.

Exposure to TCDD modulates the expression of many genes through an AhR-dependent mechanism. Nevertheless, many of these genes lack a clearly defined XRE. Recent studies have identified a novel non-consensus XRE (NC-XRE) in the promoter of the gene encoding plasminogen activator inhibitor-1 (PAI-1), which is known to be regulated by AhR activation (Huang and Elferink, 2012). Interestingly, chromatin immunoprecipitation and RNA interference studies showed that ARNT is not a component of the NC-XRE-bound AhR complex. Subsequent studies on the NC-XRE-

bound AhR complex revealed many novel Krüppel-like factor (KLF) protein family as AhR binding partners (Wilson, *et al.*, 2013). The AhR has also been shown to bind to the NF-kB subunit, RelA, to induce expression of interleukin-6 (IL-6) and c-myc (Kim *et al.*, 2000). These studies underscore the complexity of AhR transcriptional activity.

Termination of AhR Signaling

Termination of AhR signaling following transcriptional activation is required to prevent long-lasting gene modulation. Termination of AhR activity is largely achieved through proteasomal degradation. Proteasomal degradation is accomplished by transporting the AhR back to the cytoplasm through the recognition of a nuclear export signal by the CRM-1 protein (Davarinos and Pollenz, 1999). In the cytoplasm, the receptor undergoes ubiquitination and is subsequently degraded by the 26S proteasome (Ma, Baldwin and Virginia, 2000). In addition, the AhR protein itself was found to be a ligand-dependent E3 ubiquitin ligase, capable of targeting sex steroid hormone receptors for degradation (Ohtake *et al.*, 2007). Another regulatory mechanism for termination of AhR activity is through competitive inhibition by a protein called the AhR repressor. This protein shares structural similarities with the N-terminus of the AhR, which makes it possible for the repressor to compete with ARNT for dimerization with the AhR (Mimura *et al.*, 1999).

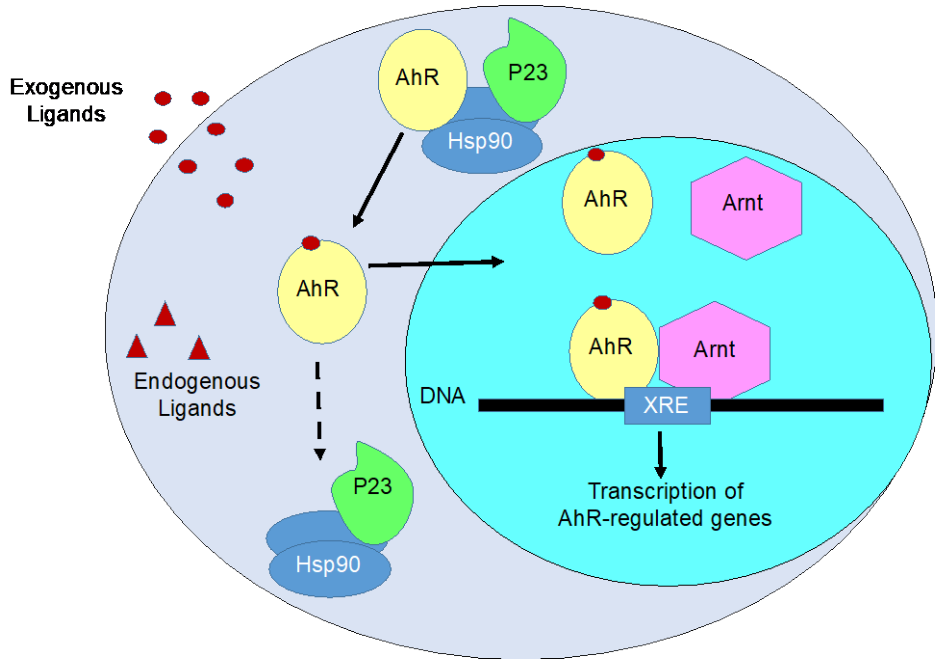

Figure 1.4 Classical Mechanism of AhR Activation

Binding of exogenous or endogenous ligands to the AhR causes the dissociation of cofactors, resulting in nuclear translocation of the AhR. In the nucleus, the AhR heterodimerizes with the AhR nuclear translocator (ARNT). The AhR-ARNT-ligand complex modulates gene transcription by binding to xenobiotic response elements (XREs).

AhR Ligands

The AhR is activated by structurally diverse ligands, including endogenous, exogenous, and dietary ligands. Endogenous ligands are those compounds and metabolites that are formed within a biological system. In contrast, exogenous AhR ligands are typically produced through anthropogenic activities. Some of these ligands are further discussed below.

Exogenous AhR Ligands

As previously discussed, exogenous AhR ligands include HAHs, such as dioxins (e.g., TCDD), furans, and polychlorinated biphenyls. Another family of exogenous AhR

ligands is polycyclic aromatic hydrocarbons (PAHs), which include the human carcinogen benzo[*a*]pyrene, as well as 3-methylcholanthrene and benzoflavones (Denison *et al.*, 2002). PAHs are primarily generated during the incomplete combustion of organic material, such as coal, wood, oil, and petrol (reviewed in Abdel-Shafy and Mansour, 2016). The carcinogenicity of PAHs has been well established, with benzo[*a*]pyrene having been classified as a "known animal carcinogen" by the U.S. Department of Health and Human Services and "probably carcinogenic to humans" by the International Agency for Research on Cancer (IARC) (International Agency for Research on Cancer, 2016). In contrast to TCDD, PAHs are extensively metabolized by the cytochrome P450-mediated oxidase system (reviewed in Abdel-Shafy and Mansour, 2016). The induction of phase I enzymes by PAHs is AhR-dependent, and these enzymes are responsible for the metabolic activation of the parent PAH compound, resulting in the production of mutagenic metabolites, DNA adduct formation, and carcinogenesis (Kondraganti *et al.*, 2003).

Endogenous AhR Ligands

The AhR was originally identified as a transcription factor that mediated the toxic effects of environmental toxicants, but the endogenous ligand for this receptor, as well as its physiological role, was unknown. Studies with AhR knockout mice demonstrated that the AhR likely played a physiological role in liver development. This was evident based on reports of reduced liver size in two different strains of AhR-null mice (Fernandez-Salguero et al., 1996; Schmidt et al., 1996). The AhR is also required for closure of the ductus venosus, which is an intrahepatic shunt in the fetal liver (Lahvis and Bradfield 1998). Finally, AhR-null mice displayed portal fibrosis, hypercellularity, impaired

retinoic acid catabolism (Schmidt *et al.*, 1996; Gonzalez and Fernandez-Salguero, 1998). It has been proposed that these abnormal phenotypic changes result from the absence of endogenous AhR activity, which results in unchecked levels of endogenously generated toxins (Fernandez-Salguero *et al.*, 1995; Lahvis and Bradfield, 1998). However, the molecule mechanisms and physiological ramifications of endogenous AhR activation are still under investigation.

Most of the endogenous ligands are byproducts of normal biochemical reactions in a cell and are classified into structurally distinct classes of chemicals. Many of the endogenous AhR ligands identified demonstrate a weak affinity for AhR binding when compared to TCDD. AhR endogenous ligands can be classified as indoles, tetrapyrroles, arachidonic acid metabolites, and other ligands. As shown in Figure 1.5, these endogenous ligands are structurally diverse. Some of the endogenous ligands are discussed below.

Indoles

Several *in vivo* and *in vitro* studies indicate that indole-containing chemicals can activate the AhR. For example, AhR activation by ultraviolet photoproducts of tryptophan and histidine was reported (Helferich and Denison, 1991). Tryptophan, and naturally occurring tryptophan metabolites, such as tryptamine and indole acetic acid, can induce AhR-dependent gene expression, suggesting that these metabolites may also be metabolized by cytochrome P450 enzymes (Heath-Pagliuso *et al.*, 1998). Indirubin and indigo, which are found in human urine, are another group of endogenous, indole-containing chemicals that have been shown to activate the AhR (Adachi *et al.*, 2001).

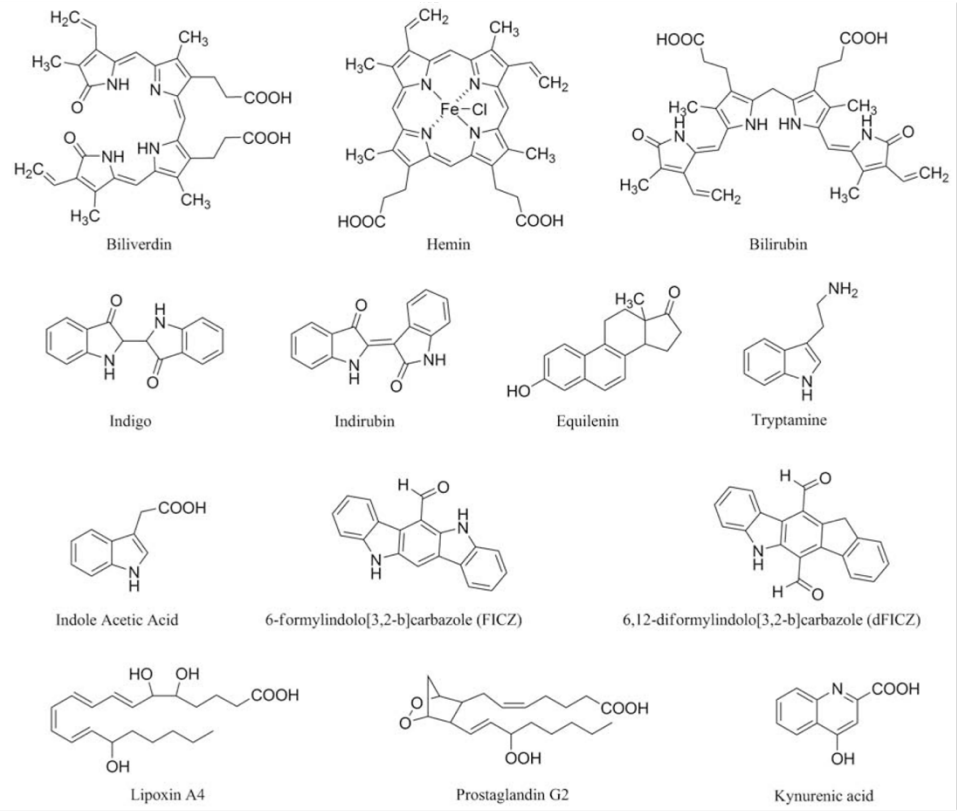

Figure 1.5 Structures of Endogenous AhR Ligands

Another chemical in the indole family, 2-(1'H-indole-3'carbonyl)-thiazole-4-carboxylic acid methyl ester (ITE), was recently reported to be a potent endogenous AhR ligand (Henry *et al.*, 2006). ITE is a tryptophan metabolite with 6 times less AhR binding affinity than TCDD (K_i values for ITE and TCDD are 3 nM and 0.5 nM, respectively) (Figure 1.6) (Song *et al.*, 2002). ITE has been reported to induce a gene expression profile that is remarkably similar to that induced by TCDD , including the induction of AhR-dependent xenobiotic-metabolizing enzymes (Henry, Welle and Gasiewicz, 2009). However, ITE did not produce any dioxin-like toxicity (Ehrlich and Kerkvliet, 2017). It has also been reported that AhR levels, which are rapidly degraded in response to agonist-induced activation, were partially restored within 24 h after ITE treatment, but not 24 h after TCDD treatment (Henry et al., 2009). This supports the notion that ITE is

readily metabolized, unlike TCDD. However, the molecular mechanism of ITE clearance is largely unknown. Rapid clearance and lack of toxicity make ITE a potential therapeutic AhR agonist.

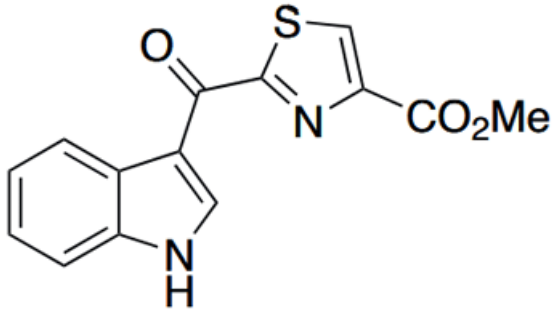

Figure 1.6 Chemical Structure of 2-(1'H-indole-3'carbonyl)-Thiazole-4-Carboxylic Acid Methyl Ester (ITE)

Tetrapyrroles

It has been reported that exogenously added hemin, biliverdin, or bilirubin induce the expression of CYP1A1 and other XRE-dependent genes in mouse hepatoma Hepa1c1c7 cells (Sinal and Bend, 1997). CYP1A1 is the gene that encodes cytochrome P4501A1, and its expression is considered a hallmark of AhR activation. Subsequent studies showed that mRNA and protein levels of CYP1A1 and CYP1A2 were elevated in congenitally jaundiced Gunn rats, which exhibit high plasma bilirubin levels due to impaired bilirubin conjugation (Kapitulnik and Gonzalez, 1993). These results support the notion that bilirubin and biliverdin are endogenous AhR ligands.

Arachidonic Acid Metabolites

TCDD is known to increase the release of arachidonic acid (AA) from the cell membrane by stimulating lipid oxidation and activating phospholipases (Denison and Nagy, 2003). Lipoxin A4, which is a lipoxygenase product of AA, can up-regulate the

expression of CYP1A1 in an AhR-dependent reporter assay (Nagy *et al.*, 2002). These findings suggest that AA metabolites are yet another class of endogenous AhR ligands.

Dietary AhR Ligands

A variety of naturally occurring, plant-derived materials have been shown to induce AhR activation. The several nutritional plant compounds such as dibenzoylmethanes, (MacDonald *et al.*, 2001) curcumin, (Ciolino *et al.*, 1998) can activate AhR. The carotenoids such as β-carotene (bC), bixin (BX), lycopene, lutein, canthaxanthin, and astaxanthin (AX) competitively bind to AhR (Jewell and O'Brien, 1999). Possibly the plants-derived materials are the largest class of natural AhR ligands to which humans and animals are exposed.

TCDD Toxicity in Rodents

Most of our knowledge about TCDD toxicity is derived from studies in which TCDD was administered to rodents. In mice, the dose of TCDD required to produce death in 50% of animals (lethal dose-50, LD_{50}) is 182 to 2570 µg/kg body weight, when administered orally (Chapman and Schiller, 1985). This wide range of concentration reflects the fact that some strains of mice express the 'b' allele of the AhR gene, which encodes an AhR protein with high affinity for ligand, compared to other strains that express the low-affinity 'd' allele (Chang *et al.*, 1993). Mice exposed to TCDD exhibited dose-related endpoints. Toxic endpoints observed at low doses of TCDD (2.4-500 ng/kg) include disturbed steroid secretion and impaired cochlear function (Baldridge *et al.*, 2015, Safe and Luebke, 2016). Effects seen at moderate doses of TCDD (0.2-30 µg/kg) include decreased thymus and spleen size, hepatomegaly, lipid accumulation, inflammation, immunosuppression, and carcinogenicity (Vos, Moore, and Zinkl, 1974; Van Miller,

Lalich and Allen, 1977; Poland and Glover, 1980). Finally, high doses of TCDD (>200 µg/kg) produced hypophagia, beta cell apoptosis, and death (Hoyeck *et al.*, 2020). These dose-dependent endpoints also varied according to species, gender, administration route, and the number of doses.

TCDD Hepatotoxicity

The liver is a target organ for TCDD-induced toxicity. The liver consists primarily of parenchymal cells called hepatocytes (80%), as well as non-parenchymal cells, including hepatic stellate cells (HSCs), sinusoidal endothelial cells, stellate cells, and Kupffer cells. The AhR is expressed in all liver cells and is highly expressed in hepatocytes. In fact, the majority of TCDD hepatotoxicity studies have focused on hepatocytes, and less is known about the ramifications of AhR signaling in non-parenchymal cell populations. In rodents, TCDD hepatotoxicity includes various endpoints, including hepatomegaly, hepatocyte necrosis and apoptosis, inflammation, fat accumulation, dysregulation of vitamin A homeostasis, and fibrosis. These endpoints are discussed in further detail below.

Hepatocyte Necrosis

TCDD has been shown to produce mild or moderate necrosis in the liver (Flower *et al*., 1973; Jones and Butler 1974). The presence of necrosis is further corroborated by the elevation of levels of alanine aminotransferase (ALT) enzymes in the serum and plasma (Pohjanvirta and Tuomisto, 1994). However, the effects of TCDD on hepatocyte apoptosis are less clear-cut and vary depending on the model system.

Steatosis

Steatosis (fatty liver) refers to intrahepatic fat accumulation that comprises at least 5% of the overall liver weight. Steatosis is also referred to as nonalcoholic fatty liver (NAFL). Steatosis can be seen as macrovesicular steatosis (large droplets) or microvesicular steatosis (small droplets). The liver is a critical organ for fat metabolism. TCDD exposure is shown to disturb liver function by altering fatty acid and triglyceride metabolism. In mice, TCDD altered hepatic gene expression related to lipid transport, partitioning, and metabolism (Kopec *et al.*, 2011). If left untreated, NAFL can progress towards a more aggressive form of liver disease called nonalcoholic steatohepatitis (NASH). In NASH, fat accumulation is associated with inflammation and fibrosis (scarring), which can lead to cirrhosis, hepatocellular carcinoma, or death.

Vitamin A Dysregulation

About 80% of the vitamin A in the body is stored in HSCs as retinol. Both endogenous and exogenous AhR activation adversely affects vitamin A homeostasis. For example, TCDD exposure has been shown to reduce vitamin A levels (Thunberg *et al.*, 1980; Pohjanvirta *et al.*, 1990; Hakansson *et al.*, 1991). There is evidence to suggest a positive correlation between TCDD-induced liver toxicity and decreased vitamin A stores (Pohjanvirta *et al.*, 1990; Fletcher, Hanberg and Håkansson, 2001). This is corroborated by a study that showed that injection of exogenous vitamin A reduced TCDD-induced body wasting, hepatomegaly, thymic atrophy, production of reactive oxygen species, and DNA damage (Alsharif and Hassoun, 2004). A more recent study from our lab also showed that TCDD inhibits lipid storage droplets in human hepatic stellate cells, LX-2 (Harvey *et al.*, 2016). These data suggest the importance of vitamin A homeostasis in

liver toxicity. Hence, it is important to study the consequences of AhR signaling in HSC activation.

Inflammation

Chronic hepatic inflammation is one of the common triggers and characteristics of liver disease. Both acute and chronic exposure to TCDD have been reported to alter the expression of inflammatory cytokines in the liver, including IL-1α, IL-1β, TNF-α , IL-6, and monocyte chemoattractant protein-1 (MCP-1) (Olivero-Verbel, Roth and Ganey, 2011; Ozeki *et al.*, 2011; Del-Campo *et al.*, 2018). Increased production of MCP-1 can attract neutrophils and monocytes, which can exacerbate inflammation. However, the mechanism by which this occurs, and which liver cell populations are directly impacted by TCDD treatment, remain unclear. Understanding how AhR signaling in diverse cell populations impacts inflammation is important for understanding the interplay within different liver cells, which is a subject addressed in this dissertation.

Hepatocellular Carcinoma

The carcinogenic effects of TCDD have been studied for the past five decades with results obtained from a variety of tissues. In rats, chronic administration of TCDD at doses as low as 0.001 µg/kg/week for 78 weeks induced cancerous tumors in various tissues including tear ducts, kidneys, skin, testes, brains, skeletal muscles, lungs and livers (Van Miller, Lalich and Allen, 1977). Mice treated with TCDD at 0.05 µg/kg/week for two years developed liver cancer and thyroid adenomas (National Toxicology Program, 1982). Male mice gavaged with 10 µg/kg every two weeks for 24 weeks developed tumors in the liver (Kennedy *et al*., 2014). Results from these animal studies indicate that TCCD is a potent carcinogen. There is no evidence to indicate that TCDD is

mutagenic, as it does not appear to bind or to damage DNA (Huff *et al.*, 1980; Pitot *et al.*, 1980). Instead, TCDD is classified as a tumor promoter (Knerr and Schrenh 2006). In the liver, TCDD appears to elicit tumorigenesis by altering hepatocyte proliferation and apoptosis. However, studies with AhR-deficient mice suggest that the AhR functions as a suppressor of liver carcinogenesis, possibly through endogenous activation (Fan *et al.*, 2010).

Modulation of Hepatocyte Proliferation

TCDD was shown to decrease the proliferation of primary hepatocyte cells from rats by suppressing DNA synthesis (Hushka and Greenlee, 1995). TCDD suppressed hepatocyte proliferation in livers of rodents that had been subjected to a partial hepatectomy (Bauman *et al.*, 1995). Another study reported that TCDD treatment shunted regeneration by reducing cyclin-dependent kinase-2 (CDK2) activity, a pivotal regulator of the G1/S phase transition (Mitchell *et al.*, 2006). TCDD can also induce AhR heterodimerization to E2F transcription factors, thereby repressing the expression of genes required for S-phase progression in the cell cycle (Puga *et al.*, 2000; Elferink, 2003). TCDD treatment suppressed hepatocyte proliferation through induction in p21Cip1 and p27Kip expression, which are negative regulators of proliferation (Kolluri *et al.*, 1999; Jackson *et al.*, 2014). However, in contrast to these studies, prolonged TCDD treatment for 30 weeks was found to increase hepatic cell proliferation (Lucier *et al.*, 1991; Tritscher *et al.*, 1995). These inconsistencies highlight the possibility of multiple mechanisms by which TCDD modulates proliferation.

Fibrosis

Fibrosis is an aberrant wound-healing process characterized by the excessive deposition of extracellular matrix (ECM) material, mainly collagen (Brenner *et al.*, 2000). The onset of fibrotic progression can be triggered by chronic injury and inflammation (Wynn, 2008). Accumulating evidence suggests a role for AhR signaling in liver fibrosis. For instance, exposure of mice to TCDD for 2 weeks elicited hepatic expression of collagen type I and markers of liver fibrosis (Pierre *et al.*, 2014). These effects were not observed in AhR knockout mice (Pierre *et al.*, 2014). A recent study reported that chronic administration of TCDD increased collagen accumulation in the mouse liver (Nault *et al.*, 2016). In addition, examination of the liver of AhR-null mice revealed the presence of fibrotic lesions despite the absence of any exogenous agonist, such as TCDD (Fernandez-Salguero *et al.*, 1995). This raises the intriguing possibility that endogenous AhR signaling may be important for repressing HSC activation and preventing the development of liver fibrosis.

Liver Fibrosis

In 2017, liver disease was the 12th leading cause of death in the United States, according to the World Health Organization. The major cause of mortality and morbidity associated with liver disease is liver cirrhosis and hepatocellular carcinoma, both of which represent advanced stages of liver disease. Liver fibrosis is characterized by an abnormal accumulation of ECM material due to increased deposition and/or reduced degradation of collagen fibers. Currently, no drugs have been approved by the Food and Drug Administration to prevent or reverse liver fibrosis. There is an urgent need to

understand the molecular mechanisms of liver fibrosis and the progression of liver disease and to identify novel therapeutic targets for treating this disease.

Liver fibrosis can be caused by a range of insults, including toxins, alcohol, hepatitis C virus infection (HCV), and drug-induced liver injury (DILI). The prevalence of HCV-induced liver fibrosis is increasing, especially in people 60 years old and above. DILI can develop following abuse of medications such as over-the-counter drugs (Lee, 2003). There are no risk factors identified for DILI, but certain individuals with genetic susceptibility and pre-existing liver disease may be particularly susceptible to DILI onset (Donepudi *et al.*, 2012). The incidence and prevalence of liver fibrosis are increasing due to confounding factors, which include type 2 diabetes, obesity, and NAFL. Type 2 diabetes and NAFL, in particular, are common causes of liver fibrosis and often coexist in patients with fibrosis (Anstee, McPherson, and Day, 2011). In fact, a recent analysis of 827 patients with advanced liver fibrosis indicates that most patients also suffer from obesity and insulin resistance (Harrison *et al.*, 2008).

Liver Injury and Inflammation

As discussed earlier, injury and inflammation are important triggers for liver fibrosis. Liver injury can be either acute or chronic. Acute liver injury is characterized by transient fibrogenesis, which lasts for days to a few weeks, and from which the injured liver tissue can recover almost completely. In contrast, during chronic liver injury, the collagen content in the liver increases. In advanced stages of fibrosis, the liver develops nodules that can hinder blood flow, which produces areas of regeneration throughout the liver that exists as nodules. This condition is referred to as cirrhosis, and it can eventually progress to hepatocellular carcinoma (Suk and Kim, 2015). The term "liver injury”

includes hepatocyte necrosis and apoptosis, steatosis, and steatohepatitis. Furthermore, inflammatory cells, such as activated Kupffer cells, which are resident macrophages, are reported to participate in liver injury and fibrogenesis by producing transforming growth factor-beta-1 (TGFβ1), which is the major driver of fibrogenesis (Norona *et al.*, 2019). Taken together, multiple pathways of liver injury and inflammation can contribute to the development of liver fibrosis.

Liver Fibrosis Reversal

Recent reports suggest that the reversibility of liver fibrosis is achievable. Accumulating evidence was documented in liver fibrosis reversal across different etiologies, including viral hepatitis, autoimmune hepatitis, and NASH (Dixon *et al.*, 2004; Brenner, 2013). Patients successfully treated for HCV showed no evidence of fibrosis upon HCV recovery, and this was confirmed by repeated biopsy (Brenner, 2013). However, the reversal of fibrosis is not possible at all advanced stages of fibrosis. In fact, patients with advanced cirrhosis failed to recover. This raises the possibility that there is a "point of no return" in liver fibrosis progression. Possibly the point of recovery is dependent on the amount of ECM remodeling that has occurred.

Extracellular Matrix

The extracellular matrix (ECM) is a dynamic component in the liver. In a healthy liver, the ECM helps maintain tissue homeostasis. In the injured liver, ECM remodeling favors the excess accumulation of ECM, predominantly collagen type I, along with fibronectin and laminin (Martinez-Hernandez, Delgado, and Amenta, 1991). During chronic liver disease, dysregulation of ECM metabolism can result in hepatic collagen levels that are eight-fold higher than those observed in the healthy liver (Wells, 2008).

Hepatic Stellate Cells

HSC are central mediators of liver fibrosis. In a healthy liver, HSCs primarily function in storing vitamin A, but they are also involved in retinoic acid homeostasis, vasoregulation through endothelial cell interactions, extracellular matrix homeostasis, drug detoxification, and immunotolerance (Senoo, 2004; Puche, Saiman and Friedman, 2013). Upon liver injury, HSCs become activated and assume a myofibroblast-like phenotype, characterized by increased proliferation, contractility, fibrogenesis, and retinoid loss (Li *et al.*, 2008). HSC activation is a complex phenomenon involving many pathways, cells, and events.

TCDD and Liver Fibrosis

The role of AhR signaling in liver fibrosis is an emerging area of research. There is evidence to indicate a role for endogenous AhR signaling in repressing fibrogenesis. For example, AhR-knockout (AhR-KO) mice have livers that are reduced in size by 50 percent and show bile duct fibrosis (Fernandez-Salguero *et al.*, 1995). The livers of AhR-KO mice also have collagen content that is 53% greater than the liver of wildtype mice (Peterson *et al.*, 2000). Whereas endogenous AhR activity appears to suppress fibrosis, exogenous AhR activation with TCDD promotes it. For example, it was recently found that, in wild-type mice that express a functional AhR, chronic TCDD treatment elicited liver fibrosis through an AhR-dependent manner (Pierre *et al.*, 2014). It is possible that treating with TCDD promotes fibrosis by preventing endogenous receptor activation, essentially resulting in de-repression of fibrogenesis. Using an AhR-KO model system in mice is not ideal for studying liver fibrosis as half of the pups were reported to have died postnatally, and the survivors exhibited diminished fertility (Fernandez-Salguero *et al.*,

1995). This project sought to investigate how AhR signaling impacts fibrosis using mice in which the AhR was selectively removed from different cell populations in the liver.

The use of experimental animal models is vital for understanding liver fibrosis. As discussed earlier, excess collagen deposition by HSCs can be triggered by multiple mechanisms. Each experimental model system can induce liver fibrosis through a different mechanism. Some of the widely used experimental models are discussed below.

Chronic Administration of Carbon Tetrachloride

Carbon tetrachloride (CCl_4) has been widely used to experimentally induce both acute and chronic liver injury. CCl_4 administration induces expression of *Cyp2e1*, which is the gene that encodes the xenobiotic metabolizing enzyme, cytochrome P450E1. This enzyme metabolizes CCl_4 into a trichloromethyl radical, which produces liver injury by eliciting lipid peroxidation in the cell membrane (Wong, Chan and Lee, 1998). CCl_4-induced liver injury is characterized by centrilobular necrosis, which is followed by fibrosis (Yu *et al.*, 2002). In fact, chronic administration of CCl_4 is a well-established model of experimental liver fibrosis (reviewed in Delire *et al.*, 2015). Our lab recently used this model to show that AhR activation by TCDD increased necroinflammation and HSC activation in the CCl_4-injured mouse liver (Lamb *et al.*, 2016a; Lamb *et al.*, 2016b). This suggests that exogenous AhR activation can exacerbate the fibrogenic response to injury.

Bile Duct Ligation

Bile duct ligation (BDL) is another classic model of experimental liver fibrosis, in which cholestatic injury drives the development of periportal biliary fibrosis. In this model, the bile duct is ligated to increase biliary pressure by obstruction (cholestasis),

which leads to mild inflammation, cytokine production, and proliferation of biliary epithelial cells (cholangiocytes), which generates reactive oxygen species (ROS) and liver damage (Georgiev *et al.*, 2008). In this model, collagen production results from the activation of portal fibroblasts as well as HSCs. The BDL model is useful for studying fibrosis reversibility because the biliary obstruction can be relieved by biliodigestive anastomosis (Abdel-Aziz *et al.*, 1990).

Chronic Administration of TCDD

In 2014, Pierre et al. reported that chronic exposure to TCDD elicited liver fibrosis (Pierre *et al.*, 2014). In this study, mice were treated with 25 µg/kg of TCDD for 2 days, 4 days, or once weekly for 42 days. Histological and biochemical examination of liver tissue confirmed that TCDD stimulated the onset of fibrosis in wildtype mice, but not in AhR-KO mice. Shortly thereafter, another lab reported that treatment of mice with TCDD for 92 days produced periportal inflammation and fibrosis (Nault *et al.*, 2016). It was further demonstrated that chronic injury from TCDD treatment dysregulated glycogen, ascorbic acid, and amino acid metabolism, which support ECM remodeling and the progression to hepatic fibrosis (Nault *et al.*, 2016). Studies described in this dissertation utilized this 92-day chronic administration of TCDD to elicit liver fibrosis and elucidate how cell-specific AhR signaling impacts HSC activation and the development of liver fibrosis.

Research Goal

The goal of this dissertation research was to determine how AhR signaling in hepatocytes and HSCs impacts HSC activation and the development of liver fibrosis. It is possible that TCDD directly activates HSCs through AhR signaling in these cells. There are several lines of evidence to support the notion that HSCs are directly cellular targets for TCDD. For example, studies from our lab previously reported that TCDD treatment increased necroinflammation and HSC activation in mice treated with CCl_4 (Lamb et al. 2016a). Furthermore, it was recently reported that treatment of mice with TCDD induced HSC activation and liver fibrosis by activating AkT and NF-kB signaling pathways (Han *et al.*, 2017). Also, *in vitro* studies from our lab demonstrated that TCDD treatment increased expression of α-smooth muscle actin (αSMA) expression, which is an HSC activation marker, in the human HSC line, LX-2 (Harvey *et al.*, 2016) (Figure 1.8). Furthermore, exposure of rodents to TCDD was found to decrease vitamin A storage, which is a well-established indicator of HSC activation (Hakansson and Hanberg, 1989). These data support the notion that TCDD could directly activate HSCs in the mouse liver, leading to the development of liver fibrosis.

However, we cannot rule out the possibility that TCDD induces HSC activation indirectly, as a secondary response to hepatocyte injury and inflammation. Studies in mice indicated that chronic TCDD exposure elicits liver fibrosis, and fibrosis is known to be a wound-healing response directly stimulated by injury and inflammation, which drive HSC activation and subsequent collagen deposition (Pierre *et al.*, 2014; Lamb *et al.*, 2016a; Nault *et al.*, 2016). Moreover, most of the studies of TCDD hepatotoxicity have focused on the consequences of AhR activation in hepatocytes. In fact, studies using

conditional AhR-KO mice demonstrated that AhR signaling in hepatocytes was required for the gross hepatotoxic effects of TCDD (Walisser *et al.*, 2005). The same study reported decreased inflammation and necrosis in hepatocyte-specific knockout mice (Walisser *et al.*, 2005). Another recent study showed a decrease in fat accumulation in liver tissues of hepatocyte-specific AhR KO mice (Tanos *et al.*, 2012). Hence, it can be concluded that AhR signaling in hepatocytes plays a crucial role in the development of necrosis, steatosis, and inflammation in TCDD-treated mice.

Hepatocyte injury and inflammation go hand-in-hand. Injury drives inflammation, and inflammation can elicit fibrogenesis by several mechanisms. For instance, apoptotic hepatocytes induce inflammation by producing profibrogenic mediators (Seki and Schwabe, 2015), which eventually induce liver fibrosis by releasing paracrine stimulators, such as ROS and fibrogenic factors (Canbay, Friedman and Gores, 2004; Li *et al.*, 2008; Lee and Friedman, 2011). Other inflammatory cells, including lymphocytes and neutrophils, can promote liver fibrosis by inducing lipid peroxidation (Casini *et al.*, 1997). Kupffer cells also have a leading role in liver fibrosis by producing ROS, cytokines, and profibrogenic stimulators (Naito *et al.*, 2004; Kolios, Valatas and Kouroumalis, 2006). Collectively, these data establish a positive correlation between inflammation and fibrosis.

In addition, there is increasing evidence to support a causal relationship between hepatic steatosis/NASH and HSC activation, the latter of which drives collagen deposition and liver fibrosis (Mann and Smart, 2002; Wobser *et al.*, 2009; Karanjia *et al.*, 2016). One report suggests that NASH progresses to and fibrosis through a mechanism that involves cytokine release from intrahepatic fat and ROS as a result of dysregulated

lipid metabolism (Cusi, 2012). These findings support the idea that chronic exposure to TCDD could elicit HSC activation indirectly as a result of TCDD-induced inflammation and steatosis. Therefore, it is evident that TCDD may indirectly activate HSC by inducing liver injury and inflammation through AhR signaling in hepatocytes (Figure 1.7). It is important to understand these secondary effects on HSC activation, because they could also play an important role in exacerbating liver fibrosis.

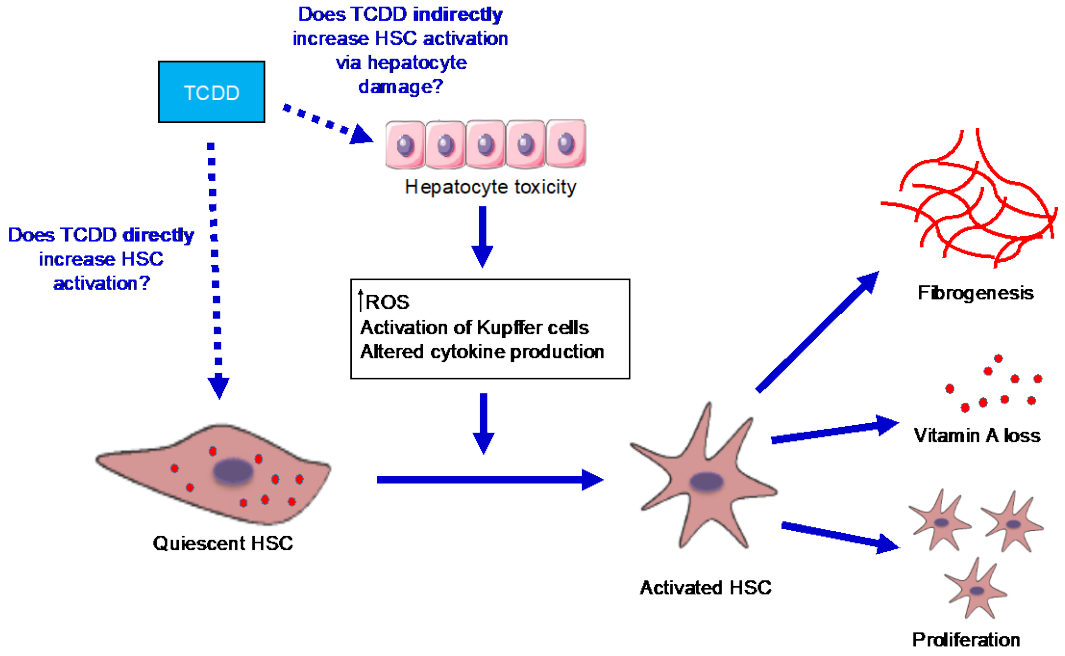

Figure 1.7 Hepatic Stellate Cell activation

Quiescent HSCs function in storing vitamin A. Upon liver injury or direct activation of HSCs, HSCs differentiate to a myofibroblast-like phenotype characterized by proliferation, fibrogenesis, and loss of vitamin A storage. Hepatocyte toxicity may increase the level of reactive oxygen species (ROS), activate Kupffer cells, and alter cytokine production.

Objectives and Hypothesis

We hypothesized that chronic TCDD treatment elicits liver fibrosis *in vivo* by directly activating HSCs. An alternate hypothesis was that TCDD treatment activated HSCs secondary to increasing liver damage, inflammation, and/or steatosis. Finally, it was possible that TCDD increased HSC activation through a combination of effects on both hepatocytes and HSCs.

In addition to understanding the cell-specific role of AhR signaling during fibrosis, we also sought to understand the discrepancy between endogenous and exogenous AhR activation as it relates to fibrosis development. It was recently reported that treatment with the endogenous nontoxic AhR agonist, ITE, reduced HSC activation and diminished liver fibrosis (Yan et al., 2019). Thereby it can be speculated that endogenous and exogenous AhR activations have different outcomes. Interestingly, understanding how AhR signaling modulates HSC activation *in vivo* is confounded by concomitant hepatocyte damage and inflammation, both of which promote HSC activation. These findings raise the intriguing possibility that HSC activation could be therapeutically targeted by novel AhR ligands to diminish liver fibrosis, which is one of the long-term goals of this research.

Studies in Chapter 2 focused on understanding how AhR signaling in HSCs and hepatocytes contributes to HSC activation during TCDD-induced liver fibrosis. Cre-Lox recombination was used to create mice with AhR-deficient hepatocytes or AhR-deficient HSCs. To induce liver fibrosis, female, adult mice were gavaged with TCDD every four days for 92 days, and HSC activation, liver damage, and inflammation were measured. Understanding the cell-specific role of AhR signaling in fibrosis is important to the

development of therapeutic AhR ligands to target and diminish HSC activation and alleviate fibrosis.

The goal of the studies in Chapter 3 was to determine the direct effects of AhR signaling on HSC gene expression in the absence of hepatocyte damage and inflammation. To accomplish this, the AhR was knocked out of the human HSC line, LX-2. Wild-type and AhR-KO cells were treated with TCDD (an exogenous AhR ligand) or ITE (an endogenous AhR ligand) for 6 days of culture, and endpoints of HSC activation, were measured. Results from these studies will be important for understating how AhR signaling directly impacts HSC gene expression. They also shed light on understanding how endogenous AhR signaling contributes to the repression of HSC activation and fibrogenesis. Results from these studies are summarized, and future studies are discussed, in the final chapter of this dissertation.

References

Abdel-Aziz, G. *et al.* (1990) 'Reversibility of hepatic fibrosis in experimentally induced cholestasis in rat', *American Journal of Pathology*, 137(6), pp. 1333–1342.

Abdel-Shafy, H. I. and Mansour, M. S. M. (2016) 'A review on polycyclic aromatic hydrocarbons: Source, environmental impact, effect on human health and remediation', *Egyptian Journal of Petroleum*, 25(1), pp. 107–123.

Adachi, J. *et al.* (2001) 'Indirubin and indigo are potent aryl hydrocarbon receptor ligands present in human urine', *The Journal of Biological Chemistry*, 276(34), pp. 31475–31478.

Alsharif, N. Z. and Hassoun, E. A. (2004) 'Protective effects of vitamin A and vitamin E succinate against 2,3,7,8-tetrachlorodibenzo-p-dioxin (TCDD)-induced body wasting, hepatomegaly, thymic atrophy, production of reactive oxygen species and DNA damage in C57BL/6J mice', *Pharmacology and Toxicology*, 95, pp. 131–138.

Anstee, Q. M., McPherson, S. and Day, C. P. (2011) 'How big a problem is non-alcoholic fatty liver disease?', *British Medical Journal*, 343(7816), pp. 201–204.

Antonsson, C. *et al.* (1995) 'Distinct roles of the molecular chaperone hsp90 in modulating dioxin receptor function via the basic helix-loop-helix and PAS domains', *Molecular and Cellular Biology*, 15(2), pp. 756–765.

Baldridge, M. G. *et al.* (2015) 'Very low-dose (femtomolar) 2,3,7,8- tetrachlorodibenzo-p-dioxin (TCDD) disrupts steroidogenic enzyme mRNAs and steroid secretion by human luteinizing granulosa cells', *Reproduction Toxicology*, 52, pp. 57–61.

Bauman, J. W. *et al.* (1995) 'Inhibitory effects of 2,3,7,8-tetrachlorodibenzo-p-dioxin on rat hepatocyte proliferation induced by 2/3 partial hepatectomy', *Cell Proliferation*, 28(8), pp. 437–451.

Beischlag, T. V. *et al.* (2002) 'Recruitment of the NCoA / SRC-1 / p160 family of transcriptional coactivators by the aryl hydrocarbon receptor/aryl hydrocarbon receptor nuclear translocator complex', *Molecular and cellular biology*, 22(12), pp. 4319–4333.

Bell, D. R. and Poland, A. (2000) 'Binding of Aryl Hydrocarbon Receptor (AhR) to AhR-interacting Protein', *The Journal of Biological Chemistry*, 275(46), pp. 36407–36414.

Bernard, A. and Fierens S. (2002) 'The Belgian PCB/Dioxin incident: a critical review of health risks evaluations', *International Journal of Toxicology*, 21(5), pp. 333–340.

Berg, M. V. *et al.* (2006) 'The 2005 World Health Organization reevaluation of human and mammalian toxic equivalency factors for dioxins and dioxin-like compounds', *Toxicological Sciences*, 93(2), pp. 223–241.

Birnbaum, L. S. (1985) 'The role of structure in the disposition of halogenated aromatic xenobiotics', *Environmental Health Perspectives*, 61, pp. 11–20.

Brenner, D. A. *et al.* (2000) 'New aspects of hepatic fibrosis', *Journal of Hepatology*, 32(1), pp. 32–38.

Brenner, D. A. (2013) 'Advances in hepatology: reversibility of liver fibrosis', *Gastroenterology and Hepatology*, 9(11), pp. 737–738.

Brenner, David A. (2013) 'Reversibility of liver fibrosis', *Gastroenterology and Hepatology*, 9(11), pp. 737–739.

Burbach, K. M. *et al.* (1992) 'Cloning of the Ah-receptor cDNA reveals a distinctive ligand-activated transcription factor', *Biochemistry*, 89, pp. 8185–89.

Canbay, A. *et al.* (2003) 'Apoptotic body engulfment by a human stellate cell line is profibrogenic', *Laboratory Investigation*, 83(5), pp. 655–663.

Casini, A. *et al.* (1997) 'Neutrophil-derived superoxide anion induces lipid peroxidation and stimulates collagen synthesis in human hepatic stellate cells: role of nitric oxide', *Hepatology*, 25(2), pp. 361–367.

Chang, C. *et al.* (1993) 'Ten nucleotide differences, five of which cause amino acid changes, are associated with the Ah receptor locus polymorphism of C57BL/6 and DBA/2 mice', *Pharmacogenetics*, pp. 312–21.

Chapman, D. E. and Schiller, C. M. (1985) 'Dose-related laboratory of pharmacology, effects of 2,3,7,8-tetrachlorodibenzo-p-dioxin in C57BL/6J and DBA/2J mice', *Toxicology and Applied Pharmacology*, 78, pp. 147–157.

Ciolino, H. P. *et al.* (1998) 'Effect of curcumin on the aryl hydrocarbon receptor and cytochrome P450 1A1 in MCF-7 human breast carcinoma cells', *Biochemestry and Pharmacology*, 56(2), pp. 197–206.

Cole, P. *et al.* (2003) 'Dioxin and cancer: a critical review', *Regulatory Toxicology and Pharmacology*, 38(3), pp. 378–388.

Coumailleau, P. *et al.* (1995) 'Definition of a Minimal Domain of the Dioxin Receptor That Is Associated with Hsp90 and Maintains Wild Type Ligand Binding Affinity and Specificity', *The Journal of Biological Chemistry*, 270(42), pp. 25291–00.

Cox, M. B. and Miller, C. A. (2004) 'Cooperation of heat shock protein 90 and p23 in aryl hydrocarbon receptor signaling', *Cell Stress and Chaperones*, 9(1), pp. 4–20.

Cusi, K. (2012) 'Role of obesity and lipotoxicity in the development of nonalcoholic steatohepatitis: pathophysiology and clinical implications', *Gastroenterology*, 142(4), pp. 711–25.

Davarinos, N. A. and Pollenz, R. S. (1999) 'Aryl hydrocarbon receptor imported into the nucleus following ligand binding is rapidly degraded via the cytosplasmic proteasome following nuclear export', *The Journal of Biological Chemistry*, 274(40), pp. 28708–28715.

Del-Campo, J. A. *et al.* (2018) 'Role of inflammatory response in liver diseases: therapeutic strategies', *World Journal of Hepatology*, 10(1), pp. 1–7.

Delire, B., Starkel, P. and Leclercq, I. (2015) 'Animal models for fibrotic liver diseases: what we have, what we need, and what is under development', *Journal of Clinical and Translational Hepatology*, 3(1), pp. 53-66.

Denis, M. *et al.* (1988) 'Association of the dioxin receptor with the mr 90,000 heat shock protein: A structural kinship with the glucocorticoid receptor', *Biochemical and Biophysical Research Communications*, 155(2), pp. 801–807.

Denison, M. S. *et al.* (2002) 'Ligand binding and activation of the Ah receptor', *Chemico-Biological Interactions*, 141(1–2), pp. 3–24.

Denison, M. S. and Nagy, S. R. (2003) 'Activation of the aryl hydrocarbon receptor by structurally diverse exogenous and endogenous chemicals', *Annual Review of Phamacology and Toxicology*, 43, pp. 309–34.

Dixon, J. B. *et al.* (2004) 'Nonalcoholic fatty liver disease: Improvement in liver histological analysis with weight loss', *Hepatology*, 39(6), pp. 1647–1654.

Donepudi, I. *et al.* (2012) 'Drug-induced liver injury', In: Pitchumoni C., Dharmarajan T. (eds) Geriatric Gastroenterology. Springer, New York, NY.

Dutkiewicz, Z. and Mikstacka, R. (2018) 'Structure-based drug design for cytochrome P450 family 1 inhibitors', *Bioinorganic Chemistry and Applications*, 2018, pp. 1–21.

Ehrlich, A. K. and Kerkvliet, N. I. (2017) 'Is chronic AhR activation by rapidly metabolized ligands safe for the treatment of immune-mediated diseases?', *Current Opinion in Toxicology*, 2, pp. 72–78.

Elferink, C. J. (2003) 'Aryl hydrocarbon receptor-mediated cell cycle control', *Progress in Cell Cycle Research*, 5, pp. 261–267.

Enan, E. and Matsumura, F. (1996) 'Identification of C-Src as the integral component of the cytosolic Ah receptor complex, transducing (TCDD) through the protein phosphorylation pathway', *Biochemical Pharmacology*, 52(96), pp. 1599–1612.

Erickson, M. D. and Kaley, R. G. (2011) 'Applications of polychlorinated biphenyls', *Environmental Science and Pollution Research*, 18(2), pp. 135–151.

Eskenazi, B. *et al.* (2018) 'The Seveso accident: a look at 40 years of health research and beyond', *Environment International*, 121(Pt 1), pp.71–84.

Fan, Y. *et al.* (2010) 'The aryl hydrocarbon receptor functions as a tumor suppressor of liver carcinogenesis', *Cancer Research*, 70(1), pp. 212–220.

Fernandez-Salguero, P. *et al.* (1995) 'Immune system impairment and hepatic fibrosis in mice lacking the dioxin-binding Ah receptor', *Science*, 268(5211), pp. 722–726.

Fernandez-Salguero, P. *et al.* (1996) 'Aryl-hydrocarbon receptor-deficient mice are resistant to 2,3,7,8-tetrachlorodibenzo-p-dioxin-induced toxicity', *Toxicology and Applied Pharmacology*, 140, pp. 173–179.

Fletcher, N., Hanberg, A. and Håkansson, H. (2001) 'Hepatic vitamin A depletion is a sensitive marker of 2,3,7,8-tetrachlorodibenzo-p-dioxin (TCDD) exposure in four rodent species', *Toxicological Sciences*, 62(1), pp. 166–175.

Flower, B. A. *et al.* (1973) 'Ultrastructural changes in rat liver cells following a single oral dose of TCDD', *Environmental Health Perspectives*, 5, pp. 141–148.

Fukunaga, B. N. *et al.* (1995) 'Identification of functional domains of the aryl hydrocarbon receptor', *The Journal of Biological Chemistry*, 270(49), pp. 29270–29278.

Fukunaga, B. N. and Hankinson, O. (1996) 'Identification of a novel domain in the aryl hydrocarbon receptor required for DNA binding', *The Journal of Biological Chemistry*, 271(7), pp. 3743–3749.

Georgiev, P. *et al.* (2008) 'Characterization of time-related changes after experimental bile duct ligation', *British Journal of Surgery*, 95(5), p. 646—656.

Gonzalez, F. J. and Fernandez-Salguero, P. (1998) 'The aryl hydrocarbon receptor studies using the ahr-null mice', *Drug Metabolism and Disposition*, 26(12), pp. 1194–1198.

Hakansson, H. *et al.* (1991) 'Effects of 2,3,7,8-tetrachlorodibenzo-p-dioxin (TCDD) on the vitamin A status of Hartley guinea pigs, Sprague-Dawley rats, C57Bl/6 mice, DBA/2 mice, and Golden Syrian hamsters', *Journal of Nutritional Science and Vitaminology*, 37(2), pp. 117–138.

Hakansson, H. and Hanberg, A. (1989) 'The distribution of [14C]-2,3,7,8-tetrachlorodibenzo-p-dioxin (TCDD) and its effect on the vitamin A content in parenchymal and stellate cells of rat liver', *Journal of Nutrition*, 119(4), pp. 573–580.

Han, M. *et al.* (2017) '2,3,7,8-Tetrachlorodibenzo-p-dioxin (TCDD) induces hepatic stellate cell (HSC) activation and liver fibrosis in C57BL6 mouse via activating Akt and NF-κB signaling pathways', *Toxicology Letters*, 273, pp. 10–19.

Hankinson, O. (1995) 'The aryl hydrocarbon receptor complex', *Annual Review of Phamacology and Toxicology*, 35, pp. 307–340.

Harrison, S. A. *et al.* (2008) 'Development and validation of a simple NAFLD clinical scoring system for identifying patients without advanced disease.', *Gut*, 57(10), pp. 1441–1447.

Harvey, W. A. *et al.* (2016) 'Exposure to 2,3,7,8-tetrachlorodibenzo-p-dioxin (TCDD) increases human hepatic stellate cell activation', *Toxicology*, 26(33), pp. 344–346.

Heath-Pagliuso, S. *et al.* (1998) 'Activation of the Ah receptor by tryptophan and tryptophan metabolites', *Biochemistry*, 37(33), pp. 11508–11515.

Helferich, W. G. and Denison, M. S. (1991) 'Ultraviolet photoproducts of tryptophan can act as dioxin agonists', *Molecular Pharmacology*, 40(5), pp. 674–678.

Henry, E. C., Welle, S. L. and Gasiewicz, T. A. (2009) 'TCDD and a putative endogenous AhR Ligand, ITE, elicit the same immediate changes in gene expression in mouse lung fibroblasts', *Toxicological Sciences*, 114(1), pp. 90–100.

Henry, E. C. et al. (2006) 'A potential endogenous ligand for the aryl hydrocarbon receptor has potent agonist activity in vitro and in vivo', *Archives of Biochemistry and Biophysics*, 450(1), pp. 967–77.

Hoyeck, M. P. *et al.* (2020) 'Long-term metabolic consequences of acute dioxin exposure differ between male and female mice', *Scientific Reports*, 10(1), pp. 1–10.

Huang, G. and Elferink, C. J. (2012) ‘A novel nonconsensus xenobiotic response element capable of mediating aryl hydrocarbon receptor-dependent gene expression.’, *Molecular Pharmacology*, 81(3), pp. 338–47.

Huff, J. E. *et al.* (1980) ‘Long-term hazards of polychlorinated dibenzodioxins and polychlorinated dibenzofurans’, *Environmental Health Perspectives*, 36, pp. 221–40.

Hushka, D. R. and Greenlee, W. F. (1995) ‘2,3,7,8-Tetrachlorodibenzo-p-dioxin inhibits DNA synthesis primary hepatocytes’, *Mutation Research*, 333, pp. 89–99.

Ikuta, T. *et al.* (1998) ‘Nuclear localization and export signals of the human aryl hydrocarbon receptor’, *The Journal of Biological Chemistry*, 273(5), pp. 2895–904.

International Agency for Research on Cancer (2011) ‘Polycyclic aromatic hydrocarbons: 15 Listings - benz[a]anthracene, benzo[b]fluoranthene, benzo[j]fluoranthene, benzo[k]fluoranthene, benzo[a]pyrene, dibenz[a,h]acridine, dibenz[a,j]acridine, dibenz[a,h]anthracene, 7H-dibenzo[c,g]carbazole, dibenzo[a,e]pyrene, dibenzo[a,h]pyrene, dibenzo[a,i]pyrene, dibenzo[a,l]pyrene, indeno[1,2,3-cd]pyrene, 5-methylchrysene’, *Report on Carcinogens : Carcinogen Profiles*, 12, pp. 353-361.

Jackson, D. P. *et al.* (2014) ‘Ah Receptor-mediated suppression of liver regeneration through NC-XRE-driven p21Cip1 expression’, *Molecular Pharmacololgy*, 85(4), pp. 533–541.

Jain, S. *et al.* (1994) ‘Potent transactivation domains of the Ah receptor and the Ah receptor nuclear translocator map to their carboxyl termini’, *The Journal of Biological Chemistry*, 269(50), pp. 31518–31524.

Jewell, C. and O’Brien, N. M. (1999) ‘Effect of dietary supplementation with carotenoids on xenobiotic metabolizing enzymes in the liver, lung, kidney and small intestine of the rat’, *The British Journal of Nutrition*, 81(3), pp. 235–42.

Jones, G. and Butler, W. H. (1974) ‘A morphological study of the liver lesion induced by 2,3,7,8-tetrachlorodibenzo-p-dioxin in rats’, *Journal of Pathology*, 112, pp. 93–97.

Kapitulnik, J. and Gonzalez, F. J. (1993) ‘Marked endogenous activation of the CYP1A1 and CYP1A2 genes in the congenitally jaundiced Gunn rat’, *Molecular Pharmacology*, 43(5), pp. 722–725.

Karanjia, R. N. *et al.* (2016) ‘Hepatic steatosis and fibrosis: non-invasive assessment’, *World Journal of Gastroenterology*, 22(45), pp. 9880–9897.

Kazlauskas, A., Poellinger, L. and Pongratz, I. (2000) ‘The immunophilin-like protein XAP2 regulates ubiquitination and subcellular localization of the dioxin receptor’, *The Journal of Biological Chemistry*, 275(52), pp. 41317–41324.

Kennedy, G. D. et al. (2014) ‘Liver tumor promotion by 2,3,7,8-tetrachlorodibenzo-p-dioxin is dependent on the aryl hydrocarbon receptor and TNF/IL-1 receptors’, *Toxicological Sciences*, 140(1), pp. 135–143.

Kim, D. W. *et al.* (2000) ‘The RelA NF-kappaB subunit and the aryl hydrocarbon receptor (AhR) cooperate to transactivate the c-myc promoter in mammary cells’, *Oncogene*, 19, pp. 5498–5506.

Kim, J. *et al.* (2003) ‘Impact of Agent Orange exposure among Korean Vietnam veterans’, *Industrial Health*, 41, pp. 149–157.

Klawans, H. L. (1987) ‘Dystonia and tremor following exposure to 2,3,7,8-tetrachlorodibenzo-p-dioxin’, *Movement Disorders*, 2(4), pp. 255–261.

Knerr, S. and Schrenk. D. (2006) ‘Carcinogenicity of 2,3,7,8-tetrachlorodibenzo-p-dioxin in experimental models’, *Molecular Nutrition & Food Research*, 50(10), pp. 897–907.

Ko, H. P. *et al.* (1997) ‘Transactivation domains facilitate promoter occupancy for the dioxin-inducible CYP1A1 gene in vivo’, *Molecular and Cellular Biology*, 17(7), pp. 3497–3507.

Kobayashi, A. *et al.* (1997) 'CBP/p300 functions as a possible transcriptional coactivator of Ah receptor nuclear translocator (Arnt)', *The Journal of Biochemistry*, 122(4), pp. 703–710.

Kogevinas, M. (2001) 'Human health effects of dioxins : cancer, reproductive and endocrine system effects', *Human Reproduction Update*, 7(3), pp. 331–339.

Kolios, G., Valatas, V. and Kouroumalis, E. (2006) 'Role of Kupffer cells in the pathogenesis of liver disease', *World Journal of Gastroenterology*, 12(46), pp. 7413–7420.

Kolluri, S. K. *et al.* (1999) 'p27(Kip1) induction and inhibition of proliferation by the intracellular Ah receptor in developing thymus and hepatoma cells', *Genes and Development*, 13(13), pp. 1742–1753.

Kondraganti, S. R. *et al.* (2003) 'Polycyclic aromatic hydrocarbon-inducible DNA adducts: evidence by 32P-postlabeling and use of knockout mice for Ah receptor-independent mechanisms of metabolic activation in vivo', *International Journal of Cancer*, 103(1), pp. 5–11.

Kopec, A. K. *et al.* (2011) 'Non-additive hepatic gene expression elicited by 2,3,7,8-tetrachlorodibenzo-p-dioxin (TCDD) and 2,2′,4,4′,5,5′-hexachlorobiphenyl (PCB153) co-treatment in C57BL/6 mice', *Toxicology and Applied Pharmacology*, 256, pp. 154–167.

Kumar, M. B. and Perdew, G. H. (1999) 'Nuclear receptor coactivator SRC-1 interacts with the Q-rich subdomain of the AhR and modulates its transactivation potential', *Gene Expression*, 8(1), pp. 273–286.

Lahvis, G. P. and Bradfield, C. A. (1998) 'Ahr null alleles: distinctive or different?', *Biochemical Pharmacology*, 56(7), pp. 781–787.

Lamb, C. L. *et al.* (2016a) '2,3,7,8-Tetrachlorodibenzo-p-dioxin (TCDD) increases necroinflammation and hepatic stellate cell activation but does not exacerbate experimental liver fibrosis in mice', *Toxicology and Applied Pharmacology*, 311, pp. 42–51.

Lamb, C. L. *et al.* (2016b) 'Aryl hydrocarbon receptor activation by TCDD modulates expression of extracellular matrix remodeling genes during experimental liver fibrosis', *BioMed Research International*, 2016, pp. 1–14.

Lee, U. E. and Friedman, S. L. (2011) 'Mechanisms of hepatic fibrogenesis', *Best Practice & Research: Clinical Gastroenterology*, 25(2), pp. 195–206.

Lee, W. M. (2003) 'Drug-induced hepatotoxicity', *New England Journal of Medicine*, 349(5), pp. 474–485.

Li, J. T. *et al.* (2008) 'Molecular mechanism of hepatic stellate cell activation and antifibrotic therapeutic strategies', *Journal of Gastroenterology*, 43(6), pp. 419–428.

Lucier, G. W. *et al.* (1991) 'Ovarian hormones enhance 2,3,7,8-tetrachlorodibenzo-p-dioxin-mediated increases in cell proliferation and preneoplastic foci in a two-stage model for rat hepatocarcinogenesis', *Cancer Research*, 51(5), pp. 1391–1397.

Ma, Q., Baldwin, K. T. and Virginia, W. (2000) '2,3,7,8-Tetrachlorodibenzo-p-dioxin-induced degradation of aryl hydrocarbon receptor (AhR) by the ubiquitin-proteasome pathway', *The Journal of Biological Chemistry*, 275(12), pp. 8432–8438.

Ma, Q. and Whitlock, J. P. (1997) 'A novel cytoplasmic protein that interacts with the Ah receptor, contains tetratricopeptide repeat motifs, and augments the transcriptional Response to 2,3,7,8-tetrachlorodibenzo-p-dioxin', *The Journal of Biological Chemistry*, 272(14), pp. 8878–8884.

MacDonald, C. J. *et al.* (2001) 'Dibenzoylmethane Modulates Aryl Hydrocarbon Receptor Function and Expression of Cytochromes P50 1A1, 1A2, and 1B1', *Cancer Res*, 61(10), pp. 3919-3924.

Mann, D. A. and Smart, D. E. (2002) 'Transcriptional regulation of hepatic stellate cell activation', *Gut*, 50(6), pp. 891–896.

Martinez-Hernandez, A., Delgado, F. M. and Amenta, P. S. (1991) 'The extracellular matrix in hepatic regeneration. Localization of collagen types I, III, IV, laminin, and fibronectin', *Laboratory Ivestigation; A Journal of Technical Methods and Pathology*, 64(2), p. 157—166.

Meyer, B. K. *et al.* (1998) 'Hepatitis B virus X-associated protein 2 is a subunit of the unliganded aryl hydrocarbon receptor core complex and exhibits transcriptional enhancer activity', *Molecular and Cellular Biology*, 18(2), pp. 978–988.

Van Miller, J. P., Lalich, J. J. and Allen, J. R. (1977) 'Increased incidence of neoplasms in rats exposed to low levels of 2,3,7,8-tetrachlorodibenzo-p-dioxin', *Chemosphere*, 9(1), pp. 537–544.

Mimura, J. *et al.* (1999) 'Identification of a novel mechanism of regulation of Ah (dioxin) receptor function', *Genes & Development*, 13(1), pp. 20–25.

Mitchell, K. A. *et al.* (2006) 'Sustained aryl hydrocarbon receptor activity attenuates liver regeneration', *Molecular Pharmacology*, 70(1), pp. 163–170.

Nagy, S. R. *et al.* (2002) 'Development of a green fluorescent protein-based cell bioassay for the rapid and inexpensive detection and characterization of Ah receptor agonists', *Toxicological Sciences*, 65(2), pp. 200–210.

Naito, M. *et al.* (2004) 'Differentiation and function of Kupffer cells', *Medical Electron Microscopy*, 37(1), pp. 16–28.

National Toxicology Program (1982) *Technical Report Series*, 209, pp. 1-49.

Nault, R. *et al.* (2016) 'Dose-dependent metabolic reprogramming and differential gene expression in TCDD-elicited hepatic fibrosis', *Toxicological Sciences*, 154(2), pp. 253–266.

Nebert, D. W., Puga, A. and Vasiliou, V. (1993) 'Role of the Ah receptor and the dioxin-inducible [Ah] gene battery in toxicity, cancer, and signal transduction', *Annals of the New York Academy of Sciences*, 685, pp. 624–640.

Norona, L. M. *et al.* (2019) 'Bioprinted liver provides early insight into the role of Kupffer cells in TGF-β1 and methotrexate-induced fibrogenesis', *PLoS ONE*, 14(1), pp. 1–19.

Ohtake, F. *et al.* (2007) 'Dioxin receptor is a ligand-dependent E3 ubiquitin ligase', *Nature letters*, 446, pp. 562–566.

Olivero-Verbel, J., Roth, R. A. and Ganey, P. E. (2011) 'Dioxin alters inflammatory responses to lipopolysaccharide', *Toxicological and Environmental Chemistry*, 93(6), pp. 1180–1194.

Ozeki, J. *et al.* (2011) 'Aryl hydrocarbon receptor ligand 2,3,7,8-tetrachlorodibenzo-p-dioxin enhances liver damage in bile duct-ligated mice', *Toxicology*, 280, pp. 10–17.

Pavuk, M., Michalek, J. E. and Ketchum, N. S. (2006) 'Prostate cancer in US air force veterans of the Vietnam war', *Journal of Exposure Science and Environmental Epidemiology*, 16(2), pp. 184–190.

Pelclova, D. *et al.* (2006) 'Adverse health effects in humans exposed to 2,3,7,8-tetrachlorodibenzo-p-dioxin (TCDD)', *Reviews on Environmental Health*, 21(2), pp. 119–138.

Peterson, T. C. *et al.* (2000) 'Hepatic fibrosis and cytochrome P450: experimental models of fibrosis compared to AHR knockout mice', *Hepatology Research*, 17(2), pp. 112–125.

Pierre, S. *et al.* (2014) 'Aryl hydrocarbon receptor-dependent induction of liver fibrosis by dioxin', *Toxicological Sciences*, 137(1), pp. 114–124.

Pitot, H. C. *et al.* (1980) 'Quantitative evaluation of the promotion by 2,3,7,8-tetrachlorodibenzo-p-dioxin of hepatocarcinogenesis from diethylnitrosamine', *Cancer Research*, 40(10), pp. 3616–3620.

Pohjanvirta, R. *et al.* (1990) 'Effects of TCDD on vitamin A status and liver microsomal enzyme activities in a TCDD-susceptible and a TCDD-resistant rat strain', *Food and Chemical Toxicology*, 28(3), pp. 197–203.

Pohjanvirta, R. and Tuomisto, J. (1994) ‘Short-term toxicity of 2,3,7,8-tetrachlorodibenzo-p-dioxin in laboratory animals: effects, mechanisms, and animal models’, *Pharmacological Reviews*, 46(4), pp. 483–549.

Poland, A. and Glover, E. (1980) ‘2,3,7,8-Tetrachlorodibenzo-p-dioxin: Segregation of toxicity with the Ah locus’, *Molecular Pharmacology*, 17(1), pp. 86–94.

Poland, A. and Knutson, J. C. (1982) ‘2,3,7,8-tetrachlorodibenzo-p-dioxin and related halogenated aromatic hydrocarbons: examination of the mechanism of toxicity’, *Annual Review of Pharmacology and Toxicology*, 22(1), pp. 517–54.

Pollenz, R. S., Sattler, C. A. and Poland, A. (1994) ‘The aryl hydrocarbon receptor and aryl hydrocarbon receptor nuclear translocator protein show distinct subcellular localizations in Hepa 1c1c7 cells by immunofluorescence microscopy’, *Molecular Pharmacology*, 45, pp. 428–438.

Pongratz, I., Mason, G. G. F. and Poellinger, L. (1992) ‘Dual roles of the 90-kDa heat shock protein hsp90 in modulating functional activities of the dioxin receptor’, *The Journal of Biological Chemistry*, 267(19), pp. 13728–13734.

Probst, M. R. *et al.* (1993) ‘Role of the aryl hydrocarbon receptor nuclear translocator protein in aryl hydrocarbon (dioxin) receptor action’, *Molecular Pharmacology*, 44, pp. 511–518.

Puche, J. E., Saiman, Y. and Friedman, S. L. (2013) ‘Hepatic stellate cells and liver fibrosis’, *Comprehensive Physiology*, 3(4), pp. 1473–1492.

Puga, A. *et al.* (2000) ‘Aromatic hydrocarbon receptor interaction with the retinoblastoma protein potentiates repression of E2F-dependent transcription and cell cycle arrest’, *The Journal of Biological Chemistry*, 275(4), pp. 2943–2950.

Reggiani, G. (1980) ‘Acute human exposure to TCDD in Seveso, Italy’, *Journal of Toxicology and Environmental Health*, 6, pp. 27–43.

Remillard, R. B. J. and Bunce, N. J. (2002) ‘Linking dioxins to diabetes: epidemiology and biologic plausibility review of epidemiologic’, *Environmental Health Perspectives*, 110(9), pp. 853–858.

Robertson, L. W. *et al.* (2018) 'PCBs risk evaluation, environmental protection, and management: 50-year research and counting for elimination by 2028', *Environmental Science and Pollution Research*, 25(17), pp. 16269–16276.

Rowlands, J. C., Mcewan, L. J. and Gustafsson, J.-A. (1996) 'Trans-activation by the human aryl hydrocarbon receptor aryl hydrocarbon receptor nuclear translocator proteins: direct interactions with basal transcription factors', *Molecular Pharmacology*, 50, pp. 538–548.

Ryan, J. J., Gasiewicz, T. A. and Brown, J. F. (1990) 'Human body burden of polychlorinated dibenzofurans associated with toxicity based on the yusho and yucheng incidents', *Toxicological Sciences*, 15(4), pp. 722–731.

Safe, T. M. and Luebke, A. E. (2016) 'Prenatal low dosage dioxin (TCDD) exposure impairs cochlear function resulting in auditory neuropathy', *Hearing Research*, 331, pp. 7–12.

Schecter, A. *et al.* (2006) 'Dioxins: an overview and history', *Environmental Science and Technology*, 101(3), pp. 419–428.

Schmidt, J. V. *et al.* (1996) 'Characterization of a murine Ahr null allele: involvement of the Ah receptor in hepatic growth and development', *Proceedings of the National Academy of Sciences of the United States of America*, 93(13), pp. 6731–6736.

Seike, N., Kashiwagi, N. and Otani, T. (2007) 'PCDD/F contamination over time in Japanese paddy soils', *Environmental Science and Technology*, 41(7), pp. 2210–2215.

Seki, E. and Schwabe, R. F. (2015) 'Hepatic inflammation and fibrosis: functional links and key pathways', *Hepatology*, 61(3), pp. 1066–1079.

Senoo, H. (2004) 'Structure and function of hepatic stellate cells', *Medical Electron Microscopy*, 37, pp. 3–15.

Sinal, C. J. and Bend, J. R. (1997) 'Aryl hydrocarbon receptor-dependent induction of cyp1a1 by bilirubin in mouse hepatoma hepa 1c1c7 cells', *Molecular Pharmacology*, 52, pp. 590–599.

Song, J. *et al.* (2002) ‘A ligand for the aryl hydrocarbon receptor isolated from lung’, *Proceedings of the National Academy of Sciences of the United States of America*, 99(23), pp. 14694–14699.

Sorg, O. *et al.* (2009) ‘2,3,7,8-Tetrachlorodibenzo-p-dioxin (TCDD) poisoning in Victor Yushchenko: identification and measurement of TCDD metabolites’, *The Lancet*, 374(9696), pp. 1179–1185.

Suk, K. T. and Kim, D. J. (2015) ‘Staging of liver fibrosis or cirrhosis: the role of hepatic venous pressure gradient measurement’, *World Journal of Hepatology*, 7(3), pp. 607–615.

Swanson, H. I. and Yang, J. (1998) ‘The aryl hydrocarbon receptor interacts with transcription factor IIB’, *Molecular Pharmacology*, 54, pp. 671–677.

Tanos, R. *et al.* (2012) ‘Role of the Ah receptor in homeostatic control of fatty acid synthesis in the liver’, *Toxicological Sciences*, 129(2), pp. 372–379.

Thunberg, T. *et al.* (1980) ‘Effect of 2,3,7,8-tetrachlorodibenzo-p-dioxin on the hepatic storage of retinol in rats with different dietary supplies of vitamin A (Retinol)’, *Archives of Toxicology*, 45(4), pp. 273–285.

Tlustos, C. *et al.* (2011) ‘The dioxin contamination incident in Ireland, 2008: analytical results and congener patterns’, *Food Additives & Contaminants: Part A: Chemistry, Analysis, Control, Exposure & Risk Assessment*, 28(3), pp. 259–272.

Tritscher, A. M. *et al.* (1995) ‘Persistence of TCDD-induced hepatic cell proliferation and growth of enzyme altered foci after chronic exposure followed by cessation of treatment in DEN initiated female rats’, *Carcinogenesis*, 16(11), pp. 2807–2811.

Vos, J. G., Moore, J. A. and Zinkl, J. G. (1974) ‘Toxicity of 2,3,7,8-tetrachlorodibenzo-p-dioxin (TCDD) in C57B16 mice’, *Toxicology and Applied Pharmacology*, 29, pp. 229–241.

Walisser, J. A. *et al.* (2005) ‘Aryl hydrocarbon receptor-dependent liver development and hepatotoxicity are mediated by different cell types’, *Proceedings of the National Academy of Sciences of the United States of America*, 102(49), pp. 17858–17863.

Wang, S. and Hankinson, O. (2002) 'Functional involvement of the Brahma/SWI2-related gene 1 protein in cytochrome P4501A1 transcription mediated by the aryl hydrocarbon receptor complex', *The Journal of Biological Chemistry*, 277(14), pp. 11821–11827.

Wells, R. G. (2008) 'Cellular sources of extracellular matrix in hepatic fibrosis', *Clinics in Liver Disease*, 12(4), pp. 1–10.

Wilhelmsson, A. *et al.* (1990) 'The specific DNA binding activity of the dioxin receptor is modulated by the 90 kd heat shock protein.', *The EMBO journal*, 9(1), pp. 69–76.

Wilson, S. R., Joshi, A. D. and Elferink, C. J. (2013) 'The tumor suppressor Kruppel-like factor 6 is a novel aryl hydrocarbon receptor DNA binding partner', *Journal of Pharmacology and Experimental Therapeutics*, 345(3), pp. 419–429.

Wobser, H. *et al.* (2009) 'Lipid accumulation in hepatocytes induces fibrogenic activation of hepatic stellate cells', *Cell Research*, 19(8), pp. 996–1005.

Wong, F. W. Y., Chan, W. Y. and Lee, S. S. T. (1998) 'Resistance to carbon tetrachloride-induced hepatotoxicity in mice which lack CYP2E1 expression', *Toxicology and Applied Pharmacology*, 153(1), pp. 109–118.

World Health Organization (WHO) (2010) 'Exposure to dioxins and dioxin-like substances: a major public health concern', *Preventing Disease Through Healthy Environments.*

Wynn, T. (2008) 'Cellular and molecular mechanisms of renal fibrosis', *Journal of Pathology*, 214(2), pp. 199–210.

Yan, J. *et al.* (2019) 'Aryl hydrocarbon receptor signaling prevents activation of hepatic stellate cells and liver fibrogenesis in mice', *Gastroenterology*, 157(3), pp. 793–806.

Yu, C. *et al.* (2002) 'Increased carbon tetrachloride-induced liver injury and fibrosis in FGFR4-deficient mice', *American Journal of Pathology*, 161(6), pp. 2003–2010.

Z, L. (2018) ‘Release of dioxins from solid waste burning and its impacts on urban human population-a review’, *Journal of Pollution Effects & Control*, 06(01), pp. 1–6.

CHAPTER TWO: CHRONIC TCDD TREATMENT INCREASES LIVER MYOFIBROBLAST ACTIVATION THROUGH AHR SIGNALING IN HEPATOCYTES

Abstract

Liver fibrosis is a pathological condition characterized by the excessive deposition of collagen by activated hepatic stellate cells (HSCs). We previously reported that exposure to the high-affinity aryl hydrocarbon receptor (AhR) ligand 2,3,7,8-tetrachlorodibenzo-*p*-dioxin (TCDD) increases HSC activation *in vitro*, raising the possibility that TCDD directly targets HSCs. However, few studies have specifically examined AhR signaling during HSC activation. Furthermore, the development of liver fibrosis *in vivo* depends on complex interactions between multiple types of *cells*, including parenchymal hepatocytes, infiltrating immune cells, as well as HSCs. Recent reports indicate that chronic exposure of mice to TCDD elicits liver fibrosis with concomitant changes observed in hepatocyte metabolism, inflammatory cytokine production, HSC activation, and ECM deposition. The goal of this project was to use mice with AhR-deficient hepatocytes ($AhR^{\Delta Hep}$) or AhR-deficient HSCs ($AhR^{\Delta HSC}$) to determine how AhR activity in these cell populations impacts liver injury, inflammation, HSC activation, and collagen deposition during TCDD-induced liver fibrosis. Control are referred as $AhR^{fl/fl}$ mice. To induce liver fibrosis, mice were gavaged with TCDD (100 µg/kg) or peanut oil (vehicle) every four days for 92 days. Based on serum levels of alanine aminotransferase, this dose of TCDD produced minimal hepatocyte necrosis that

was consistent across all backgrounds. Exposure to TCDD induced marked hepatic steatosis in $AhR^{fl/fl}$ mice and $AhR^{\Delta HSC}$ mice, but not in $AhR^{\Delta Hep}$ mice, indicating that hepatocyte AhR signaling mediated TCDD-induced steatosis. TCDD treatment increased inflammatory cell infiltration in the liver of all mouse genotypes. In $AhR^{fl/fl}$ mice, TCDD increased expression of the HSC activation markers *Col1a1, Timp1,* and *Col3a1*. TCDD produced a similar effect in $AhR^{\Delta HSC}$ mice but failed to elicit HSC activation in $AhR^{\Delta Hep}$ mice. Increased collagen mRNA expression was not consistent with collagen protein expression, with all mouse genotypes possessing low hepatic collagen protein, indicating the possibility of TCDD-induced ECM turnover through a mechanism that does not depend on AhR signaling in hepatocytes or HSCs. We conclude that chronic TCDD exposure increases HSC activation indirectly through a mechanism that requires AhR signaling in hepatocytes. It is possible that hepatic steatosis contributes to HSC activation in TCDD-treated mice, whereas hepatocyte necrosis and hepatic inflammation do not appear to play a major role.

Introduction

The aryl hydrocarbon receptor (AhR) is a ligand-activated transcription factor that belongs to the basic helix-loop-helix Per/ARNT/Sim family of proteins (Hankinson, 1995). The AhR is well studied for mediating the toxicity of numerous environmental contaminants, including 2,3,7,8-tetrachlorodibenzo-*p*-dioxin (TCDD) (Fernandez-Salguero *et al.*, 1996). Upon ligand binding, the cytoplasmic AhR translocates to the nucleus, where it heterodimerizes with the AhR nuclear translocator (ARNT) and binds to conserved DNA sequences, which include a classical xenobiotic response element (XRE), as well as a recently identified non-consensus XRE, to modulate the expression of target genes (Huang and Elferink, 2012).

It is well established that TCDD toxicity is AhR-dependent, yet, at the organism level, mechanisms of toxicity are poorly understood (Fernandez-Salguero *et al.*, 1996). For example, transcriptome-wide studies revealed that exposure to TCDD upregulates the expression of numerous genes that do not contain XREs (Huang and Elferink, 2012). At the molecular level, increased gene transcription of non-XRE-containing genes could potentially be explained by TCDD/AhR-mediated epigenetic modifications and/or the recruitment of alternative cofactors to the AhR/ARNT complex (Patrizi and de Cumis, 2018). However, at the tissue or organ level, it is likely that increased expression of non-XRE-containing genes at least partially reflects a compensatory response of various cell populations to TCDD-induced tissue injury or dysfunction. Because the AhR is widely expressed across all cell types, it has been difficult to distinguish between the direct cellular effects of TCDD and the indirect effects that occur due to compensatory cellular responses within the same tissue.

Liver fibrosis is a pathological condition in which chronic injury and/or unresolved inflammation drive the excessive deposition of extracellular matrix (ECM) proteins by hepatic stellate cells (HSCs) (reviewed in Wynn, 2008). In the healthy liver, HSCs are quiescent and function in the storage of vitamin A. However, upon liver injury, these cells become activated and assume a myofibroblast-like phenotype characterized by retinoid loss, increased proliferation, contractility, and fibrogenesis. In 2014, Pierre et al. reported that chronic exposure of mice to TCDD produced liver fibrosis (Pierre, Chevallier, Teixeira-clerc, *et al.*, 2014). Exposure to TCDD for two weeks increased expression of genes encoding HSC activation markers and inflammatory cytokines. Histological features of fibrosis were observed after six weeks of TCDD treatment. These effects were AhR-dependent, as they were not observed in AhR knockout mice treated with TCDD. In mice, a single bolus of TCDD has been shown to produce hepatic steatosis and immune cell infiltration (Boverhof *et al.*, 2005). It has been proposed that repeated TCDD treatment promotes the progression of steatosis to steatohepatitis with fibrosis, resulting in a condition similar to non-alcoholic fatty liver disease (NAFLD) seen in humans (Pierre, Chevallier, Teixeira-clerc, *et al.*, 2014; Fader *et al.*, 2015). In support of this, Fader et al. demonstrated that treatment of mice with TCDD every 4 days for 28 days dose-dependently altered expression of genes associated with hepatic lipid metabolism, increased the accumulation of fat droplets within the liver, and increased the number of $F4/80^{+}$ cells (macrophages) in the liver (Fader *et al.*, 2015). Nault et al. extended this study to show that treatment of mice with TCDD for 92 days not only increased hepatic fat accumulation and inflammation, but also produced hepatic collagen deposition and differential expression of matrisome genes consistent with HSC activation

(Nault *et al.*, 2016). Furthermore, fibrosis development correlated with the reorganization of metabolic activities in hepatocytes, including the redirection of glycogen, ascorbic acid, and proline metabolism to support ECM remodeling.

The development of liver fibrosis is a complex phenomenon that involves many pathways and cell types. Initial damage to hepatocytes and/or cholangiocytes initiates the infiltration of immune cells to the liver. Persistent inflammation triggers profibrotic signaling that further increases inflammation and elicits HSC activation, resulting in the deposition of ECM proteins, including collagen. It is well known that the liver is a target organ for TCDD toxicity, with endpoints that include hepatomegaly, moderate elevation in serum alanine aminotransferase (ALT) levels, and modest periportal inflammation. Studies using mice with hepatocyte-specific deletion of the AhR demonstrate that each of these endpoints of TCDD toxicity requires a functional AhR in hepatocytes (Walisser *et al.*, 2005). Although parenchymal hepatocytes comprise ~80% of the cells in the liver, the AhR is expressed in all liver cell populations, including the remaining non-parenchymal cells, which are comprised of HSCs, sinusoidal endothelial cells, cholangiocytes, and resident macrophages (Kupffer cells). In mice with the hepatocyte-specific AhR knockout, TCDD treatment still induced the expression of the classic AhR-regulated genes, *Cyp1a1* and *Cyp1b1*, and this was attributed to AhR signaling in non-parenchymal cell populations (Walisser *et al.*, 2005). However, less is known regarding the effects of TCDD on these cell populations.

It is possible that HSCs are direct cellular targets for TCDD during the development of liver fibrosis. It has been reported that HSC express a functional AhR and that the half-life of TCDD in HSCs is 52 days (compared to 13 days in hepatocytes)

(Håkansson and Hanberg, 1989). However, studies with isolated rat HSCs found that a single dose of TCDD had no effect on expression of the HSC activation marker, alpha-smooth muscle actin (αSMA) (Hanberg, Kling and Hakansson, 1996). In contrast, we previously found TCDD treatment increased proliferation and αSMA expression in a human HSC line, LX-2 (Harvey *et al.*, 2016). Interestingly, under typical cell culture conditions, LX-2 cells exist in a quasi-activated state. It is possible that a single dose of TCDD is not sufficient for increasing the activation of freshly isolated, quiescent HSCs (Hanberg, Kling and Hakansson, 1996), but that it was sufficient for increasing endpoints of activation in cells that were at least partially activated (Harvey et al., 2016). Thus, it is possible that TCDD treatment could directly activate HSCs.

It is also possible that TCDD could activate HSCs and subsequently elicit fibrosis by enhancing injury and inflammation. In fact, liver damage, inflammation, steatosis, and increased mechanotension by cross-linking of ECM proteins are considered triggers for HSC activation. One report suggests that the engulfment of hepatocyte apoptotic bodies by HSCs can promote HSC activation (Canbay *et al.*, 2003). This can occur when the apoptotic bodies are engulfed by Kupffer cells, which induces the release of profibrogenic mediators and pro-inflammatory cytokines (Canbay *et al.*, 2003b). Inflammatory cells drive HSC activation through the release of reactive oxygen species (ROS) and profibrogenic mediators (Canbay, Friedman and Gores, 2004; Li *et al.*, 2008; Lee and Friedman, 2011). Inflammatory cells, such as lymphocytes and neutrophils, can also activate HSCs by inducing lipid peroxidation (Casini *et al.*, 1997). Thus, Kupffer cells play a large role in HSC activation by inducing ROS production, cytokine release,

and profibrogenic stimulation (Naito *et al.*, 2004; Kolios, Valatas and Kouroumalis, 2006).

The goal of this study was to investigate the cell-specific role of AhR activation during the development of liver fibrosis. We used Cre-Lox technology to generate mice with a hepatocyte-specific or HSC-specific AhR knockout to determine the respective contributions of hepatocyte damage, steatosis, inflammation on HSC activation and the development of liver fibrosis.

Materials and Methods

Generation of Mice with AhR-Deficient Hepatocytes or AhR-Deficient HSCs

Mice expressing the floxed AhR gene ($Ahr^{tm3.1Bra}$/J, The Jackson Laboratory, Bar Harbor, ME), referred to as $AhR^{fl/fl}$, were crossbred to produce male $AhR^{fl/fl}$ mice. For hepatocyte-specific AhR knockout mice, referred to as $AhR^{\Delta Hep}$ mice, female mice that expressed the Cre recombinase transgene under the albumin reporter (Alb-Cre mice) (B6N.Cg-Speer6-ps1$^{Tg(Alb\text{-}Cre)21Mgn}$/J, The Jackson Laboratory) were bred to male $AhR^{fl/fl}$ mice to produce $AhR^{fl;Alb\text{-}Cre}$ offspring. $AhR^{fl;Alb\text{-}Cre}$ female mice were then bred to $AhR^{fl/fl}$ male mice to generate mice that were $AhR^{fl/fl}$ and hemizygous for Alb-Cre. $AhR^{fl/fl}$ mice and wild-type Alb-Cre were used as controls.

Similarly, to generate mice with an HSC-specific AhR knockout, referred to as $AhR^{\Delta HSC}$ mice, we used female mice that expressed Cre recombinase under control of the human glial fibrillary acidic protein (GFAP) promoter (referred to as GFAP-Cre) (FVB-Tg(GFAP-cre)25Mes/J, The Jackson Laboratory). These mice were crossbred with male $AhR^{fl/fl}$ mice to produce $AhR^{fl;\ GFAP\text{-}Cre}$ offspring. $AhR^{fl;\ GFAP\text{-}Cre}$ female mice were then bred with $AhR^{fl/fl}$ male mice to generate $AhR^{fl/fl}$ mice that were heterozygous for GFAP-

Cre. Several reports suggest that GFAP-Cre specifically target HSCs (Kocabayoglu *et al.*, 2016; Ceni *et al.*, 2017; Alsamman *et al.*, 2018).

Animal Treatment

TCDD (98% pure; Cambridge Isotope Laboratories, Andover, MA) was dissolved in anisole and diluted in peanut oil to create a working stock of 10 µg/mL. Mice were gavaged with either 100 µg/kg TCDD diluted in peanut oil or with peanut oil alone (referred to as "Vehicle") every 4 days for 92 days. At the end of the study, mice were euthanized, and sera and liver tissue were collected (Figure 2.1). Liver was either flash-frozen in liquid nitrogen or fixed in UltraLight Zinc Formalin Fixative (PSL Equipment, Vista, CA). Flash-frozen tissue and sera were stored at -80°C until assayed. For each treatment group, 8-11 mice were used. Mice were housed in microisolator cages with a 12:12 hour light/dark cycle. Food and water were available ad libitum. Bodyweight was monitored and recorded every 4 days, and liver weight was measured immediately after euthanasia. All protocols and experiments were approved by the Institutional Animal Care and Use Committee at Boise State University.

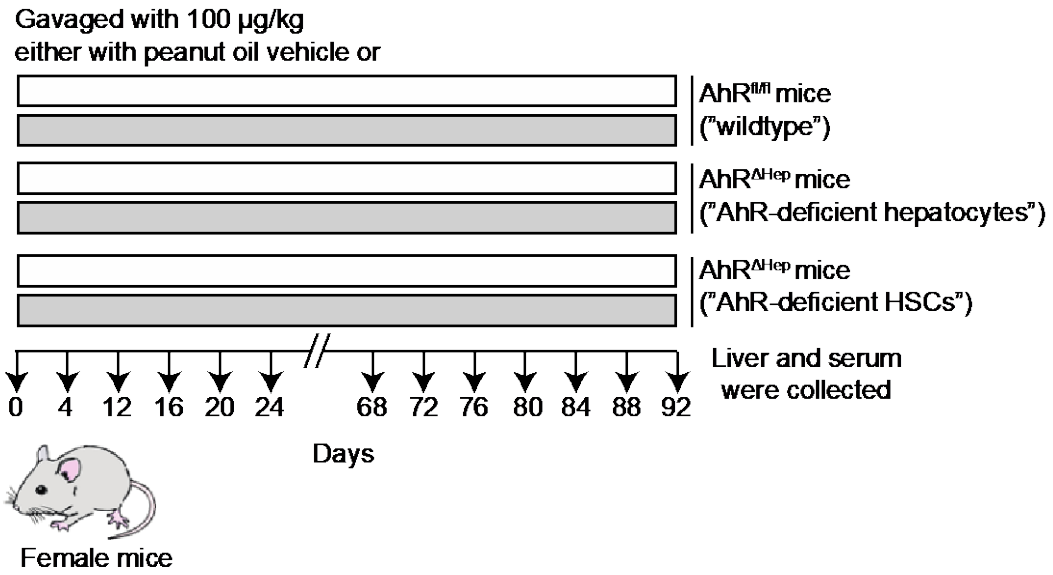

Figure 2.1 Mouse Treatment Schedule

Female mice were used at 8-9 weeks of age. Mice were on one of three different genetic backgrounds: $AhR^{fl/fl}$ (control); $AhR^{\Delta Hep}$ (hepatocyte-specific AhR knockout); $AhR^{\Delta HSC}$ (HSC-specific AhR knockout). Mice were gavaged with 100 µg/kg TCDD (gray) or vehicle (white) every four days for 92 days and then euthanized. Eight to 11 mice were used in each treatment group.

Serum Alanine Aminotransferase (ALT) Assay

Alanine aminotransferase (ALT) is a hepatocyte-specific enzyme that is released into the blood upon injury. To measure serum ALT levels, we used an Infinity^{TM} ALT (GPT) (Thermo Fisher Scientific, Waltham, MA) according to the manufacturer's protocol. Sera was diluted 1:5 in PBS, and samples were run in duplicates.

Inflammatory Cell Infiltration Staining

Liver sections (5-µm thick) were stained with hematoxylin and eosin (H&E) to measure inflammatory cell infiltration as described elsewhere (Junqueira, Bignolas and Brentani, 1979). Stained tissues were imaged using a compound microscope (Olympus BX53). For densitometry, the pixel content of the outlined regions in five fields per

mouse was quantified using ImageJ software (US National Institutes of Health) and expressed as a percentage of total pixels.

Collagen Staining

Liver sections were stained with Sirius Red to visualize collagen as described elsewhere (Junqueira, Bignolas and Brentani, 1979). The slides were imaged using a compound microscope (Olympus BX53). For densitometry, the pixel content of the red in five separate fields per mouse was quantified using ImageJ software and expressed as a percentage of total pixels.

Lipid Staining

Frozen liver tissues were embedded in optimal cutting temperature (OCT) reagent, and 10-µm sections were cut using a Cryostat Leica CM1950. Sections were mounted on glass slides. Slides were incubated in 100% propylene glycol for 2 min and stained with 0.7% Oil Red O (Alfa Aesar, Tewksbury, MA) solution dissolved in 100% propylene glycol for 15 min. The slides were then rinsed with distilled water and incubated with 85% propylene glycol for 1 min. Excess Oil Red O/ propylene glycol was removed by rinsing with distilled water. Tissues were then counterstained with Mayer's hematoxylin Gill No. 3 (Sigma-Aldrich, St. Louis, MO) for 1 min. Slides were imaged using a compound microscope (Olympus BX53). The pixel content of the red regions in five separate fields per mouse was counted using Image software and expressed as a percentage of total pixels.

Measurement of mRNA Expression by Quantitative Real-Time PCR (qRT-PCR)

mRNA was extracted from 10 mg of frozen liver tissue using the E.Z.N.A.® Total RNA Kit (Omega Bio-Tek, Norcross, GA). RNA purity was assessed using a

Nanodrop (Thermo Fisher Scientific, Waltham, MA). mRNA was reverse transcribed using a commercially available High-Capacity cDNA Reverse Transcription Kit (Thermo Fisher Scientific, Waltham, MA). cDNA was then amplified using gene-specific primers (Table 3.1) and Roche FastStart essential DNA green master reaction mix. Amplification was performed using a LightCycler® 96 Thermocycler (Roche, Indianapolis, IN). Samples were run in duplicate, and 8-11 samples were used in each treatment group. Gene expression was normalized to GAPDH, and the relative expression was estimated using the ΔΔCq method (Livak and Schmittgen, 2001). mRNA levels are expressed as fold-change (mean ± SEM) relative to vehicle-treated $AhR^{fl/fl}$ mice.

Table 2.1 Primer Sequences

Gene	Primer Sequence (5'to 3')	Temp. (°C)
Acta2	TCC TCC CTG GAG AAG AGC TAC TAT AGG TGG TTT CGT GGA TGC	60
Ccl2	ACT GAA GCC AGC TCT CTC TTC CTC TTC CTT CTT GGG GTC AGC ACA GAC	60
Col1a1	GTC CCT GAA GTC AGC TGC ATA TGG GAC AGT CCA GTT CTT CAT	60
Col3a1	CCT GGT GGA AAG GGT GAA AT CGT GTT CCG GGT ATA CCA TTA G	62
Cyp1a1	GCC TTC ATT CTG GAG ACC TTC C CAA TGG TCT CTC CGA TGC	60
Fgf21	CCG CAG TCC AGA AAG TCT CC CTG CAG GCC TCA GGA TCA AA	62
Gapdh	CAA TGA CCC CTT CAT TGA CC GAT CTC GCT CCT GGA AGA TG	60
Mmp13	GCC CTG GGA AGG AGA GAC TCC AGG GGA TTC CCG CAA GAG TCG CAG G	60
Timp1	CAC GGG CCG CCT AAG GAA CG GGT CAT CGG GCC CCA AGG GA	67
Tgfb1	TGC TAA TGG TGG ACC GCA A CAC TGC TTC CCG AAT GTC TGA	55

RNA-Sequencing and Data Analysis

mRNA extraction, library preparation, and sequencing were performed at the Novogene Corporation Inc. (Sacramento, CA). In brief, mRNA was isolated from 10 mg

of liver tissue using poly-T oligo-attached magnetic beads. RNA quality was determined using the Nano 6000 assay kit of the Bioanalyzer 2100 system (Agilent Technologies, CA, USA), and samples with an RNA integrity number (RIN) > 6.8 were used for library preparation. Transcriptome libraries were prepared using NEBNext® Ultra™ RNA Library Prep Kit for Illumina (Biolabs, Ipswich, MA), and quality was determined by Qubit2.0 and Agilent 2100. Finally, these libraries were sequenced on an Illumina Nova 6000 platform, and 150-bp paired-end reads were generated with a read depth of ~20M per sample. Raw data were analyzed for the Per base sequence quality (>30), Per sequence GC content, adapter (universal Illumina adapter), and adapter removal using FASTQC v0.11.9. Reads were mapped to the mouse reference genome (GRCm38 release 96) using HISAT2 v2.1.0 (Kim, Langmead and Salzberg, 2015). Aligned reads were counted using HTSeq v0.11.3 (Anders, Pyl and Huber, 2015). The obtained counts were analyzed for differential expression using the Median-Ratio-Normalization method (Maza *et al.*, 2013) with Deseq2 v1.22.2 (Love, Huber and Anders, 2014). Fold-change was calculated relative to counts in vehicle-treated $AhR^{fl/fl}$ mice. Gene expression was considered differentially expressed if the adjusted *p*-value was < 0.05. The enrichment analysis of the differentially expressed genes (DEGs) was performed in Cytoscape v3.7.0 using the ClueGov2.5.1 visualization tool.

Statistical Analysis

Statistical significance was determined based on a two-way ANOVA with Bonferroni testing ($p<0.05$) using GraphPad Prism 8.01 software (GraphPad Software, La Jolla, CA). Unless otherwise noted, data represent mean ± SEM. Means that do not share a letter are significantly different from each other.

Results

AhR Activity in $AhR^{\Delta Hep}$ Mice and $AhR^{\Delta HSC}$ Mice

To confirm the cell-specific knockout of AhR, we measured the hepatic mRNA expression of *Cyp1a1*, which encodes cytochrome P450 1A1, and *Cyp1b1*, which encodes cytochrome P450 1B1. *Cyp1a1* and *Cyp1b1* are AhR-regulated genes, and the expression of these genes is an accepted hallmark of AhR activation. In $AhR^{fl/fl}$ and $AhR^{\Delta HSC}$ mice, TCDD treatment significantly increased *Cyp1a1* mRNA expression (Figure 2.2 A). However, in $AhR^{\Delta Hep}$ mice, the TCDD-mediated induction of *Cyp1a1* was not statistically significant. Similarly, TCDD treatment significantly increased *Cyp1b1* mRNA expression in $AhR^{fl/fl}$ and $AhR^{\Delta HSC}$ mice but not in $AhR^{\Delta Hep}$ mice (Figure 2.2 B). Given that hepatocytes make up ~90% of the cells in the liver, it is not surprising that expression of Cyp1a1 and Cyp1b1 was markedly reduced in mice with the hepatocyte-specific AhR knockout. In the $AhR^{\Delta Hep}$ mice, the small TCDD-induced increase in *Cyp1a1* and *Cyp1b1* presumably reflects the contribution from non-parenchymal cells of the liver (Walisser *et al.*, 2005).

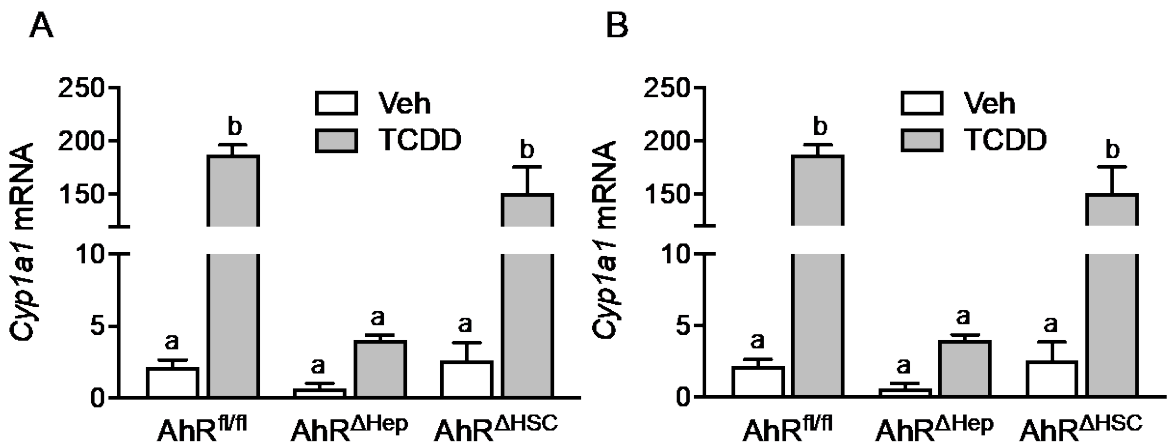

Figure 2.2 Assessing AhR Activity in AhR$^{\Delta Hep}$ Mice and AhR$^{\Delta HSC}$ Mice

Hepatic mRNA levels of *Cyp1a1* (A), and *Cyp1a1* (B) are expressed as fold-change (mean ± SEM) relative to vehicle-treated AhR$^{fl/fl}$ mice ($p < 0.05$). Means that do not share a letter are significantly different from each other ($p < 0.05$).

Hepatotoxic Effects of Mice Treated with TCDD

In order to evaluate the impact of TCDD-induced hepatotoxicity on HSC activation in our model system, we investigated gross markers of hepatotoxicity. In response to TCDD, all mice showed marked hepatomegaly, which was determined by the increase in the liver-to-body weight ratios (Figure 2.3A). Serum activity levels of alanine aminotransferase (ALT) were measured as a marker of hepatocellular necrosis. ALT is a liver-specific enzyme that catalyzes the synthesis of alanine from glutamate, released into the blood following liver injury, namely hepatocyte lysis. Chronic TCDD treatment produced minimal liver damage, regardless of AhR knockout (Figure 2.3B).

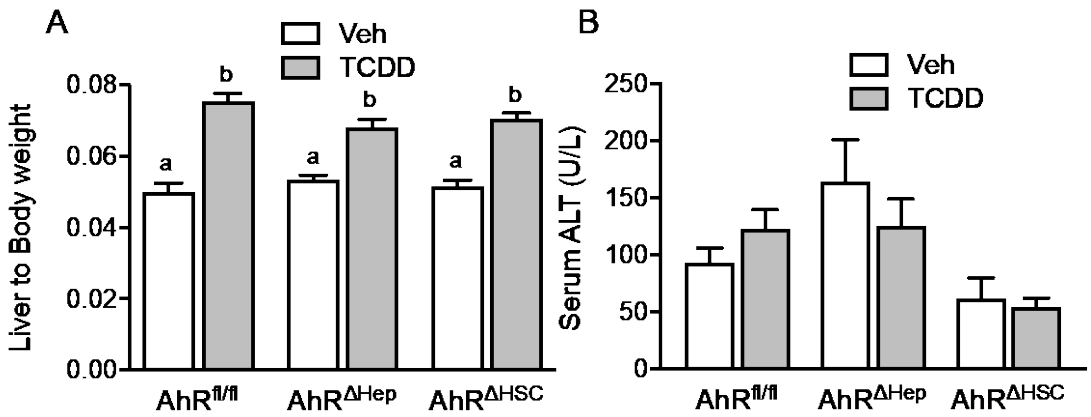

Figure 2.3 Hepatotoxic Effects of TCDD-Treated Mice

(A) Liver weight to body weight ratios after 92 days of treatment. (B) Data represent mean (± SEM) serum ALT levels. Means that do not share a letter are significantly different from each other ($p < 0.05$).

TCDD-Induced Inflammatory Cell Infiltration Occurs Independently of AhR Signaling in Hepatocytes and HSCs.

To identify the inflammatory cell infiltration, the liver tissues were stained with H&E. TCDD treatment increased inflammatory cell infiltration around the portal regions, regardless of AhR knockout (Figure 2.4A, B). We also quantified the mRNA levels of inflammation marker *Ccl2*, which encodes monocyte chemoattractant protein-1 (MCP-1). The TCDD-treated *Ccl2* mRNA expression in $AhR^{fl/fl}$ and $AhR^{\Delta Hep}$ mice reveals a relative increase compared to $AhR^{\Delta Hep}$ mice, when compared to vehicle-treated mice (Figure 2.4C).

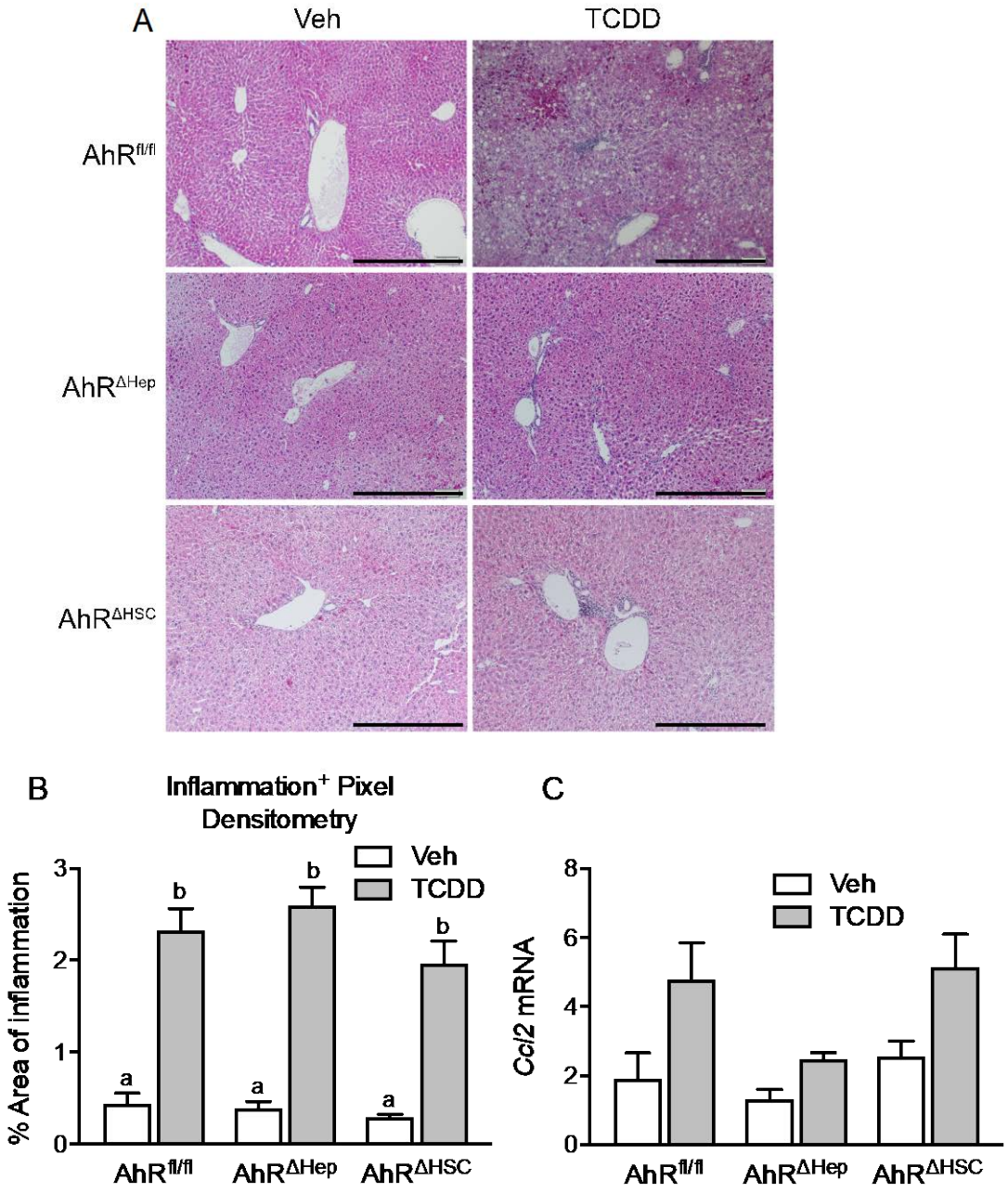

Figure 2.4 TCDD Treatment Induces Inflammation in the Livers of Both $AhR^{\Delta Hep}$ and $AhR^{fl/fl}$ Mice.

(A) H&E-stained liver tissue from vehicle- and TCDD-treated mice (100X magnification; scale bar = 500 µm). (B) Pixel content of the inflammatory regions was quantified in five fields per mouse and expressed as a percentage of total pixels. (C) Hepatic mRNA levels of *Ccl2* are expressed as fold-change (mean ± SEM) relative to vehicle-treated $AhR^{fl/fl}$ mice. Means that do not share a letter are significantly different from each other ($p < 0.05$).

TCDD Treatment Does Not Induce Lipid Deposition in the Livers of $AhR^{\Delta Hep}$ Mice.

It is well established that AhR activation causes spontaneous fatty liver (Fernandez-Salguero *et al.*, 1996). However, the cell-specific role of AhR remains largely unknown. To determine the cell-specific contribution of AhR signaling in mediating hepatic steatosis, which in turn can affect HSC activation, we measured the lipid deposition in the liver. TCDD treatment induced both macrosteatosis and microsteatosis in $AhR^{fl/fl}$ mice and $AhR^{\Delta HSC}$. In contrast, livers from the $AhR^{\Delta Hep}$ mice did not show any marked lipid accumulation upon TCDD treatment (Figure 2.5A). Quantification of lipid staining revealed a significant increase in Oil Red O-positive pixels in $AhR^{fl/fl}$ mice and $AhR^{\Delta HSC}$ mice, when compared to vehicle-treated mice. However, oil Red O staining was minimal in $AhR^{\Delta Hep}$ mice (Figure 2.5B). mRNA levels of *Fgf21*, which is a hepatokine that reflects liver fat accumulation (Rusli *et al.*, 2016), were significantly increased in TCDD-treated $AhR^{fl/fl}$ and $AhR^{\Delta HSC}$ mice but not in $AhR^{\Delta Hep}$ mice (Figure 2.5C). This supports the Oil Red O staining. Furthermore, to determine the cell-specific role of AhR in lipid metabolism, makers of lipid accumulation, fatty acid synthesis, and β-oxidation were assessed using RNA-seq (Figure 2.6). Results indicate that expression of the CD36 (*Cd36*) gene, which encodes a membrane protein capable of taking up circulating fatty acids (Abumrad *et al.*, 1993), was induced significantly following TCDD treatment in $AhR^{fl/fl}$ and $AhR^{\Delta HSC}$ mice but not in $AhR^{\Delta Hep}$ mice. Expression of fatty acid synthase (*Fasn*) and long-chain fatty acid ligase (*Acsl1*), both of which encode proteins crucial for fatty acid synthesis, were repressed in $AhR^{fl/fl}$ and $AhR^{\Delta HSC}$ mice treated with TCDD. Most genes pertaining to β-oxidation demonstrated at least a marginal repression in $AhR^{fl/fl}$ and $AhR^{\Delta HSC}$ mice, but not in $AhR^{\Delta Hep}$ mice following TCDD treatment.

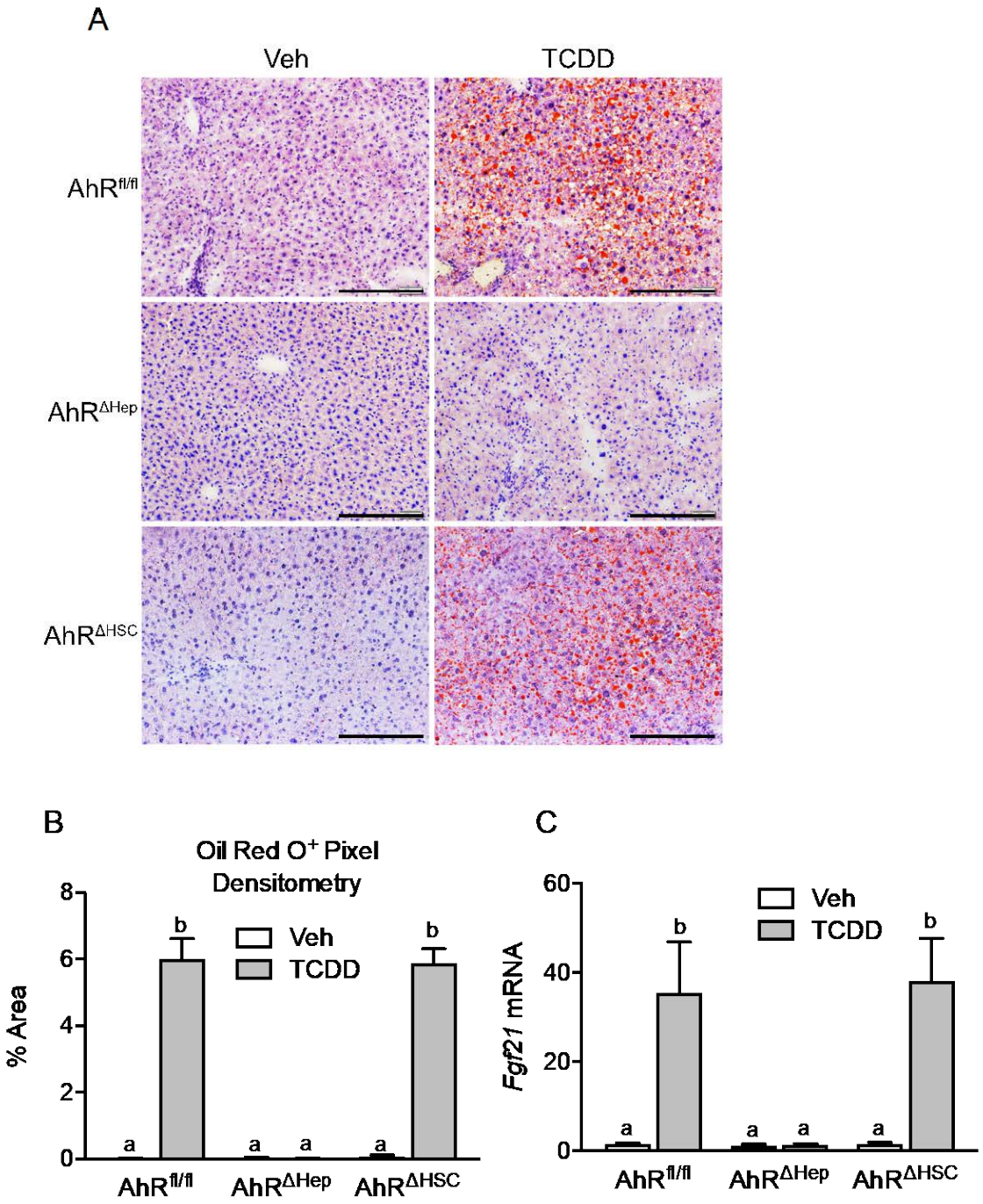

Figure 2.5 TCDD Treatment Does Not Induce Lipid Deposition in the Livers of $AhR^{\Delta Hep}$ mice.

A) Oil Red O stained liver tissue from TCDD-treated mice (200X magnification; scale bar = 200 µm). (B) The pixel content of the red regions was quantified in five fields per mouse and expressed as a percentage of total pixels. (C) Hepatic mRNA levels of *Fgf21* are expressed as fold-change (mean ± SEM) relative to vehicle-treated $AhR^{fl/fl}$ mice (n=8-11). Means that do not share a letter are significantly different from each other ($p < 0.05$).

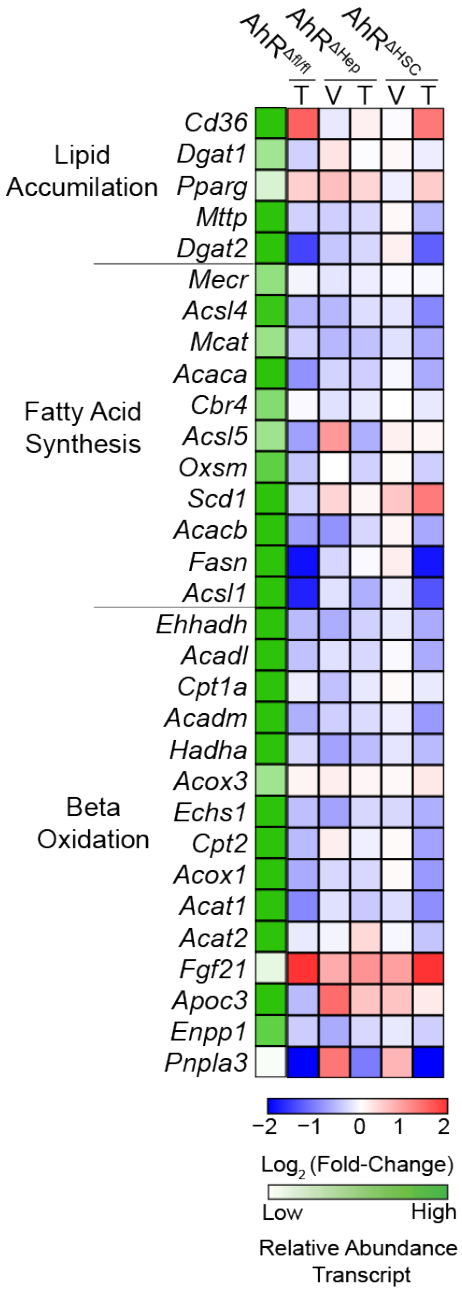

Figure 2.6 TCDD Treatment Modulated Genes Associated With Lipid Metabolism in AhR$^{\Delta Hep}$ mice.

RNA-seq was used to assess the expression of lipid accumulation, fatty acid synthesis, and beta-oxidation genes. Gene expression for all treatment groups was normalized to vehicle-treated AhR$^{fl/fl}$ mice. Blue tiles indicate repression, and red tiles indicate induction of gene expressions. Relative transcript abundance depicts the mean of the normalized transcript counts of all samples in each individual genes, normalizing for sequencing depth. Green tiles indicate a high (>1000) relative transcript abundance and white tiles indicate a low (<10) relative transcript abundance. The letters V and T represents Vehicle and TCDD treatments, respectively.

TCDD Treatment Increases HSC Activation Markers in the Livers of $AhR^{fl/fl}$ and $AhR^{\Delta HSC}$ Mice, But Not in $AhR^{\Delta Hep}$ Mice.

To determine how AhR ablation impacted HSC activation following chronic TCDD treatment, the expression of several HSC activation markers was investigated. The mRNA and protein levels of HSC activation marker, α-smooth muscle actin (αSMA) was measured by RT-qPCR and immunofluorescence staining. TCDD treatment elicited minimal changes in αSMA mRNA and protein levels (Supplementary Figure 2.1). Other markers of HSC activation, namely collagen type I (*Col1a1*), collagen type III (*Col3a1*), and tissue inhibitor of metalloproteinases-1 (*Timp1*), were assessed by RT-qPCR. *Col1a1*, *Col3a1,* and *Timp1* mRNA expression were significantly increased in TCDD-treated $AhR^{fl/fl}$ mice and $AhR^{\Delta HSC}$ mice, compared to vehicle-treated mice. However, in $AhR^{\Delta Hep}$ mice, the TCDD-induced increase was minimal for all three genes (Figure 2.7A, B, and C). HSC activation markers were also assessed using RNA-seq to determine the cell-specific effects of AhR knockout. Genes such as *Tgfb1*, and *Tgfb2* were unaffected by AhR knockout (Figure 2.7D).

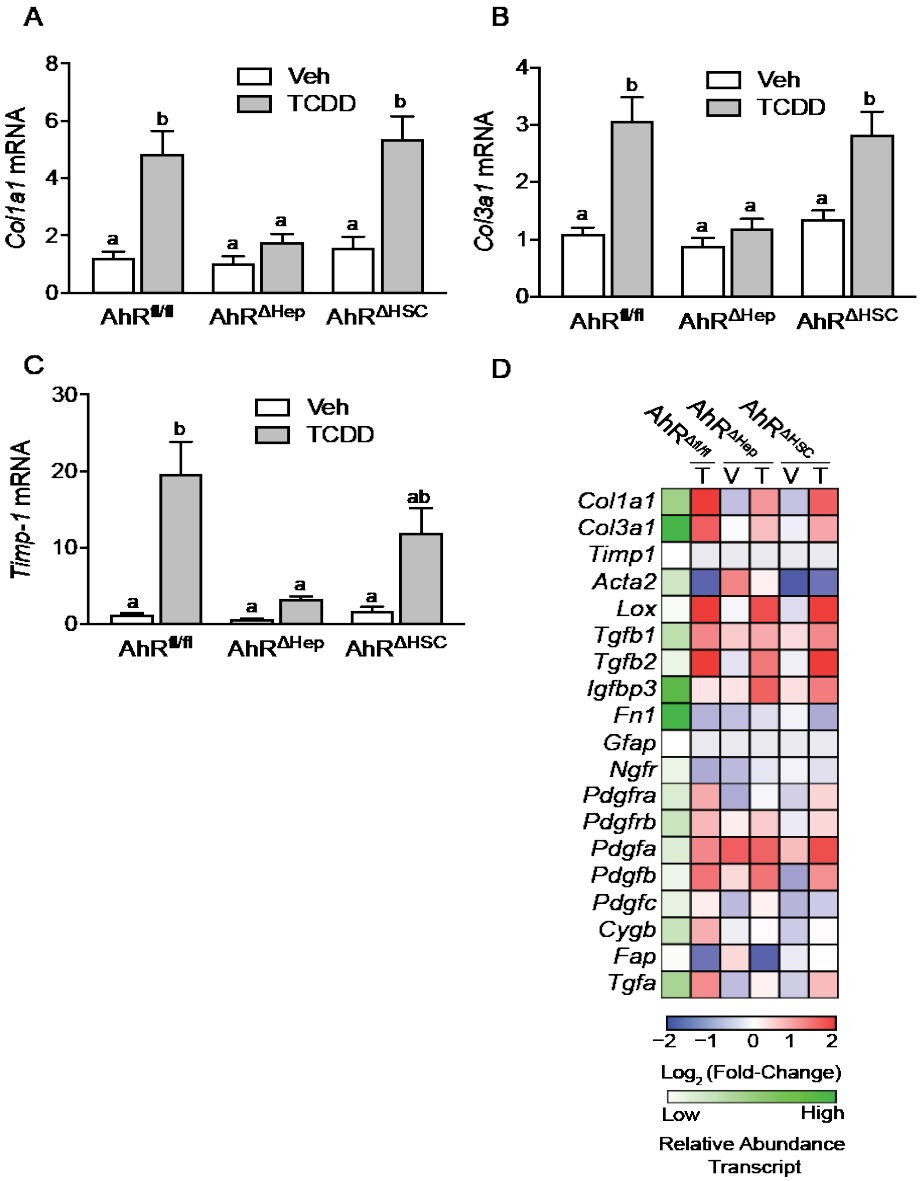

Figure 2.7 TCDD Increases HSC Activation Markers in AhR$^{fl/fl}$ Mice But Not in AhR$^{\Delta Hep}$ Mice.

(A-C) Hepatic mRNA levels of HSC activation markers *Col1a1*, *Timp-1*, and *Col3a1*. mRNA levels are expressed as fold-change (mean ± SEM) relative to vehicle-treated AhR$^{fl/fl}$ mice (n=8-11). Means that do not share a letter are significantly different from each other ($p < 0.05$). (D) RNA-seq was used to assess expression of HSC activation associated genes. Gene expression for all treatment groups was normalized to vehicle-treated AhR$^{fl/fl}$ mice. Blue tiles indicate repression, and red tiles indicate induction of gene expressions. Relative transcript abundance depicts the mean of the normalized transcript counts of all samples for each gene, normalizing for sequencing depth. Green tiles indicate a high (>1000) relative transcript abundance, and white tiles indicate a low (<10) relative transcript abundance. The letters V and T represent Vehicle and TCDD treatment, respectively.

TCDD Induced Collagen Expression and Modulated Extracellular Matrix Remodeling Genes Regardless of AhR-Knockout.

To visualize hepatic collagen content, liver tissues were stained with Sirius Red. This revealed that TCDD induced periportal fibrosis across all the groups regardless of AhR knockout (Figure 2.8A). However, the Sirius Red quantification revealed that the change across all the groups was minimal (Figure 2.8B). The minimal change may be attributed to the degradation of collagen fibers by matrix metalloproteases (MMPs). To investigate how TCDD impacts extracellular matrix remodeling genes in cell-specific knockout mice, we measured the mRNA expression of several genes by RT-qPCR and differential gene expression by RNA-sequencing. mRNA levels of *Tgfβ1* and *Mmp13* (which encodes matrix metallopeptidase 13) increased upon TCDD treatment regardless of AhR knockout (Figure 2.9A, B). The TCDD-induced expression of lysyl oxidase (*Lox*) mRNA was similar levels across all genotypes (Figure 2.9C).

The RNA-seq data revealed that *Col1a1, Col3a1, Col6a1, Col6a2*, and *Col6a3* expression was induced in $AhR^{fl/fl}$ and $AhR^{\Delta HSC}$ mice upon TCDD treatment (Figure 2.9D). In contrast, the increase in $AhR^{\Delta Hep}$ mice was minimal or absent upon TCDD treatment. TCDD also induced expression of *Mmp2, Mmp9, Mmp13,* and *Mmp14* genes, regardless of AhR knockout. TCDD increased mRNA expression of *Serpine1* (which encodes PAI-1), *Plat* (which encodes tissue plasminogen activator; tPA), and *Plau* (which encodes plasminogen activator, urokinase; uPA) in $AhR^{fl/fl}$ and $AhR^{\Delta HSC}$ mice but not in $AhR^{\Delta Hep}$ mice.

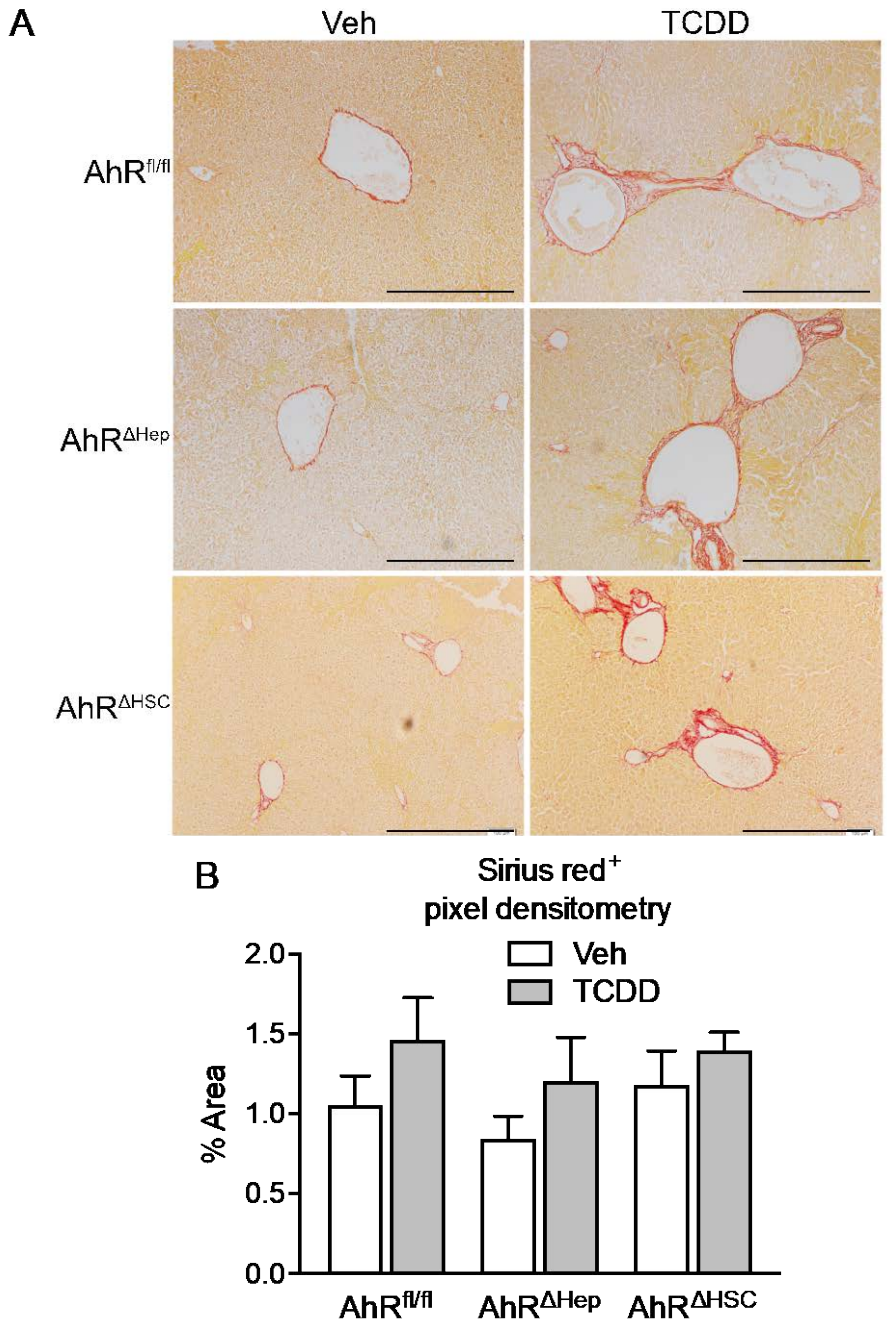

Figure 2.8 Chronic TCDD Treatment Induced Collagen Expression in the Liver Regardless of AhR-Knockout

(A) Sirius Red-stained liver tissue from vehicle- and TCDD-treated mice (100X magnification; scale bar = 500 µm). (B) Densitometry of Sirius Red-staining in five sections per mouse (8-11 mice per treatment group).

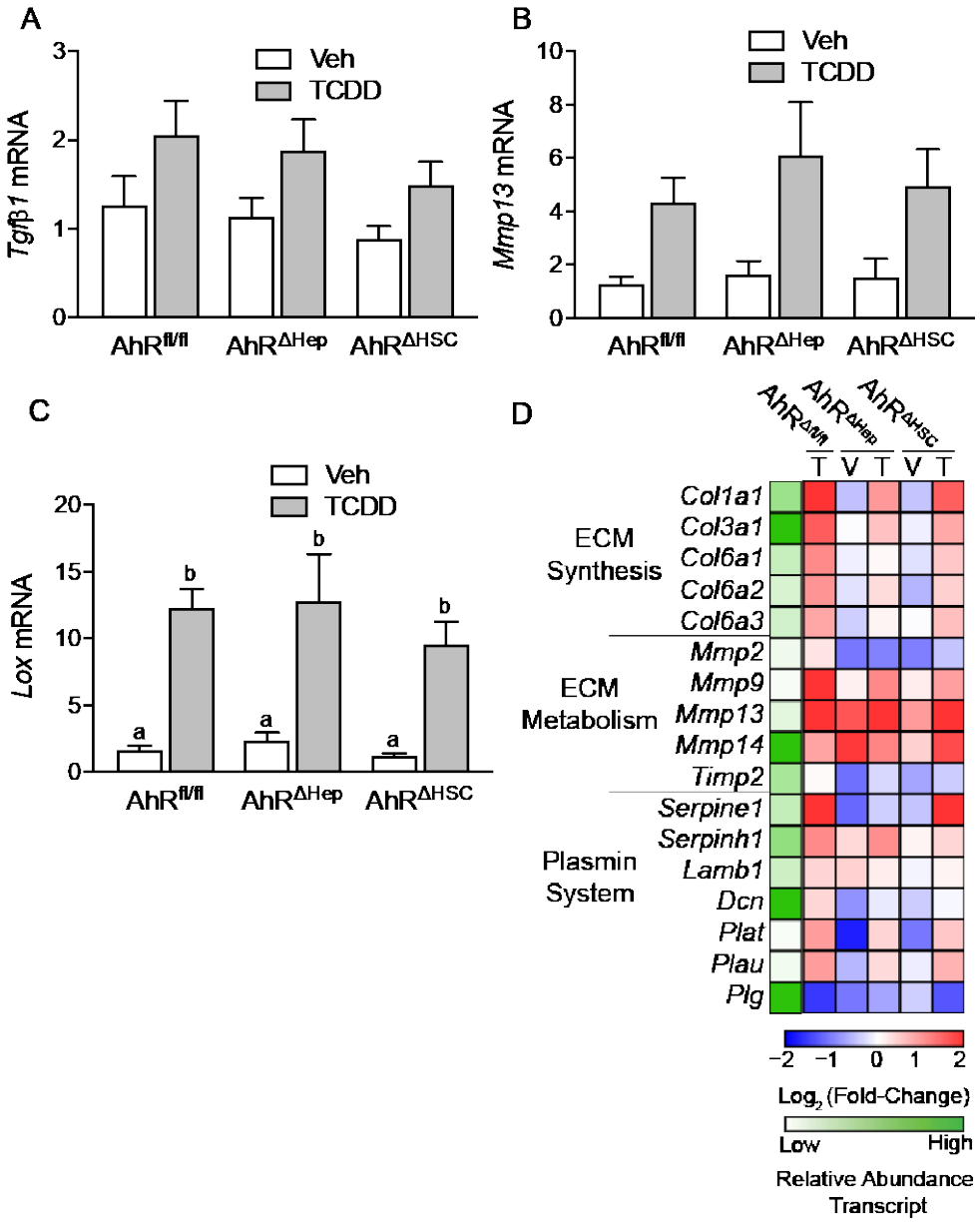

Figure 2.9 TCDD Treatment Modulated Expression of Extracellular Matrix Remodeling Genes Regardless of AhR-Knockout

(A-C) Hepatic mRNA levels of the pro-fibrogenic mediators *Tgfβ1*, *Mmp13*, and *Lox* are expressed as fold-change (mean ± SEM) relative to vehicle-treated $AhR^{fl/fl}$ mice (n=8-11). Means that do not share a letter are significantly different from each other ($p < 0.05$). (D) RNA-seq was used to assess the expression of ECM remodeling-related genes. Gene expression for all treatment groups was normalized to vehicle-treated $AhR^{fl/fl}$ mice. Blue tiles indicate repression of gene expression, and red tiles indicate the induction of gene expression. Relative transcript abundance represents the mean of the normalized transcript counts of all samples. Green tiles indicate a high (>1000) relative transcript abundance, and white tiles indicate a low (<10) relative transcript abundance. The letters V and T represent Vehicle and TCDD treatments, respectively.

Discussion

The present study investigated the cell-specific role of AhR signaling in hepatocytes and HSCs during liver injury, inflammation, and HSC activation incurred by chronic exposure to TCDD. To address the cell-specific contributions, we used mice in which the AhR was removed from either hepatocytes or from HSCs. A recent study has demonstrated that TCDD treatment increases HSC activation *in vitro* (Harvey *et al.*, 2016). This led us to speculate that chronic exposure to TCDD may also directly activate HSCs in the mouse liver.

No marked elevation in serum ALT levels was observed among treatment groups (Figure 2.3B), possibly due to the clearance of ALT by Kupffer cells, as the last dose of TCDD was given on day 88, and serum was collected on day 92 (Radi *et al.*, 2011). This was further supported by the fact that the half-life of ALT is 48 hours (Dufour *et al.*, 2000). This mild liver damage is consistent with previous reports in which mice were exposed to chronic TCDD treatment (Fernandez-Salguero *et al.*, 1996; Nault *et al.*, 2016). Overall, a more extensive liver damage would likely have been observed if mice had been treated with a higher dose of TCDD due to the fact that the mice used in our experiments contained the relatively insensitive 'd' allele of the AhR.

Our results indicate that chronic exposure to TCDD induced periportal fibrosis and inflammation, which is consistent with a previous report (Nault *et al.*, 2016). However, we observed a relatively mild induction of fibrosis, based on minimal distribution and intensity of Sirius red-stained fibers throughout the liver. It is possible that the dose selected for these experiments failed to elicit robust tissue injury, inflammation, and/or fibrogenesis. This was supported by the observation that no

treatment-related deaths were observed (data not shown), unlike other studies that reported having more than 50% of treatment-related deaths. Our findings indicate that TCDD-induced collagen-synthesis is dependent on AhR signaling in hepatocytes. Further, the repression of *Col6a2* and *Col6a3* mRNA expression in $AhR^{\Delta Hep}$ mice supports the fact that AhR signaling in hepatocytes is an absolute requirement for collagen gene expression.

We and others have previously shown that TCDD modulates expression of ECM remodeling genes in the liver (Andreasen et al., 2006; Pierre *et al.*, 2014; Lamb *et al.*, 2016). It is possible that chronic TCDD treatment enhances the turnover of collagen by enhancing collagenase activity, thereby limiting the accumulation of collagen. Our results indicate that the mRNA expression of matrix metalloproteinases, and genes in the plasminogen activator/plasmin system, which in turn regulate MMP activation, did not change much in cell-specific knockout mice. Interestingly, expression of the gene encoding PAI-1 (*Serpine1*), which is a negative regulator of MMP activity, was severely repressed in $AhR^{\Delta Hep}$ mice, but this did not correlate with reduced MMP expression.

In this study, ECM stiffness was not directly measured. Several studies have demonstrated the role of ECM stiffness in HSC activation during the development of liver fibrosis (Priya and Sudhakaran, 2008; Saneyasu, Akhtar and Sakai, 2016). The predominant ECM protein in fibrosis is collagen. A recent study reported that LOX depended on the mechanism of collagen cross-linking in liver fibrosis in carbon tetrachloride-treated mice (Liu *et al.*, 2016). Based on earlier studies, the mechanical tension can be generated as a result of inflammation (Liu *et al.*, 2016) or through a TGFβ1-mediated pathway. Both promote the covalent cross-linking by LOX for

stabilization of collagen (Van Der Slot *et al.*, 2005). Our results indicate that TCDD treatment produced a similar level of inflammatory cell infiltration and *Lox* and *Tgfb1* mRNA expression regardless of AhR knockdown. Hence, it can be predicted that hepatic stiffness would also be similar among genotypes.

Numerous HSC activation markers have been identified, some of which are induced while others are repressed. The expression of some HSC activation markers depends on the model system, and some of these activation markers could require secondary signals obtained through injury and inflammation. For instance, in the present study, although elevated *Acta2* mRNA and protein levels are considered hallmarks of HSC activation, TCDD did not elicit remarkable expression of this marker (Supplementary Fig. S2). It is possible that the dose selected in this study was not sufficient to induce a significant change in mRNA and protein expression. However, other reported activation markers such as type I collagen (*Col1a1*), tissue inhibitor of matrix metalloproteinase-1 (*Timp1*), and type III collagen (*Col3a1*) (Hemmann *et al.*, 2007; Mannaerts *et al.*, 2013) reveal that AhR signaling in hepatocytes is important for HSC activation during TCDD-induced liver fibrosis. Furthermore, RNA-seq did not identify any changes in gene expression that would explain decreased HSC activation in $AhR^{\Delta Hep}$ mice.

Our findings corroborate previous reports that activation of AhR by TCDD induces hepatic steatosis (Walisser *et al.*, 2005; Lee *et al.*, 2008; Xu *et al.*, 2016). In addition, our data suggest that AhR signaling in HSCs is not an absolute requirement for steatosis. The lack of steatosis observed in $AhR^{\Delta Hep}$ mice could indicate that steatosis contributes to HSC activation in this model system. The relationship between steatosis

and HSC activation is fairly well documented. For example, it has been reported that HSC activation correlates with steatosis during human liver fibrosis (Reeves *et al.*, 1996; Feldstein *et al.*, 2005). Another study reported that hepatic steatosis accelerates the activation and proliferation of HSCs through the activation of the phosphatidylinositol 3-kinase (PI-3-kinase) pathway (Wobser *et al.*, 2009), which is known to contribute to HSC proliferation and collagen secretion (Friedman, 2000). Furthermore, hepatic steatosis induces the expression of the profibrogenic genes TGF-β, tissue inhibitor of metallo-proteinase-1 (TIMP-1), TIMP-2, and matrix-metalloproteinase-2, as well as nuclear-factor kappaB-dependent expression of MCP-1 in HSCs, all leading to HSC activation (Wobser *et al.*, 2009). Increasing evidence suggests the association of hepatic steatosis and lipid peroxidation (Macdonald *et al.*, 2001) with mitochondrial abnormalities, which induce overproduction of reactive oxygen species, can activate HSCs (Caldwell *et al.*, 1999). Furthermore, Cyp2e1 expression was increased in NAFLD (Aubert *et al.*, 2011), which can activate HSCs and increase type I collagen secretion (Nieto *et al.*, 1999). Finally, *Fgf21*, a hepatokine and a potential plasma marker for NAFLD (Rusli *et al.*, 2016). During liver injury, FGF21 is produced from hepatocytes and HSCs and has been shown to directly induce HSC activation (Schumacher and Guo, 2016). It was reported that AhR signaling in hepatocytes attenuates FGF21 expression (Girer *et al.*, 2016). It is possible that the TCDD-induced *Fgf21* levels in our model system represent a secondary effect of steatosis. Hence, it can be predicted that decreased HSC activation in $AhR^{\Delta Hep}$ mice treated with TCDD could result from decreased lipid accumulation.

TCDD-mediated differential expression of lipid metabolism suggests that TCDD induces lipid accumulation and decreases β-oxidation in a hepatocyte-specific, AhR-

dependent manner. Genes pertaining to lipid accumulation (*Cd36, Dgat2*), de novo synthesis of fatty acids (*Fasn, Acsl1*), and β-oxidation of fatty acids (*Fgf21, Pnpla3*) were among the most induced genes. CD36 is a glycoprotein that facilitates membrane transport of fatty acids. It was previously shown that hepatocyte-specific disruption of CD36 attenuates fatty liver in the high-fat diet-fed mice (Wilson *et al.*, 2016). Our data support this finding. Interestingly, a decrease in *Dgat2* expression in $AhR^{\Delta Hep}$ mice, which largely determines hepatic de novo synthesis of triglycerides (Wurie, Buckett and Zammit, 2012), suggests that TCDD induces fatty acid accumulation and prevents triglyceride synthesis through a mechanism that relies on AhR signaling in hepatocytes. It can be speculated that TCDD decreases de novo synthesis of fatty acids through *Fasn* and *Acsl,* which are dependent on hepatocyte AhR signaling. Our data show that TCDD decreases gene expression for phospholipase 3 *(Pnpla3).* The deletion of the *Pnpla3* variant *Pnpla3 I148M* has been shown to increase hepatic steatosis (Wurie, Buckett and Zammit, 2012). In summary, increased steatosis is dependent on hepatocyte-specific AhR, which occurs mostly by elevation of *Cd36* and repression of *Pnpla3.*

In conclusion, results from this study indicate that chronic TCDD exposure indirectly increases HSC activation through a mechanism that requires AhR signaling in hepatocytes. It is possible that hepatic steatosis contributes to HSC activation in TCDD-treated mice, whereas hepatocyte necrosis and hepatic inflammation do not appear to play a major role, although the precise mechanism remains unclear. TCDD-induced synthesis and degradation of collagen in fibrosis are independent of AhR signaling in hepatocytes and HSCs. Collectively, results from this project imply that it may be more fruitful to strategically target AhR signaling in hepatocytes, instead of in HSCs directly, when

developing new therapeutic AhR ligands to modulate HSC activation and limit or reverse liver fibrosis.

Supplementary Data

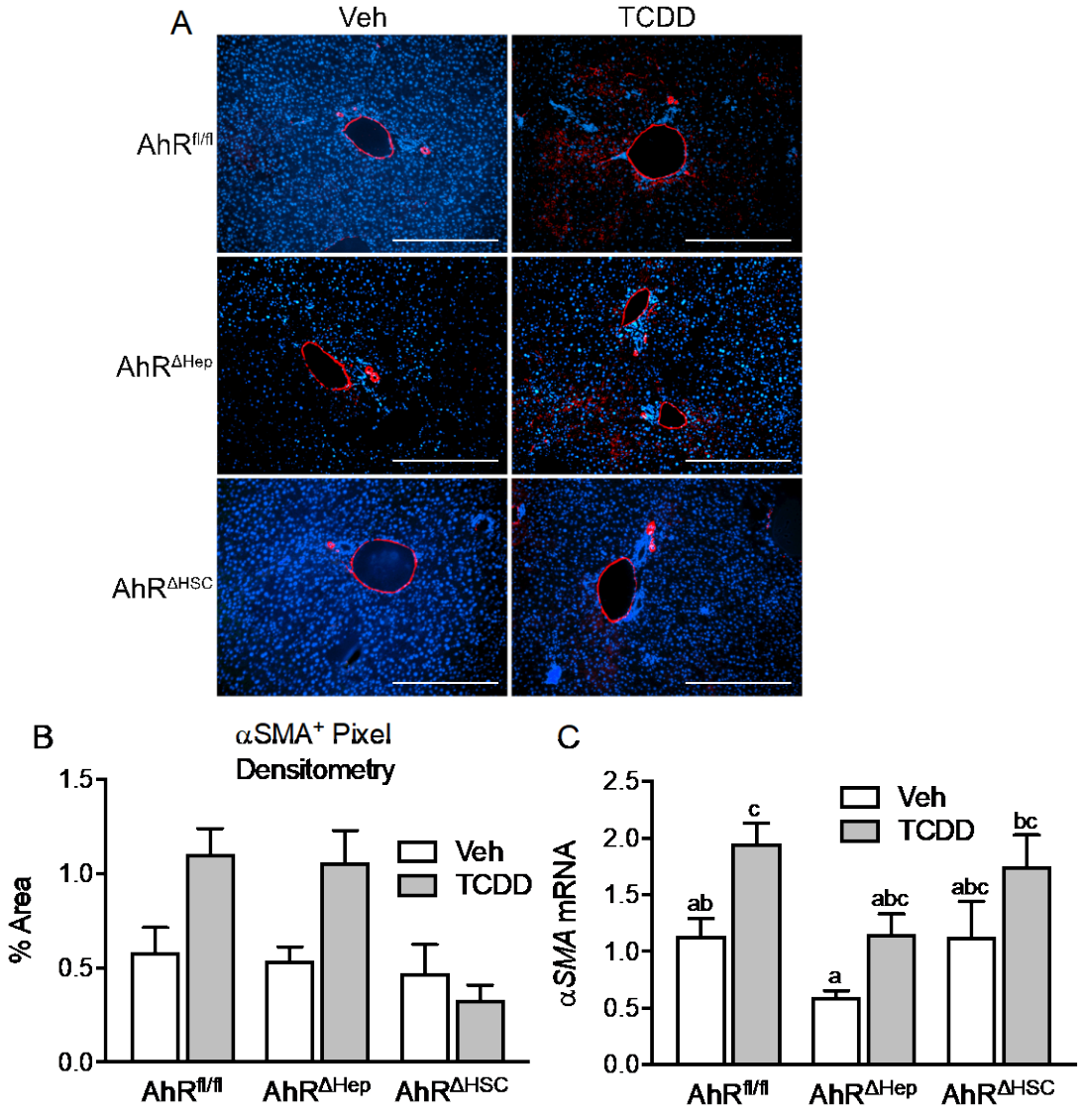

Supplementary Figure 2.1 Protein and mRNA Levels of αSMA

(A) αSMA immunofluorescence stained liver tissue from vehicle- and TCDD-treated mice (100X magnification and scale bar = 500 µm) across all the groups. The αSMA expression was measured using fluorescence microscopy (anti-αSMA, red; DAPI, blue). Scale bar = 100 µm. (B) The pixel content of the red regions was quantified in five fields per mouse and expressed as a percentage of total pixels. (C) Hepatic mRNA levels of *FGF-21* are expressed as fold-change (mean ± SEM) relative to vehicle-treated $AhR^{fl/fl}$ mice (n=8-11). Means that do not share a letter are significantly different from each other ($p < 0.05$).

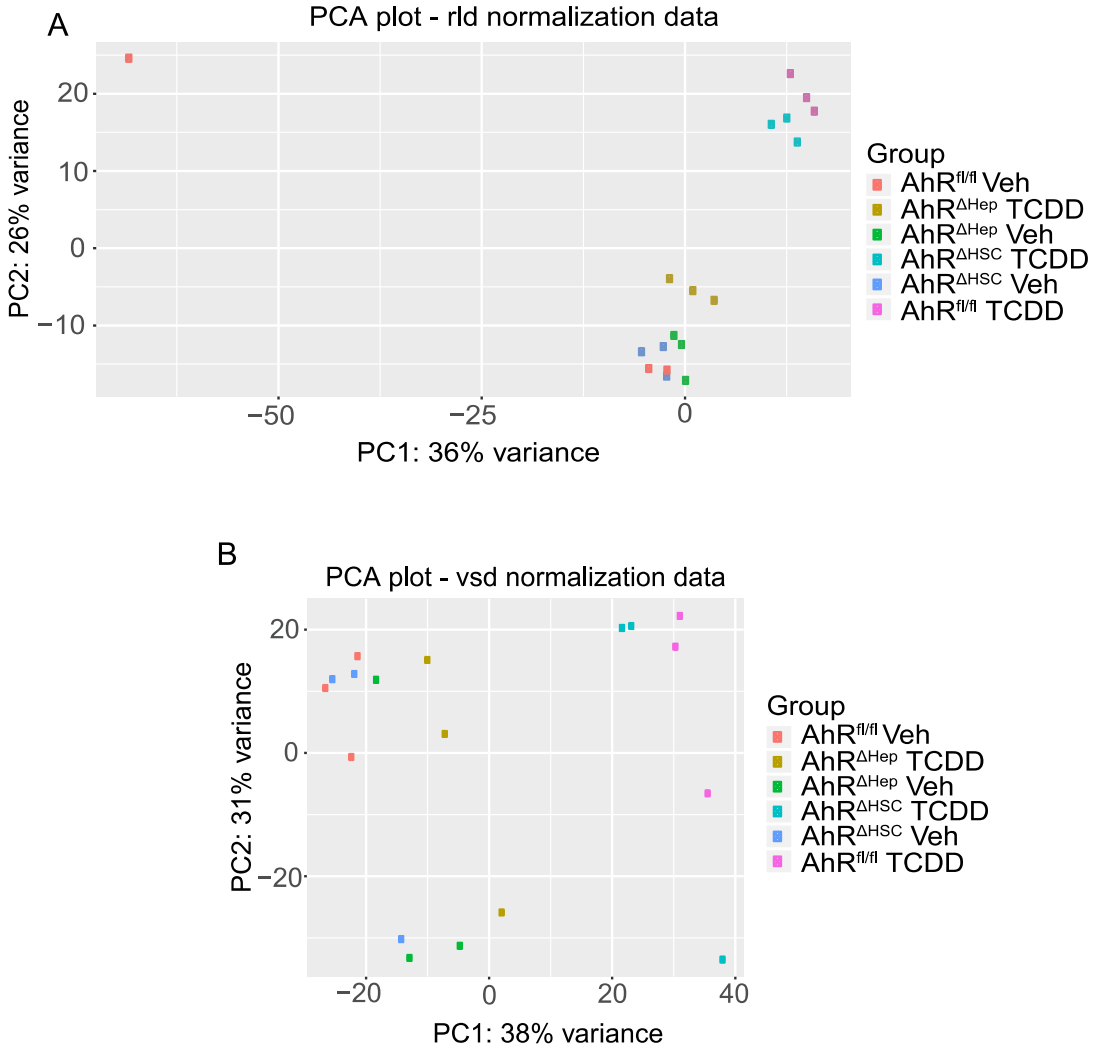

Supplementary Figure 2.2 Analysis of Gene Expression Variances Using Principal Component Analysis (PCA).

(A) PCA analysis of gene expression across the treatments in both wild-type and AhR-deficient LX-2 cells**.** The components PC1 and PC2 define the x- and y-axis, respectively. The distance between any two points represents the variance in gene expression between them. (A) PCA plot was generated using the rlog transformation (rld) function of normalized count data. (B) PCA plot was generated using the variance stabilizing transformation (VST) function of normalized count data.

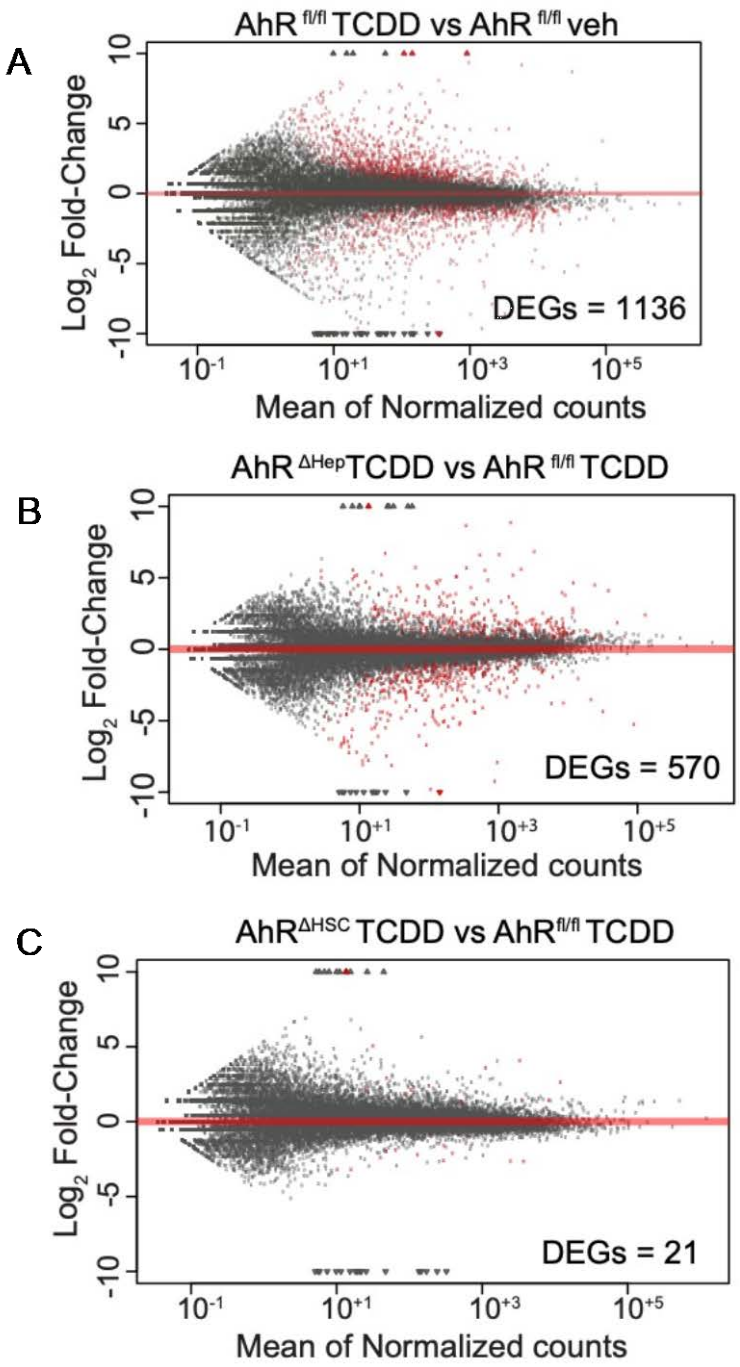

Supplementary Figure 2.3 MA Plots of Differentially Expressed Genes

(A-E) MA plots for differentially expressed genes (red) enriched for the defined comparisons shown on the bottom of each figure. The X- and Y-axis of the plots indicates the "mean of normalized counts" and $\log_2$ fold-change, respectively.

References

Abumrad, N. A. *et al.* (1993) 'Cloning of a rat adipocyte membrane protein implicated in binding or transport of long-chain fatty acids that is induced during preadipocyte differentiation. Homology with human CD36', *The Journal of Biological Chemistry*, 268(24), pp. 17665–17668.

Alsamman, M. *et al.* (2018) 'Endoglin in human liver disease and murine models of liver fibrosis-A protective factor against liver fibrosis', *Liver International*, 38(5), pp. 858–867.

Anders, S., Pyl, P. T. and Huber, W. (2015) 'HTSeq-A python framework to work with high-throughput sequencing data', *Bioinformatics*, 31(2), pp. 166–169.

Andreasen, E. A., Mathew, L. K. and Tanguay, R. L. (2006) 'Regenerative growth is impacted by TCDD: gene expression analysis reveals extracellular matrix modulation', *Toxicological Sciences*, 92(1), pp. 254–269.

Aubert, J. *et al.* (2011) 'Increased expression of cytochrome P450 2E1 in nonalcoholic fatty liver disease: mechanisms and pathophysiological role', *Clinics and Research in Hepatology and Gastroenterology*, pp. 630–637.

Boverhof, D. R. *et al.* (2005) 'Temporal and dose-dependent hepatic gene expression patterns in mice provide new insights into TCDD-mediated hepatotoxicity', *Toxicological Sciences*, 85(2), pp. 1048–1063.

Caldwell, S. H. *et al.* (1999) 'Mitochondrial abnormalities in non-alcoholic steatohepatitis', *Journal of Hepatology*, 31(3), pp. 430–434.

Canbay, A. *et al.* (2003) 'Apoptotic body engulfment by a human stellate cell line is profibrogenic', *Laboratory Investigation*, 83(5), pp. 655–663.

Canbay, A. *et al.* (2003b) 'Kupffer cell engulfment of apoptotic bodies stimulates death ligand and cytokine expression', *Hepatology*, 38, pp. 1188–1198.

Canbay, A., Friedman, S. and Gores, G. J. (2004) 'Apoptosis: the nexus of liver injury and fibrosis', *Hepatology*, 39(2), pp. 273–278.

Casini, A. *et al.* (1997) 'Neutrophil-derived superoxide anion induces lipid peroxidation and stimulates collagen synthesis in human hepatic stellate cells: role of nitric oxide', *Hepatology*, 25(2), pp. 361–367.

Ceni, E. *et al.* (2017) 'The orphan nuclear receptor COUP-TFII coordinates hypoxia-independent proangiogenic responses in hepatic stellate cells', *Journal of Hepatology*, 66(4), pp. 754–764.

Dufour, D. R. *et al.* (2000) 'Diagnosis and monitoring of hepatic injury. I. Performance characteristics of laboratory tests', *Clinical Chemistry*, 46(12), pp. 2027–2049.

Fader, K. A. *et al.* (2015) '2,3,7,8-tetrachlorodibenzo-p-dioxin alters lipid metabolism and depletes immune cell populations in the Jejunum of C57BL/6 mice', *Toxicological Sciences*, 148(2), pp. 567–580.

Feldstein, A. E. *et al.* (2005) 'Hepatic stellate cells and fibrosis progression in patients with nonalcoholic fatty liver disease', *Clinical Gastroenterology and Hepatology*, pp. 384–389.

Fernandez-Salguero, P. *et al.* (1996) 'Aryl-hydrocarbon receptor-deficient mice are resistant to 2,3,7,8-tetrachlorodibenzo-p-dioxin-induced toxicity', *Toxicology and Applied Pharmacology*, 140, pp. 173–179.

Friedman, S. L. (2000) 'Molecular Regulation of Hepatic Fibrosis, an Integrated Cellular Response to Tissue Injury, *The Journal of Biolologocal Chemistry*, 275, pp. 2247–2250.

Girer, N. G. *et al.* (2016) 'Hepatic aryl hydrocarbon receptor attenuates fibroblast growth factor 21 expression', *The Journal of Biological Chemistry*, 291(29), pp. 15378–15387.

Håkansson, H. and Hanberg, A. (1989) 'The distribution of [14C]-2,3,7,8-tetrachlorodibenzo-p-dioxin (TCDD) and its effect on the vitamin A content in parenchymal and stellate cells of rat liver', *Journal of Nutrition*, 119(4), pp. 573–580.

Hanberg, A., Kling, L. and Hakansson, H. (1996) 'Effect of 2,3,7,8-tetrachlorodibenzo-p-dioxin (TCDD) on the hepatic stellate cell population in the rat', *Chemosphereere*, 32(6), pp. 1225–1233.

Hankinson, O. (1995) 'The Aryl hydrocarbon receptor complex', *Annual Review of Phamacology and Toxicology*, 35, pp. 307–340.

Harvey, W. A. *et al.* (2016) 'Exposure to 2,3,7,8-tetrachlorodibenzo-p-dioxin (TCDD) increases human hepatic stellate cell activation', *Toxicology*, 26(33), pp. 344–346.

Hemmann, S. *et al.* (2007) 'Expression of MMPs and TIMPs in liver fibrosis-a systematic review with special emphasis on anti-fibrotic strategies', *Journal of Hepatology*, 46(5), pp. 955–975.

Huang, G. and Elferink, C. J. (2012) 'A novel nonconsensus xenobiotic response element capable of mediating aryl hydrocarbon receptor-dependent gene expression', *Molecular Pharmacology*, 81(3), pp. 338–347.

Junqueira, L. C. U., Bignolas, G. and Brentani, R. R. (1979) 'Picrosirius staining plus polarization microscopy, a specific method for collagen detection in tissue-sections', *The Histochemical Journal*, 11(4), pp. 447–455.

Kim, D., Langmead, B. and Salzberg, S. L. (2015) 'HISAT: a fast spliced aligner with low memory requirements', *Nature Methods*, 12(4), pp. 357–360.

Kocabayoglu, P. *et al.* (2016) 'Induction and contribution of β-PDGFR signaling by hepatic stellate cells to liver regeneration after partial hepatectomy in mice', *Liver International*, 36(6), pp. 874–882.

Kolios, G., Valatas, V. and Kouroumalis, E. (2006) 'Role of Kupffer cells in the pathogenesis of liver disease', *World Journal of Gastroenterology*, 12(46), pp. 7413–7420.

Lamb, C. L. *et al.* (2016a) '2,3,7,8-Tetrachlorodibenzo-p-dioxin (TCDD) increases necroinflammation and hepatic stellate cell activation but does not exacerbate experimental liver fibrosis in mice', *Toxicology and Applied Pharmacology*, 311, pp. 42–51.

Lamb, C. L. *et al.* (2016b) 'Aryl hydrocarbon receptor activation by TCDD modulates expression of extracellular matrix remodeling genes during experimental liver fibrosis', *BioMed Research International*, 2016, pp. 1–14.

Lee, J. H. *et al.* (2008) 'A novel role for the dioxin receptor in fatty acid metabolism', *Gastroenterology*, 28(2), pp. 4439–4448.

Lee, U. E. and Friedman, S. L. (2011) 'Mechanisms of hepatic fibrogenesis', *Best Practice & Research: Clinical Gastroenterology*, 25(2), pp. 195–206.

Li, J. T. *et al.* (2008) 'Molecular mechanism of hepatic stellate cell activation and antifibrotic therapeutic strategies', *Journal of Gastroenterology*, 43(6), pp. 419–428.

Liu, S. B. *et al.* (2016) 'Lysyl oxidase activity contributes to collagen stabilization during liver fibrosis progression and limits spontaneous fibrosis reversal in mice', *FASEB Journal*, 30(4), pp. 1599–1609.

Livak, K. J. and Schmittgen, T. D. (2001) 'Analysis of relative gene expression data using real-time quantitative PCR and the 2(-Delta Delta C(T)) method', *Methods*, 25(4), pp. 402–408.

Love, M. I., Huber, W. and Anders, S. (2014) 'Moderated estimation of fold change and dispersion for RNA-seq data with DESeq2', *Genome Biology*, 15(12), pp. 550–571.

Macdonald, G. A. *et al.* (2001) 'Lipid peroxidation in hepatic steatosis in humans is associated with hepatic fibrosis and occurs predominately in acinar zone 3', *Journal of Gastroenterology and Hepatology (Australia)*, 16(6), pp. 599–606.

Mannaerts, I. *et al.* (2013) 'Gene expression profiling of early hepatic stellate cell activation reveals a role for igfbp3 in cell migration', *PLoS ONE*, 8(12), pp. 1–13.

Maza, E. *et al.* (2013) 'Comparison of normalization methods for differential gene expression analysis in RNA-Seq experiments: a matter of relative size of studied transcriptomes', *Communicative and Integrative Biology*, 6(6), pp. 1–8.

Naito, M. *et al.* (2004) 'Differentiation and function of Kupffer cells', *Medical Electron Microscopy*, 37(1), pp. 16–28.

Nault, R. *et al.* (2016) 'Dose-dependent metabolic reprogramming and differential gene expression in TCDD-elicited hepatic fibrosis', *Toxicological Sciences*, 154(2), pp. 253–266.

Nieto, N. *et al.* (1999) 'CYP2E1-mediated oxidative stress induces collagen type I expression in rat hepatic stellate cells', *Hepatology*, 30(4), pp. 987–996.

Patrizi, B. and de Cumis, M. S. (2018) 'TCDD toxicity mediated by epigenetic mechanisms', *International Journal of Molecular Sciences*, 19(12), pp. 1–15.

Pierre, S., Chevallier, A., Teixeira-Clerc, F., *et al.* (2014) 'Aryl hydrocarbon receptor-dependent induction of liver fibrosis by dioxin', *Toxicological Sciences*, 137(1), pp. 114–124.

Priya, S. and Sudhakaran, P. R. (2008) 'Cell survival, activation and apoptosis of hepatic stellate cells: modulation by extracellular matrix proteins', *Hepatology Research*, 38(12), pp. 1221–1232.

Radi, Z. A. *et al.* (2011) 'Increased serum enzyme levels associated with kupffer cell reduction with no signs of hepatic or skeletal muscle injury', *American Journal of Pathology*, 179(1), pp. 240–247.

Reeves, H. L. *et al.* (1996) 'Hepatic stellate cell activation occurs in the absence of hepatitis in alcoholic liver disease and correlates with the severity of steatosis', *Journal of Hepatology*, 25(5), pp. 677–683.

Rusli, F. *et al.* (2016) 'Fibroblast growth factor 21 reflects liver fat accumulation and dysregulation of signalling pathways in the liver of C57BL/6J mice', *Scientific Reports*, 6(July), pp. 1–16.

Saneyasu, T., Akhtar, R. and Sakai, T. (2016) 'Molecular cues guiding matrix stiffness in liver fibrosis', *BioMed Research International*, pp. 1–11.

Schumacher, J. D. and Guo, G. L. (2016) 'Regulation of hepatic stellate cells and fibrogenesis by fibroblast growth factors', *BioMed Research International*, 2016, pp. 1–8.

Van Der Slot, A. J. *et al.* (2005) 'Elevated formation of pyridinoline cross-links by profibrotic cytokines is associated with enhanced lysyl hydroxylase 2b levels', *Biochimica et Biophysica Acta - Molecular Basis of Disease*, 1741(1–2), pp. 95–102.

Walisser, J. A. *et al.* (2005) 'Aryl hydrocarbon receptor-dependent liver development and hepatotoxicity are mediated by different cell types', *Proceedings of the National Academy of Sciences of the United States of America*, 102(49), pp. 17858–17863.

Wilson, C. G. *et al.* (2016) 'Hepatocyte-specific disruption of CD36 attenuates fatty liver and improves insulin sensitivity in HFD-fed mice', *Endocrinology*, 157(2), pp. 570–585.

Wobser, H. *et al.* (2009) 'Lipid accumulation in hepatocytes induces fibrogenic activation of hepatic stellate cells', *Cell Research*, 19(8), pp. 996–1005.

Wurie, H. R., Buckett, L. and Zammit, V. A. (2012) 'Diacylglycerol acyltransferase 2 acts upstream of diacylglycerol acyltransferase 1 and utilizes nascent diglycerides and de novo synthesized fatty acids in HepG2 cells', *The FEBS journal*, 279(17), pp. 3033–3047.

Wynn, T. A. (2008) 'Cellular and molecular mechanisms of fibrosis', *Journal of Pathology*, 214(2), pp. 199–210.

Xu, C.-X. *et al.* (2016) 'Aryl hydrocarbon receptor deficiency protects mice from diet-induced adiposity and metabolic disorders through increased energy expenditure', *International Journal of Obesity*, 39(8), pp. 1300–1309.

CHAPTER THREE: ROLE OF ARYL HYDROCARBON RECEPTOR SIGNALING IN HEPATIC STELLATE CELL ACTIVATION USING LX-2 CELLS

Abstract

Accumulating evidence suggests a complex role for aryl hydrocarbon receptor (AhR) signalig in liver fibrosis. Fibrosis is an abnormal wound healing response characterized by excessive deposition of collagen by activated hepatic stellate cells (HSCs). We recently reported that AhR signaling increases HSC activation in vitro and in the liver of mice treated with chronic carbon tetrachloride. In contrast, another recent study reported that AhR prevents the activation of HSC and liver fibrosis. To investigate the mechanistic roles by which AhR signaling regulates HSC activation, we sought to create a novel modified human HSC line, LX-2, that does not express a functional AhR. To disrupt AhR gene expression, CRISPR/Cas9 technology was used, which allowed for precise and targeted mutation of exons 2 within the AhR gene. The wildtype and AhR-knocked out (AhR-KO) LX-2 cells were treated with a prototypical exogenous AhR ligand, 2,3,7,8-tetrachlorodibenzo-p-dioxin (TCDD), or the non-toxic endogenous AhR ligand 2-(1' H-indole-3'-carbonyl)-thiazole-4-carboxylic acid methyl ester (ITE) and incubated for 6 days for culture-induced activation. RNA-sequencing data revealed 9720 differentially expressed genes (DEGs) in untreated AhR-KO LX-2 cells compared to untreated wildtype LX-2 cells. AhR gene deletion was found to increase the protein and mRNA expression of alpha-smooth muscle actin (αSMA) and mRNA expression of several other HSC activation markers, such as collagen type III (COL3A) and insulin-like

growth factor binding protein 3 (IGFBP3). AhR gene deletion from LX-2 cells decreased cell proliferation and altered the expression of proliferation-related genes, including CCND1 (cyclin1) and CDKN1A (p21). Extracellular matrix remodeling (ECM) genes were also modulated in AhR-KO LX-2 cells, which indicates that endogenous AhR activation may play a role in ECM remodeling. No significant differences were observed in the activation of LX-2 cells treated with TCDD and ITE ligands. We conclude that endogenous AhR activation prevents HSC activation and modulates the expression of genes associated with proliferation and ECM remodeling.

Introduction

Liver fibrosis is a wound healing process characterized by the excessive deposition of extracellular matrix (ECM) proteins by activated hepatic stellate cells (HSCs) (Wynn, 2008). The role and importance of HSCs as primary collagen-producing cells contributing to liver fibrosis is well established (Fernandez-Salguero et al., 1996; Moreira, 2007; Iwaisako et al., 2014). Some important triggers for HSC activation are cytokine and profibrogenic mediators produced during hepatocyte injury and inflammation (Casini et al., 1997; Canbay et al., 2003; Kisseleva and Brenner, 2008). Activated HSCs are characterized by increased proliferation, the production of cytokines and profibrogenic mediators, and the synthesis of ECM proteins, such as collagen type I (Tsukamoto, 1999; Kisseleva and Brenner, 2007). The cytokines and profibrogenic mediators produced from HSCs can function in an autocrine stimulus (Tsukamoto, 1999). Overall, HSC activation is a complex event interplayed by many cells and stimuli, and understanding the molecular mechanism is essential for liver fibrosis therapeutics.

Several studies have implicated a role for aryl hydrocarbon receptor (AhR) in mediating HSC activation and liver fibrosis (Fernandez-Salguero *et al.*, 1996; Harvey *et al.*, 2016; Nault *et al.*, 2016). The AhR is a ubiquitously expressed, soluble receptor that functions as a ligand-activated transcription in response to endogenous and exogenous ligands (Nguyen and Bradfield, 2008). The AhR is important for mediating the toxicity associated with exposure to environmental toxicants, such as 2,3,7,8-tetrachlorodibenzo-*p*-dioxin (TCDD) (Fernandez-Salguero et al., 1996). It was later discovered that AhR activation by endogenous ligands contributes to the regulation of physiological processes such as cell cycle regulation, inflammation, development, and immunity, although mechanisms by which this occurs are incompletely understood (Nebert and Karp, 2009; Puga, Ma and Marlowe, 2009; Thatcher et al., 2015). Understanding how endogenous ligands impact AhR activation in HSCs is important for determining the likelihood that AhR signaling could be therapeutically targeted to diminish liver fibrosis.

The role of AhR signaling in HSC activation is unclear. We previously reported that sub-chronic exposure to TCDD results in increased necroinflammation and HSC activation, while a single treatment of TCDD also increased expression of HSC activation markers *in vitro* (Harvey *et al.*, 2016; Lamb *et al.*, 2016a). This was corroborated by a recent study that showed that TCDD induced HSC activation via activating protein kinase-B/Akt and NF-kB signaling pathways (Han et al., 2017). In contrast, treatment with the non-toxic, endogenous AhR agonist, 2-(1'H-indol-3'-carbonyl) thiazole-4-carboxylic acid methyl ester (ITE) has been reported to reduce HSC activation and mitigate liver fibrosis (Yan et al., 2019). Furthermore, primary cells isolated from HSC-specific AhR knockout mice showed increased HSC activation (Yan et al., 2019). These

inconsistencies suggest the possibility that the AhR elicits different signaling pathways and transcription profiles in response to exogenous and endogenous ligands. Understanding how AhR signaling modulates HSC activation *in vivo* is typically confounded by concomitant hepatocyte damage and inflammation, both of which promote HSC activation. Therefore, to understand the discrepancies of AhR signaling in HSCs at the cellular and molecular level, it would be ideal to use a model system in which hepatocyte damage and inflammation were absent.

The goal of this study was to determine how exogenous and endogenous AhR signaling impacts HSC activation in the absence of hepatocyte damage and inflammation. We used CRISPR/Cas9 technology to create a AhR-deficient variant of the human HSC line, LX-2. LX-2 cells were originally isolated from a healthy human liver and immortalized by transfection with SV40 T-antigen (Xu et al., 2005). These cells display a quasi-activated phenotype and express a functional AhR (Harvey et al., 2016). Gene expression in LX-2 cells is remarkably similar to human HSCs (Xu et al., 2005). These characteristics of LX-2 cells make it an ideal *in vitro* model to study AhR signaling in HSCs. We hypothesized that AhR activation with the endogenous agonist ITE would repress activation in wildtype LX-2 cells compared to untreated and TCDD-treated cells. We further hypothesized that this repression would be absent in AhR-deficient LX-2 cells and in wild-type LX-2 cells treated with an AhR antagonist (CH223191).

Materials and Methods

LX-2 Cell Culture

Human LX-2 cells (Merck, Kenilworth, NJ), were cultured in Dulbecco's modified Eagle's medium (DMEM) supplemented with 5% fetal bovine serum (FBS;

Biowest, Riverside, MO), 1 mM sodium pyruvate, and 100 U/mL penicillin/streptomycin in a 5% CO2 humidified atmosphere incubator at 37 °C. Cell passage was performed on 70% confluent cells by trypsinization with 0.25% trypsin-EDTA (Sigma, St. Louis, MO).

Generation of AhR-Knockout LX-2 Cells Using CRISPR/Cas 9

A Gene Knockout Kit for human AHR was purchased from Synthego (Redwood City, CA). The online Synthego design tool (https://design.synthego.com/#/) was used to design three unique guide RNA (gRNA) sequences to target exon-2 of the human *AHR* gene. All gRNAs from the kit were conjugated to the Synthego modified EZ scaffold. A gRNA sequence that targeted the human *RELA* gene served as a positive control, as the editing efficiency of this gRNA was previously established. gRNA sequences were computationally analyzed for potential off-target effects using COSMID online software (Cradick et al., 2014). Ribonucleoproteins (RNPs) were prepared according to the manufacturer's specifications. In brief, 30 μM of gRNA was incubated with 20 pmol of Cas9 nuclease (from *Streptococcus pyogenes*) containing two nuclear localization sequences for 10 minutes at room temperature in 1X Tris-EDTA (TE) buffer, pH 8.0. LX-2 cells were transfected using the Cell Line Nucleofector™ Kit V, according to the manufacturer's specifications (LONZA, Basel, Switzerland). Briefly, LX-2 cells were trypsinized at 70% confluency, and 2×10^6 cells were resuspended in 93 μL of Nucleofector Solution V and 7 μL of previously prepared individual RNPs. Electroporation was performed using a Nucleofector™ II/2b Device (LONZA, Basel, Switzerland) on program Y-01. After transfection, LX-2 cells were grown for 3 passages. Then cells were trypsinized, 50,000-100,000 cells were lysed, and DNA was collected using the GeneArt® Genomic Cleavage Detection Kit (Thermo Fisher Scientific,

Waltham, MA). A region around exon 2 of the human AhR gene was amplified by PCR using designed primers (Invitrogen, Carlsbad, CA) (Supplementary Table S1). Amplified products were sequenced at the Molecular Research Core Facility at Idaho State University (Pocatello, ID) using the Applied Biosystems 3130xl Genetic Analyzer. Genome editing of exon 2 was analyzed using Inference of CRISPR Edits (ICE) (Synthego, https://ice.synthego.com/#/), which compares sequencing results from treated and untreated RNPs. Single-cell clones were isolated (Supplementary Materials and Methods). DNA from individual clones was sequenced, and the purity and editing efficiency (percentage of cells carrying mutations) was determined using ICE analysis.

Chemical Treatment of LX-2 Cells

TCDD was purchased from Cambridge Isotope Laboratories (Andover, MA); ITE was purchased from Sigma (St. Louis, MO); CH233191 was purchased from Fisher Scientific (Waltham, MA). Working stocks of 1 μM and 1 nM were prepared by diluting each chemical in dimethyl sulfoxide (DMSO). LX-2 cells ($2x10^4$ cells) were plated in tissue culture plates or on 22 x 22 mm glass coverslips. After reaching 30-70 % confluency, cells were treated with 10 nM TCDD (Harvey *et al.*, 2016), 1 μM ITE (Yoshida et al., 2012), or 1 μM CH223191 (Walla et al., 2012; Yoshida et al., 2012) at 0.1% vol/vol. Controls consisted of cells treated with an equivalent volume of DMSO alone (0.1% vol/vol) or cells that were left untreated altogether. One to six days after treatment, cells were collected by trypsinization (0.25% trypsin-EDTA; Sigma, St. Louis, MO) for analysis.

Proliferation Assay

Viable LX-2 cells were counted using a hemocytometer based on trypan blue dye exclusion. The trypsinized cells were diluted from 200 μL to 1200 μL with DMEM media to obtain raw counts of 20 to 40 cells per image. For field counting, cells in DMEM were diluted with trypan blue in a 1:1 ratio. Cells from two fields for each sample were counted in a light microscope with 100X magnification. Each treatment had 3 samples. The percentage of dead cells in each treatment was less than 1%.

Immunofluorescence Detection of αSMA

LX-2 cells ($2x10^4$ cells) were plated on 22 x 22 mm glass coverslips and treated as described above. After 6 days of incubation, cells were fixed by incubating coverslips in 2% paraformaldehyde for 15 minutes. Cells were then permeabilized by a 15-minute incubation in phosphate buffered saline (PBS) containing 0.1% Triton X-100, and antigen retrieval was achieved using PBS containing 0.5% SDS. Non-specific regions were blocked with PBS containing 5% bovine serum albumin (BSA) for 45 minutes at room temperature. Cells were incubated overnight at 4°C with mouse anti-αSMA monoclonal antibody (MS-113-PO, Thermo Fisher Scientific, Waltham, MA) diluted 1:100 in PBS containing 0.5 % BSA. Coverslips were washed five times in PBS containing 0.5% BSA and incubated with a 1:200 dilution of Cy-3 conjugated AffiniPure donkey anti-mouse IgG polyclonal antibody (715-165-150, Jackson ImmunoResearch Laboratories, West Grove, PA) for an hour in the dark at room temperature. Following a total of 5 washes with PBS containing 0.5% BSA, cells were incubated with 4',6-diamidino-2-phenylindole (DAPI) for 5 minutes in the dark at room temperature, to counterstain cell nuclei. Coverslips were washed 3 times with PBS and mounted using VECTASHIELD

antifade mounting medium (Vector Laboratories, Burlingame, CA). Cells were imaged using an EVOS® FL (Life Technologies, Carlsbad, CA) at 200X magnification using fluorescence from an RFP cube to visualize αSMA and a DAPI cube to visualize DAPI. Coverslips with primary antibody alone or secondary antibody alone served as negative controls.

RNA-Sequencing and Data Analysis

LX-2 cells ($2x10^4$ cells) were treated as described above. After 6 days, cells were collected and shipped on dry ice to Novogene Corporation Inc. (Sacramento, CA), where mRNA extraction, eukaryotic transcriptome library preparation (PCR-based), and sequencing were performed. Briefly, mRNA was isolated using poly-T oligo-attached magnetic beads. mRNA quality was determined using an RNA Nano 6000 assay kit for the Bioanalyzer 2100 system (Agilent Technologies, CA, USA); only samples with an RNA integrity number (RIN) >6.8 were used for library preparation. The libraries were prepared using NEBNext® Ultra™ RNA Library Prep Kit for Illumina (Biolabs, Ipswich, MA), and quality was determined by Qubit2.0 and Bioanalyzer 2100. Libraries were sequenced on an Illumina Nova 6000 platform, and 150 bp paired-end reads were generated with a read depth of ~20M per sample.

RNA-sequencing (RNA-seq) data analysis was performed in house. Raw data were analyzed for per base sequence quality (>30), per sequence GC content, and adapter (universal Illumina adapter) removal using FASTQC v0.11.9. The sequencing reads were mapped to the human reference genome (GRCh38 release 99) using HISAT2 v2.1.0 (Kim, Langmead and Salzberg, 2015). Aligned reads were counted using HTSeq v0.11.3 (Anders, Pyl and Huber, 2015), and the counts were then analyzed for differential gene

expression using median-ratio-normalization (Maza et al., 2013) with Deseq2 v1.22.2 (Love, Huber and Anders, 2014). Fold-changes were calculated by comparing counts in all the treatments relative to CTRLs. Genes with an adjusted p-value < 0.05 were considered differentially expressed. Enrichment analysis of differentially expressed genes (DEGs) was performed in Cytoscape v3.7.0 using the ClueGo v2.5.1 visualization tool.

Measurement of mRNA Expression by Quantitative Real-Time PCR (qRT-PCR)

LX-2 cells were treated as described. mRNA was collected using the E.Z.N.A.® Total RNA Kit (Omega Bio-Tek, Norcross, GA). RNA purity was assessed using a Nanodrop 2000c (Thermo Scientific, Waltham, MA), and 500 μg of mRNA was reverse transcribed using a High-Capacity cDNA Reverse Transcription Kit (Thermo Fisher Scientific, Waltham, MA). Gene-specific primers (Table 1) were purchased from Invitrogen (Carlsbad, CA) and used to amplify cDNA using FastStart Essential DNA Green Master reaction mix (Roche, Indianapolis, IN) and a LightCycler® 96 Thermocycler (Roche, Indianapolis, IN). Samples were run in duplicate, and 3 samples were used in each treatment group. Gene expression was normalized to *β-ACTIN*, and the relative expression was estimated using the ΔΔCq method (Livak and Schmittgen, 2001). mRNA levels are expressed as fold-change (mean ± SEM) relative to untreated, wildtype LX-2 cells that were collected on day 0.

Statistical Analysis

Statistical significance was determined using a two-way ANOVA with Bonferroni testing ($p < 0.05$) using GraphPad Prism 8.01 software (GraphPad Software, La Jolla, CA). Unless otherwise noted, data represent mean ± SEM. Means that do not share a letter are significantly different from each other ($p < 0.05$).

Table 3.1 Primer Sequences

Gene	Primer Sequence (5'to 3')	Temp.(℃)
β-ACTIN	GAT GAG ATT GGC ATG GCT TT	51
	GAG AAG TGG GGT GGC TT	
ACTA2	TCT GGA GAT GGT GTC ACC CAC AAT	61
	AAT AGC CAC GCT CAG TCA GG	
CCDN1	ATC AAG TGT GAC CCG GAC TG	52
	CTT GGG GTC CAT GTT CTG CT	
CDKN1A	CTG CCG AAG TCA GTT CCT TGT TGA	54
	CAT GGC GCC TCC TCT G	
CDKN1B	GCT AAC TCT GAG GAC ACG CAT	52
	TGT TTT GAG TAG AAG AAT CGT CGG	
COL1A1	GGA ATG AAG GGA CAC AGA GGT T	52
	AGT AGC ACC ATC ATT TCC ACG A	
COL3A1	TCT GAG GAC CAG TAG GGC ATG ATT	67
	AAT CAA TGC CCC AGT CAC CT	
CYP1A1	GAA TGA GAA GTT CTA CAG	43
	CAA GAC GAT GTT AAT GAT	
CYP1B1	CAC TGC CAA CAC CTC TGT CTT	57
	CAA GGA GCT CCA TGG ACT CT	
IL1B	TCG CCA GTG AAA TGA TGG CT	53
	TGG AAG GAG CAC TTC ATC TGT T	
CCL2	AAT CAA TGC CCC AGT CAC CT	54
	GGG TCA GCA CAG ATC TCC TT	
PDGFRB	GGA GAG GGC AGT AAG GAG GA	54
	GAA GCC GCA TGG TGT CCT TG	
TIMP1	CTG TTG TTG CTG TGG CTG ATA G	58
	CGC TGG TAT AAG GTG GTC TGG	
TIMP2	GAC GGC AAG ATG CAC ATC AC	63
	GAG ATG TAG CAC GGG ATC ATG G	

Results

Generation and Validation of AhR-Knockout in LX-2 Cells

To inhibit AhR activity in LX-2 cells, a CRISPR associated endonuclease (Cas9 protein) was delivered using three different guide RNAs (gRNAs) designed to produce site-specific editing in exon 2 (Figure 3.1A). Transfection of LX-2 cells with RNPs that contained either gRNA-1 or gRNA-3 produced low CRISPR/Cas9-mediated editing efficiency compared to RNPs containing gRNA for RELA (Figure 3.1B). In contrast, the delivery of RNPs containing gRNA-2 produced about twice as many mutations compared to gRNA-RELA. About 33% of these mutations were indels, and 30% were frameshift mutations. Sequence analysis of clones transfected with gRNA-2 led to the selection of one clone (clone-2) that contained a 14-nucleotide deletion and demonstrated 98% editing efficiency (data not shown). AhR activity was subsequently measured based on the TCDD-induced expression of a gene set known to be regulated by AhR activation: *CYP1A1* (which encodes cytochrome P450 1A1) (Figure 3.1C) and *CYP1B1* (which encodes cytochrome P450 1B1) (Figure 3.1D). TCDD treatment induced expression of both genes to varying extents in wildtype LX-2 cells but failed to do so in clone-2 cells. Therefore, cells from clone-2 were selected for use in subsequent experiments and given the designation "AhR-KO" LX-2 cells.

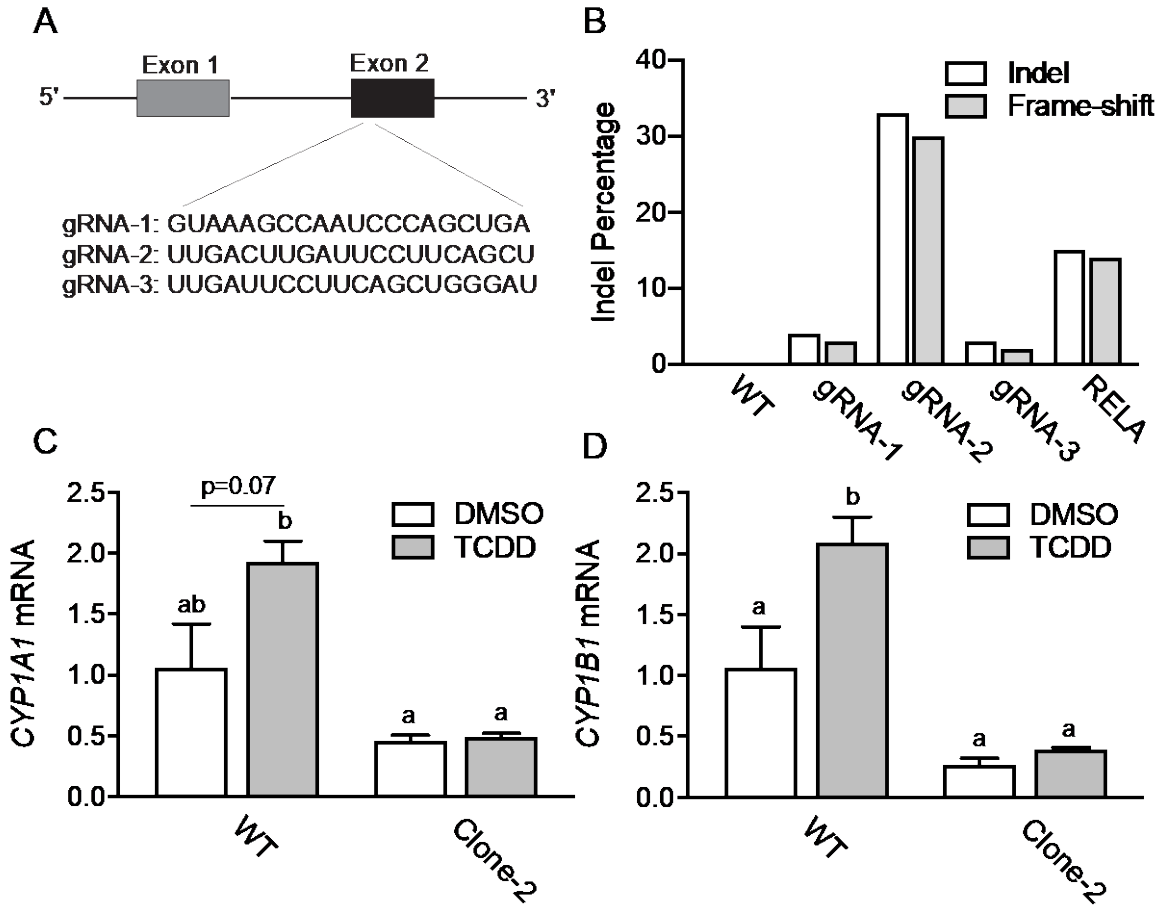

Figure 3.1 Generation and Validation of AhR-Knockout LX-2 cells Using CRISPR/Cas9

(A) Representation of the gRNA target region in AhR exon-2 and the designed sequences to edit the coding sequence on this exon. (B) Cleavage efficiency was determined using the online Synthego ICE tool. The total editing frequency of each gRNA is indicated as Insertion-deletion (Indel) percentage. (C and D) AhR-KO and wildtype LX-2 cells were treated with DMSO or 10 nM TCDD for 24 hours. mRNA levels of AhR-modulated genes, *CYP1A1*, and *CYP1B1*, are expressed as fold-change (mean ± SEM) relative to DMSO-treated wildtype LX-2 cells. Three samples were used for each treatment group; each sample was run in duplicate. Means that do not share a letter are significantly different from each other ($p < 0.05$).

Assessing AhR Activity in Wildtype and AhR-KO LX-2 Cells

To confirm AhR activity in wildtype cells and AhR ablation in AhR-KO cells, we measured the mRNA expression of *CYP1A1* and *CYP1B1*, which are known AhR-regulated genes. Treatment with TCDD and ITE significantly increased expression of

these genes in wildtype LX-2 cells but not in AhR-KO cells (Figure 3.2A and B). Gene expression was significantly reduced in wild-type LX-2 cells treated with the AhR antagonist, CH22319.

Proliferation Is Reduced in AhR-KO Cells

One of the characteristics of HSC activation is increased proliferation. We found that the number of wild-type LX-2 cells increased throughout the 6-day culture period. However, proliferation was markedly reduced in AhR-KO cells (Figure 3.3A-C). The change in proliferation after DMSO, ITE, and CH223191 treatments was not significant (Figure 3.3A-C). In the AhR-KO cells, no statistically significant changes in proliferation were observed for untreated and treated cells (Figure 3.3A-C).

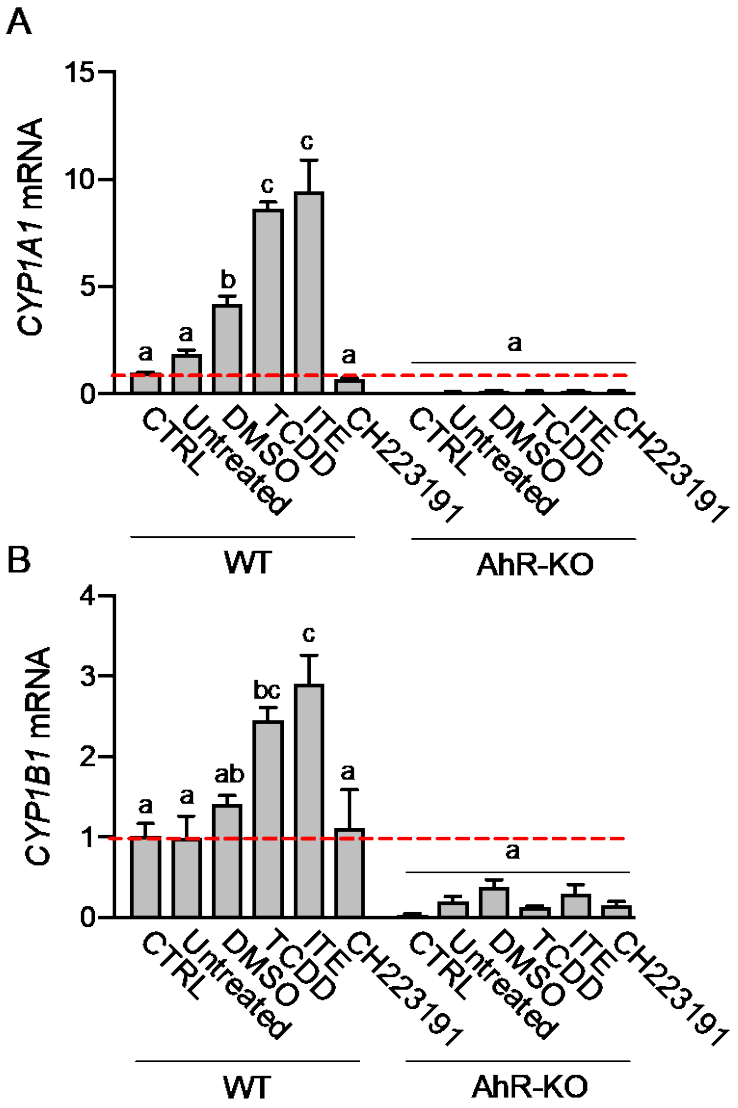

Figure 3.2 Assessing AhR Activity in Wildtype and AhR-KO LX-2 Cells

Wildtype and AhR-KO LX-2 cells were treated for 6 days with 10 nM TCDD, 1 μM ITE, or 1 μM CH223191. Graphs show the mean fold-change (mean ± SEM) in mRNA expression relative to untreated, wildtype LX-2 cells collected on day 0 denoted as control (CTRL) for *CYP1A1* (A), and *CYP1B1* (B) genes; fold-change of 1, indicated by the red-dashed line. Three samples were used for each treatment group; each sample was run in duplicate. Means that do not share a letter are significantly different from each other ($p < 0.05$).

Proliferation was further analyzed at the transcriptional level by measuring mRNA expression of several well-established proliferation markers. In untreated

wildtype cells, the mRNA expression of *CCND1* (cyclin D1) increased throughout the culture period. Upon treatment with TCDD and ITE, the expression was significantly higher. Treatment with the AhR inhibitor, CH223191, did not change expression of *CCND1* compared to TCDD and ITE treated cells. However, *CCND1* mRNA expression in AhR-KO cells failed to increase across all the treatments (Figure 3.4A). Negative proliferation regulator p21 (encoded by *CDKN1A*) mRNA expression significantly increased in AhR-KO cells in culture induced activation and upon treatment with TCDD and ITE (Figure 3.4B) but failed to increase in wildtype cells across all the treatments. Another negative regulator of proliferation, *CDKN1B,* which encodes p27Kip1, showed the opposite effect, as mRNA expression significantly decreased in AhR-KO cells in comparison with TCDD- and ITE-treated wildtype cells (Figure 3.4C). No overt differences were observed for mRNA expression of *PDGFRB,* which encodes platelet derived growth factor receptor-beta. PDGFRB is a receptor for PDGF, which is a potent mitogen for HSCs (data not shown). Similarly, RNA-seq analysis revealed decreased expression of several proliferation markers in AhR KO cells (Figure 3.5).

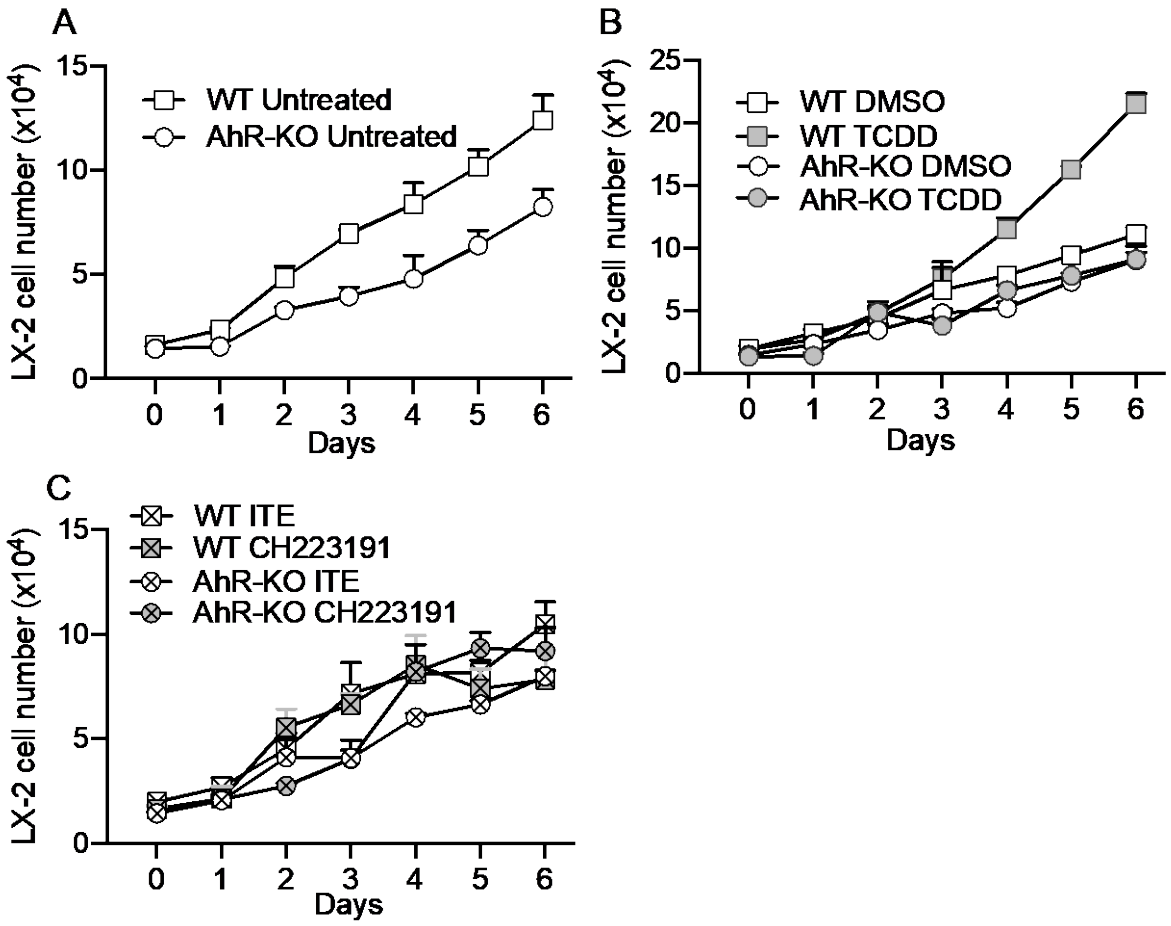

Figure 3.3 Proliferation Is Reduced in AhR KO Cells.

(A-C) Wildtype and AhR-KO LX-2 cells were treated for 6 days with 10 nM TCDD, 1 μM ITE, or 1 μM CH223191. Viable cell number were counted daily using a hemacytometer and trypan blue exclusion. Data represent the mean ±SEM. Three samples were used for each treatment group and each experiment was performed twice.

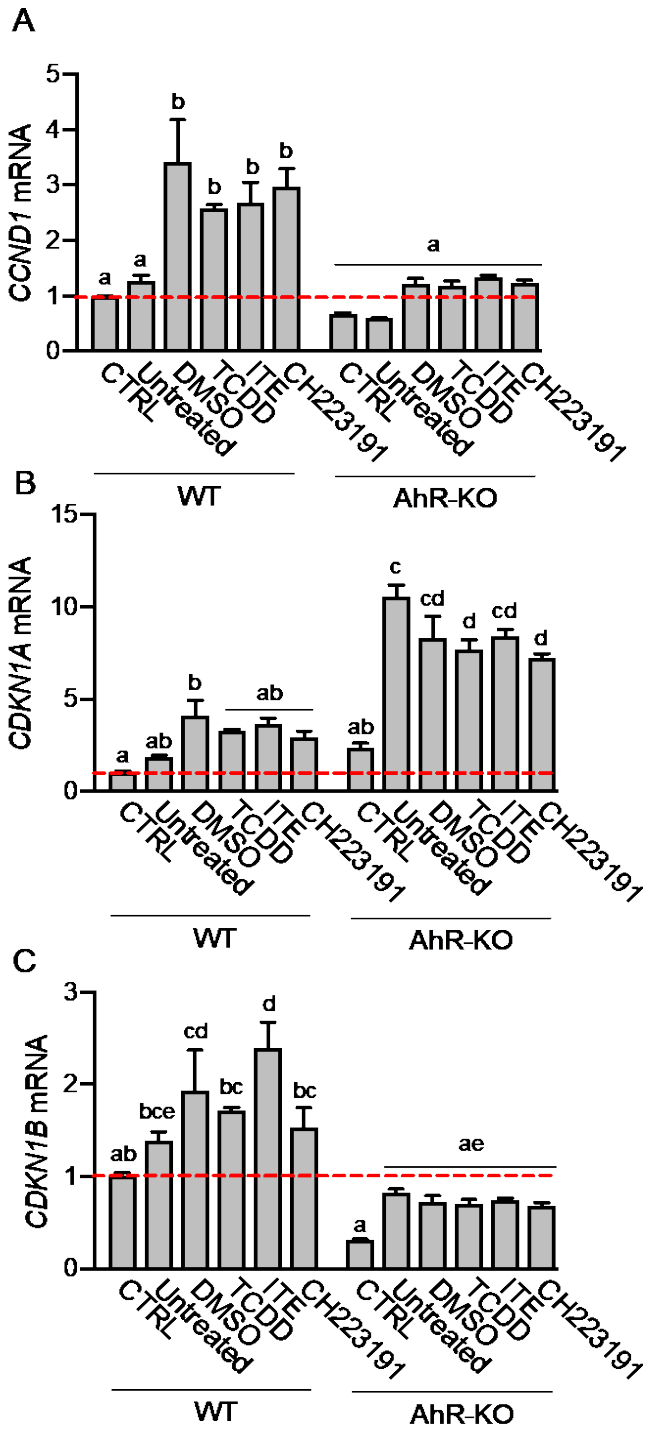

Figure 3.4 Expression of Cell Cycle Regulatory Genes Is Altered in AhR KO Cells.

Graphs show the mean fold-change (mean ± SEM) in mRNA expression relative to the wildtype control (CTRL) for cycle cycle regulatory genes *CCND1* (A), *CDKN1A* (B), and *CDKN1B* (C); fold-change of 1, indicated by the red-dashed line. Means that do not share a letter are significantly different from each other ($p < 0.05$).

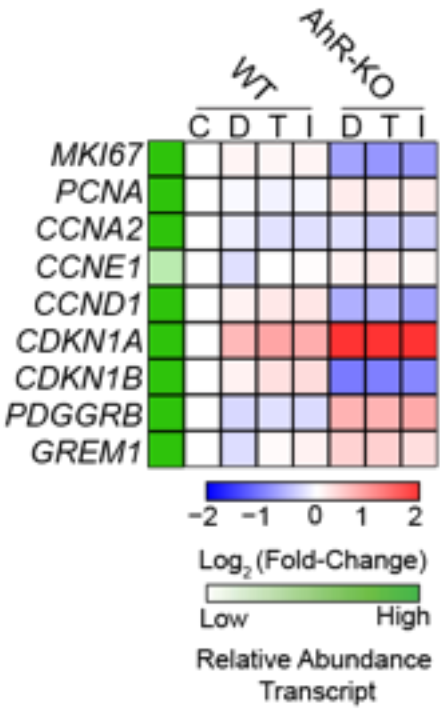

Figure 3.5 Heatmap Showing Expression of Cell Cycle Regulatory Genes in Treated Wildtype and AhR-KO Clls

RNA-seq was used to assess expression of cell cycle regulatory genes. Gene expression for all treatment groups was normalized to wildtype CTRL. Blue tiles indicate repression, and red tiles indicate induction of gene expressions. Relative transcript abundance depicts the mean of the normalized transcript counts of all samples for individual genes, normalizing for sequencing depth. Green tiles indicate a high (>1000) relative transcript abundance and white tiles indicate a low (<10) relative transcript abundance. Letters on top represents the following: C = CTRL; D = DMSO T = TCDD, I = ITE, C = CH223191.

AhR Removal Altered the Expression of Inflammatory Cell Infiltration Markers and Genes Associated with Nuclear Receptors.

To assess the role AhR signaling plays in mediating cytokine production, we measured the mRNA levels of *IL1B* and *CCL2*. In wildtype cells, TCDD and ITE increased expression of both genes, and DMSO treatment also increased gene expression compared to untreated cells, albeit to a lesser extent than ITE and TCDD treatments. Unexpectedly, *IL1B* mRNA expression was severely repressed in AhR-KO cells across

all treatments (Figure 3.6A). Similarly, mRNA expression of *CCL2* was repressed in AhR-KO cells compared to respective treatments in wildtype cells (Figure 3.6B). HSCs also express diverse groups of nuclear transcription factor receptors such as liver X receptor (encoded by *NR1H3*), farnesoid X receptor (FXR; encoded by *NR1H4*), PPARγ (encoded by *PPARG*), PPARδ (encoded by *PPARD*), vitamin D receptor (encoded by *VDR*), REV-ERBα (encoded by *NR1D1*) and nuclear receptor subfamily 4 group A member 1 (encoded by *NR4A1*). *NR1H3* and *VDR* expression showed no changed across all treatments within the wildtype and AhR-KO cells. *NR1H4*, *NR4A1*, and *PPARG* expression increased following AhR ablation in all treatments. In contrast, *PPARD* expression decreased after AhR ablation regardless of treatment (Figure 3.6C).

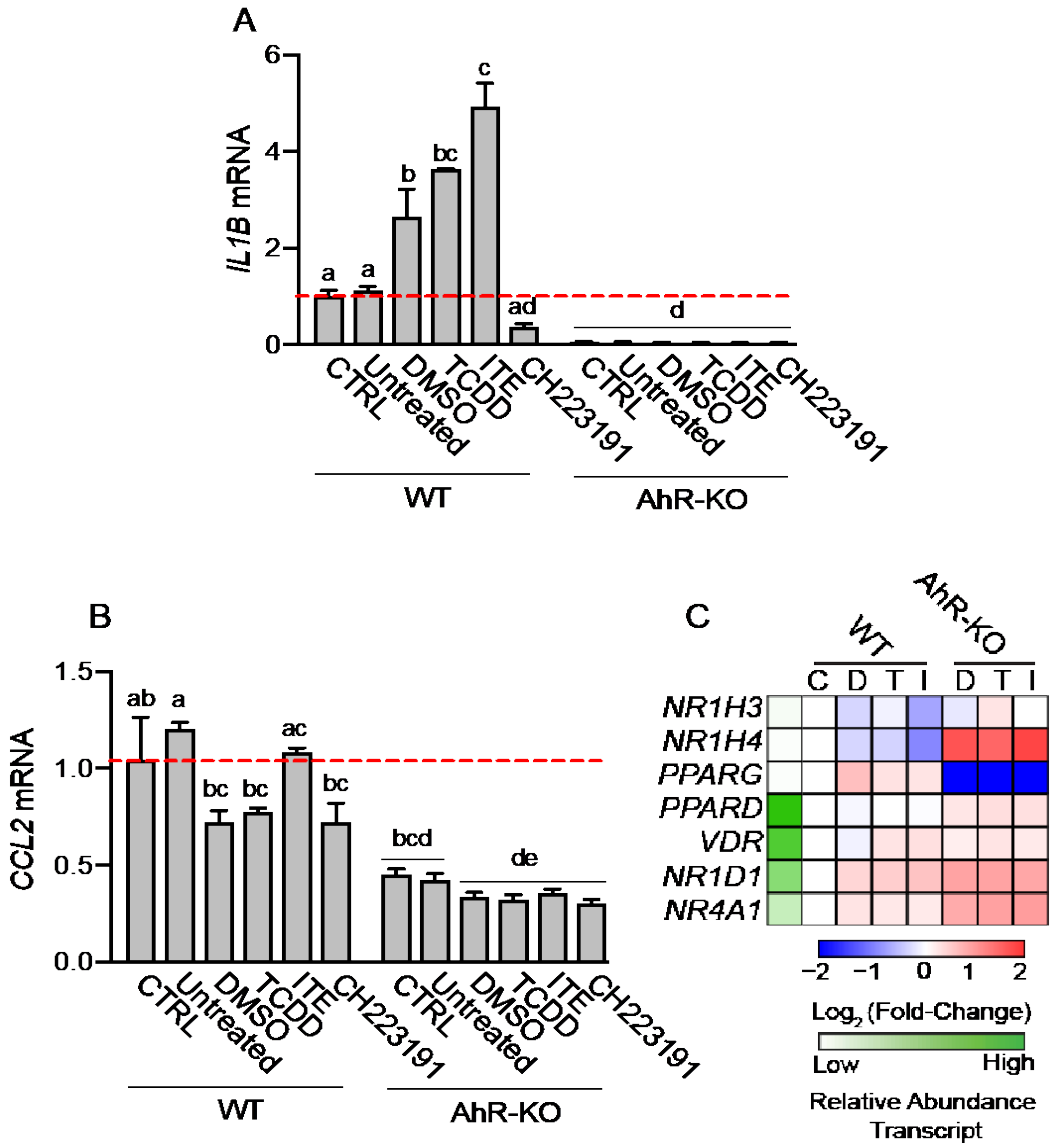

Figure 3.6 Cytokine and Nuclear Receptor Gene Expression is Modulated in AhR-KO Cells

Graphs show the mean fold-change (mean ± SEM) in mRNA expression relative to the wildtype control (CTRL) for *IL1B* (A) and *CCL2* (A) genes; fold-change of 1, indicated by the red-dashed line. Three samples were used for each treatment group; each sample was run in duplicate. Means that do not share a letter are significantly different from each other ($p < 0.05$). (C) RNA-seq was used to assess expression of nuclear receptor-related genes. Gene expression for all treatment groups was normalized to wildtype CTRL. Blue tiles indicate repression, and red tiles indicate induction of gene expressions. Relative transcript abundance depicts the mean of the normalized transcript counts of all samples for individual genes, normalizing for sequencing depth. Green tiles indicate a high (>1000) relative transcript abundance, and white tiles indicate a low (<10) relative transcript abundance. Letters on top represent the following: C = CTRL; D = DMSO T = TCDD, I = ITE, C = CH223191.

Knockout of AhR Increased LX-2 Cell Activation

To test whether AhR promotes HSC activation, we measured the protein levels of the HSC activation marker, αSMA, in wildtype and AhR-KO LX-2 cells. Immunofluorescence revealed that αSMA levels increased in AhR-KO cells (Figure 3.7A). Quantification of αSMA staining revealed that TCDD and ITE treatments decreased the expression of αSMA levels in comparison to untreated and DMSO treated wildtype LX-2 cells. The αSMA levels were not affected by CH223191 treatment. In the AhR-KO cells, αSMA levels increased in comparison to respective treatments in wildtypes (Figure 3.7B). The mRNA expression of *ACTA2* (which encodes αSMA) and *COL3A1* (which encodes collagen type III, alpha 1) showed a similar trend of gene induction in AhR-KO cells compared to wildtype cells (Figure 3.8A and B). However, no changes in *ACTA2* expression were detected in wildtype cells treated with TCDD and ITE. A similar trend was observed for *COL3A1* mRNA expression, as expression increased in AhR-KO cells regardless of treatment. Expression of *COL1A1*, which encodes collagen type I, and *TIMP1*, which encodes tissue inhibitors of metalloproteinases 1, was slightly, but not significantly, diminished in AhR-KO cells (Figure 3.8C and D). RNA-seq analysis revealed that *COL3A1*, *TGFB2*, *IGFBP3*, *FN1*, *PDGFRB*, *EDN1*, and *TGFA* were induced across all treatments in AhR-KO cells. In contrast, expression of *COL1A1*, *LOX*, *TGFβ1*, *PDGA*, *PDGFB*, and *PDGFC* were all repressed across in AhR-KO cells regardless of treatment (Figure 3.8E).

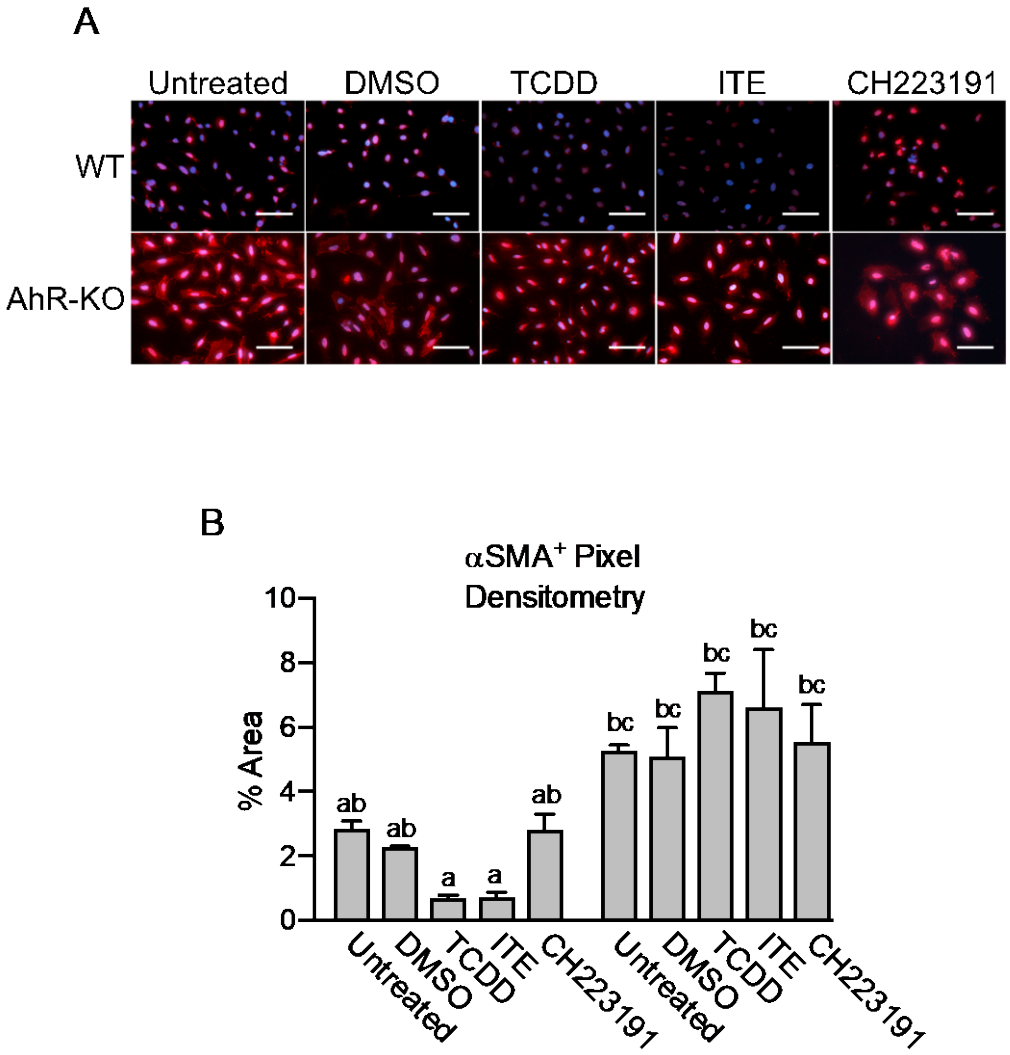

Figure 3.7 Increased αSMA Expression in AhR-KO LX-2 Cells

(A) Wildtype and AhR-KO LX-2 cells were treated with 10 nM TCDD or 1μM ITE or 1 μM CH223191 or equivalent DMSO (0.1% vol/vol) or left untreated altogether. αSMA expression was measured using fluorescence microscopy (anti-αSMA, red; DAPI, blue). Scale bar = 100 μm. (B) The pixel content of the red regions was quantified in five separate fields per sample and expressed as a percentage of the total number of pixels. Means that do not share a letter are significantly different from each other ($p < 0.05$).

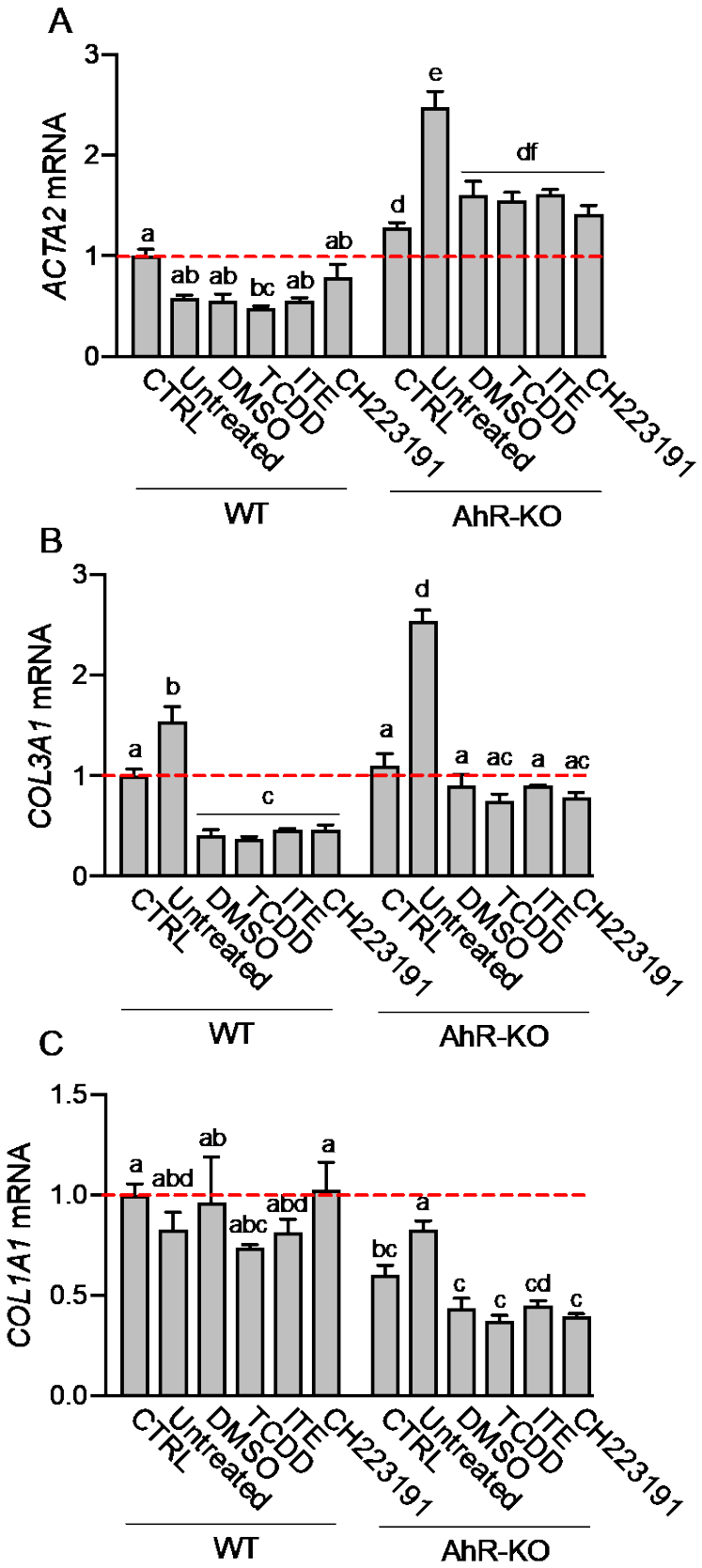
A
ACTA2 mRNA
3
2
1
0
a
ab
ab
bc
ab
ab
d
e
df
CTRL
Untreated
DMSO
TCDD
ITE
CH223191
WT
AhR-KO
B
COL3A1 mRNA
b
c
ac
C
COL1A1 mRNA
1.5
1.0
0.5
0.0
abd
abc
cd

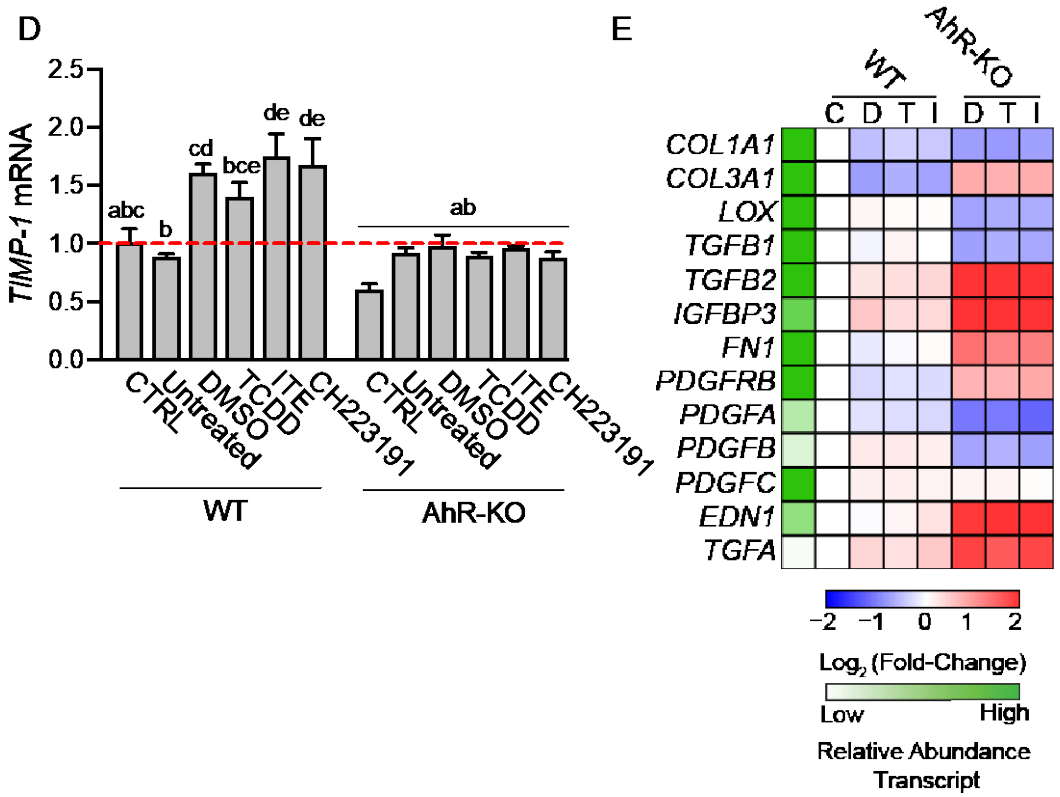

Figure 3.8 HSC Activation Markers in Wildtype and AhR-KO LX-2 Cells

Graphs show the mean fold-change (mean ± SEM) in mRNA expression relative to the wildtype control (CTRL) for HSC activation marker genes *ACTA2* (A), *COL3A1* (B), *COL1A1* (C), and *TIMP1* (D); fold-change of 1, indicated by the red-dashed line. Three samples were used for each treatment group; each sample was run in duplicate. Means that do not share a letter are significantly different from each other ($p < 0.05$). (E) RNA-seq was used to assess expression of HSC activation-related genes. Gene expression for all treatment groups was normalized to wildtype CTRL. Blue tiles indicate repression, and red tiles indicate induction of gene expressions. Relative transcript abundance depicts the mean of the normalized transcript counts of all samples for individual genes, normalizing for sequencing depth. Green tiles indicate a high (>1000) relative transcript abundance, and white tiles indicate a low (<10) relative transcript abundance. Letters on top represent the following: C = CTRL; D = DMSO T = TCDD, I = ITE, C = CH223191.

Expression of Extracellular Matrix Remodeling Genes Is Modulated in AhR-KO LX-2 Cells

TIMP2 expression increased in wildtype cells and AhR-KO cells in all treatment groups (Figure 3.9). Expression of fibrillar collagen genes *COL1A1*, *COL3A1*, and *COL4A5* was minimally impacted in wild-type cells, whereas *COL6A3*, a microfibril-

forming collagen, was markedly repressed (Figure 3.). Gene expression for *COL3A1*, and *COL4A5* showed moderate induction across all treatments in AhR-KO cells, while *COL6A2* and *COL6A3* showed robust repression. No treatment in wildtype cells elicited gene expression changes for the gelatinase *MMP2*, which was repressed in AhR-KO cells regardless of treatment. The scarcely expressed *MMP3*, which encodes the ECM remodeling protein stromolysin-1, showed moderate-to-high gene induction across all treatments in both wildtype and AhR-KO cells. Similarly, expression of *MMP9*, which encodes a gelatinase, was reduced in all treatment groups regardless of AhR expression. The mRNA expression of *PLAT* (tPA), the tissue-type plasminogen activator, was slightly increased in wildtype cells following TCDD and ITE treatments but was repressed in AhR-KO cells treated with DMSO, TCDD, or ITE. The mRNA levels of *SERPINE1* (PAI-1), a tPA inhibitor, and *SERPINH1*, a collagen synthesis chaperone, showed moderate repression in wildtype cells upon TCDD and ITE treatments but were moderately increased in AhR-KO cells upon DMSO, TCDD, and ITE treatment.

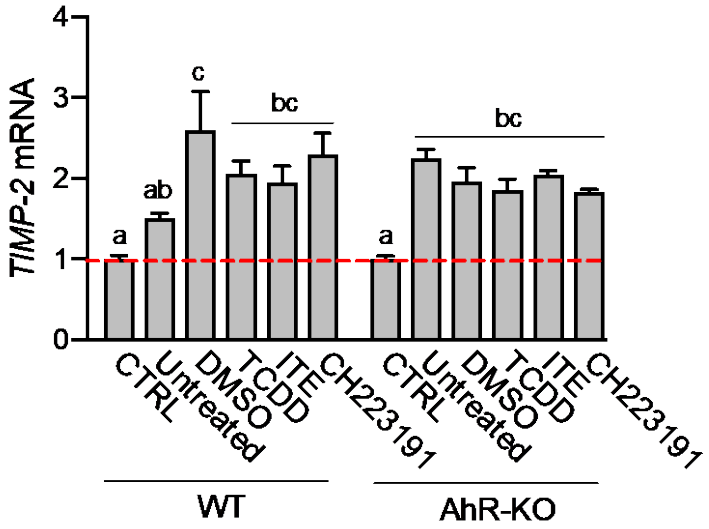

Figure 3.9 Expression of ECM Remodeling Genes in Wildtype and AhR-KO LX-2 Cells

Graphs show the mean fold-change (mean ± SEM) in *TIMP-2* mRNA expression relative to the wildtype control (CTRL); fold-change of 1, indicated by the red-dashed line. Three samples were used for each treatment group; each sample was run in duplicate. Means that do not share a letter are significantly different from each other ($p < 0.05$).

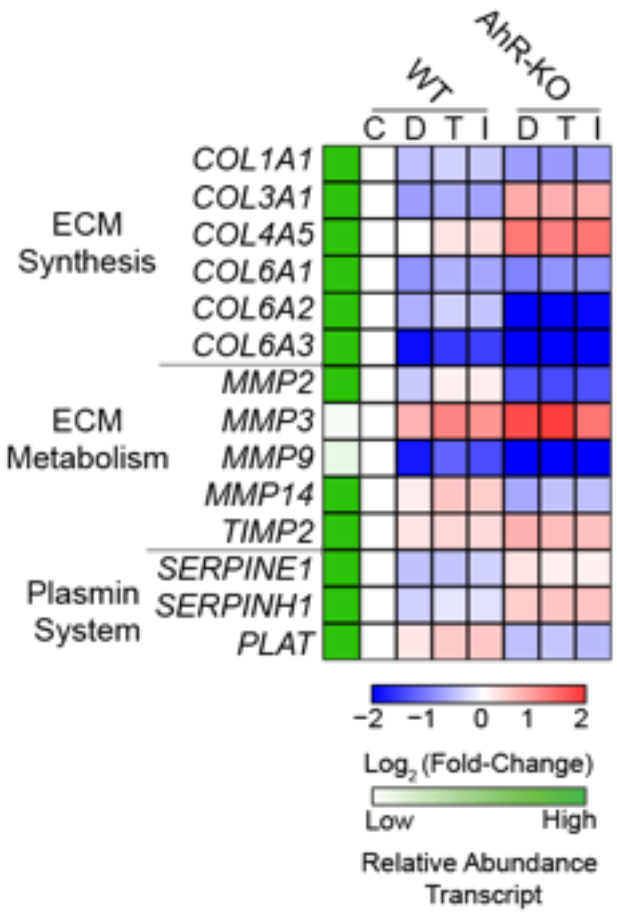

Figure 3.10 ECM Remodeling Markers in Wildtype and AhR-KO LX-2 Cells

Gene expression for all treatment groups was normalized to wildtype CTRL. Blue tiles indicate repression, and red tiles indicate induction of gene expressions. Relative transcript abundance depicts the mean of the normalized transcript counts of all samples for individual genes, normalizing for sequencing depth. Green tiles indicate a high (>1000) relative transcript abundance, and white tiles indicate a low (<10) relative transcript abundance. Letters on top represent the following: C = CTRL; D = DMSO T = TCDD, I = ITE, C = CH223191.

Discussion

The present study investigated the mechanistic role of AhR signaling in HSC activation. Several studies have suggested both a pro-fibrotic and an anti-fibrotic role of AhR signaling during HSC activation and the development of liver fibrosis. For instance, our lab showed that TCDD increases HSC activation in mouse and *in vitro* models of experimental liver fibrosis (Harvey *et al.*, 2016; Lamb *et al.*, 2016a). In contrast, treatment with the endogenous AhR agonist, ITE, reduced HSC activation and liver fibrosis in mice (Yan et al., 2019). These findings raise the intriguing possibility that HSC activation could be therapeutically targeted by AhR ligands to mitigate progression of liver fibrosis.

Results from this study indicate that removal of AhR signaling altogether increased LX-2 cell activation, which supports the notion endogenous AhR activity could repress HSC activation. Unexpectedly, LX-2 cell proliferation was diminished in the absence of the AhR.

To our knowledge, this is the first report of a stable AhR knockout in LX-2 cells. The AhR-KO cells were confirmed for single-clonal purity using the Inference of CRISPR edits (ICE) tool (https://ice.synthego.com/#/). Approximately 98% of the population from the selected clone was shown to be from a single cell (Supplementary Fig. S1B). Further, AhR-knockout was confirmed by the significant reduction of mRNA expression of *CYP1A1* and *CYP1B1*, which are AhR-regulated genes known to be induced upon TCDD treatment. Light-microscopic morphology of AhR-KO LX-2 cells were similar to wildtype cells (data not shown). This cell line may prove useful for advancing our knowledge of AhR biology in a pure population of HSCs *in vitro*.

The conflicting pro- and anti-fibrotic roles of AhR signaling during HSC activation and collagen deposition merit further investigation (Harvey *et al.*, 2016; Lamb *et al.*, 2016a; Yan *et al.*, 2019). It is possible that conflicting results are due to cell-specific roles of AhR and the influence of injury and inflammation during HSC activation during in vivo models. Our findings support the notion that AhR functionality is crucial for repressing HSC activation, as evidenced by the increase in αSMA protein and mRNA expression following AhR knockout. This observation corroborates another report in which primary mouse cells isolated from HSC-specific AhR knockout mice showed increased expression of activation markers (Yan et al., 2019). Interestingly, results from this present study suggest that gene expression of some HSC activation markers increased following AhR knockout, and while others decreased. This suggests that HSC activation could occur through "tiered" activation, with some markers requiring additional stimuli from secondary or tertiary signals, possibly from injury or inflammation.

We previously reported that TCDD treatment increased proliferation of cultured LX-2 cells (Harvey *et al.*, 2016). In contrast, primary mouse HSCs isolated from HSC-specific AhR knockout mice reportedly showed a significant increase in proliferation after culture-induced activation for 48 hours, but wildtype primary mouse HSCs failed to elicit a similar response (Yan et al., 2019). Overall, the role of AhR in regulating cell proliferation is unclear. Interestingly, we observed a lag period of 48 hours before cells commenced proliferation upon TCDD treatment (Harvey *et al.*, 2016). Based on all these data it can be speculated that the role of AhR on proliferation is time-dependent. Our data indicate that AhR signaling is required for optimal LX-2 cell proliferation, which is evident from the decrease in proliferation in AhR-KO cells. Interestingly, in wildtype

cells, TCDD treatment increased proliferation, whereas ITE treatment did not. It is possible that exogenous and endogenous ligands activate unique signaling cascades to produce these disparate effects.

HSC activation is characterized by increased proliferation and increased expression of genes involved in fibrogenesis. Recent reports suggest that AhR-mediated inhibition of HSC activation occurs independently of proliferation (Yan et al., 2019). This is corroborated by our data, in which removal of the AhR appeared to decrease cell proliferation but not activation. It is possible that endogenous AhR activity positively regulates cell cycle progression through expression of *CCND1* and *CDKN1A*, which positively and negatively regulate passage through the G1/S checkpoint of the cell cycle, respectively. *CDKN1A* encodes the Cip/Kip inhibitor, p21Cip1, the expression of which would be expected to halt proliferation. Endogenous AhR activation may be preventing the upregulation of *CDKN1A* mRNA. A decrease in *CDKN1B* mRNA expression in AhR-KO without affecting the proliferation suggests that the reduction of proliferation in AhR-KO cells is independent of *CDKN1B* and dependent on *CDKN1A*.

It is known that activated HSCs produce diverse mitogenic and fibrogenic cytokines and cytokine receptors for autocrine and paracrine signaling. On one hand, our data demonstrate that AhR knockout significantly decreased *CCL2* mRNA expression, which functions as an autocrine stimulus, as well as a monocyte and lymphocyte chemoattractant (Marra et al., 1993; Marra et al., 1999). It is possible that *CCL2* had a limited role in our model system towards HSC activation. Another important cytokine mediator, IL-1B, was recently shown to reduce αSMA expression in human HSCs. Data from our study suggest that *IL1B* expression is severely repressed in AhR-KO cells. This

led us to speculate that one of the mechanisms by which endogenous AhR signaling prevents HSC activation is by inducing *IL1B* expression. On the other hand, expression of the transcription factor receptor *NR1H4*, which is known to modulate HSC activation by inhibiting glucose and lipid metabolism, was significantly increased upon AhR knockout (Kong *et al.*, 2009). In contrast, expression of *PPARG*, which encodes another nuclear receptor known to negatively modulate HSC activation (Hazra *et al.*, 2004), was significantly decreased in AhR-KO LX-2 cells. These positive and negative regulatory events could be the direct result of AhR knockdown, or they could reflect secondary effects elicited to compensate for the knockdown.

Our data showed that TCDD and ITE altered the expression of only a subset of genes involved in ECM remodeling, which implies that the induction of some of these genes may require additional signaling from injury and/or inflammation. For example, *TGFB1* and *COL1A1* gene expression were not affected by TCDD and ITE treatments. Previous studies have shown that TCDD treatment modulates ECM remodeling genes *in vivo* (Lamb et al., 2016b). Interestingly, AhR removal had minimal effects on the expression of these two genes, implying that endogenous AhR signaling play a minimal role in regulating gene expression for *TGFB1* and *COL1A1*. It is possible that AhR is required for the expression of *MMP2*, *MMP9*, and *MMP14* genes. Interestingly, *MMP3* gene expression increased upon AhR activation and further increased upon AhR removal. For example, knocking out the AhR from LX-2 cells slightly induced *SERPINE1* (PAI-1) and *SERPINH1* expression and decreased *PLAT* (tPA). Hence it is possible that AhR removal reduces levels of plasmin, which is known to convert pro-MMPs into enzymatically active MMPs. It is possible that the AhR is regulating the expression of

certain genes directly. Further investigation will be needed to assess how endogenous AhR activity impacts MMP expression. This could occur through a direct effect or by indirectly modulating expression of MMPs, TIMPs, and other regulators in the plasmin system.

In conclusion, we established a novel AhR-KO LX-2 cell line to study the endogenous and exogenous role of AhR activation. This enabled us to study the role of AhR signaling in HSC activation without the involvement of hepatic inflammation and injury, which are typically present in *in vivo* models of experimental liver fibrosis. Our findings provide further evidence to support a role for endogenous AhR activity in repressing HSC activation. In the absence of endogenous AhR activity, LX-2 cell proliferation decreased, while endpoints of activation increased. Future studies should include an examination of the distinct signaling pathways used during HSC proliferation and activation to identify unique targets that could potentially be modulated by therapeutic AhR ligands to reduce or reverse HSC activation and curtail liver fibrosis.

Supplementary Material and Methods

Generation of AhR-KO LX-2 cells

Sanger-Sequencing

The region around exon-2 of the AhR gene was amplified using the primers listed in Supplementary Table S1. The PCR protocol consisted of a 10-minute enzyme activation at 95°C, followed by 40 cycles (30 seconds at 95°C, 30 seconds at the annealing temperature, and 30 seconds at 72 C), and a final extension for 7 minutes at 72°C. Cleaning and sequencing of the PCR product was carried out at the Molecular Research Core Facility (Idaho State University, Pocatello, ID). Briefly, cleaned PCR

products were quantified using the Qubit 2.0 Fluorometer and prepared for sequencing using the BigDye® Terminator v3.1 Cycle Sequencing Kit (Applied Biosystems, Cat. #4337455) and sequenced on an Applied Biosystems 3130xl Genetic Analyzer with a 3130xl⁄3100 Genetic Analyzer 16-Capillary Array, 50 cm. Sequencing base calls were determined by Sequence Analysis Software v6.0 using the default analysis settings.

Single Clone Isolation of AhR Mutant Clones

After nucleofection with the gRNA-2 RNP, LX-2 cells were plated on a 10-cm culture dish (1000 cells/dish) and incubated for 10 days. On day 11, individual clones were collected with sterile pipet tips and transferred to 96-well tissue-culture plates. Thirty-four clones were selected this way and expanded in culture for several days. DNA was then isolated from these clones, and the region around exon-2 was amplified. The quality of the PCR product was assessed by resolving it on a 2% agarose gel and visualizing bands with ethidium bromide (Supplementary Figure 3.S1A). The PCR products were then analyzed by Sanger sequencing using the protocol described above.

Supplementary Data

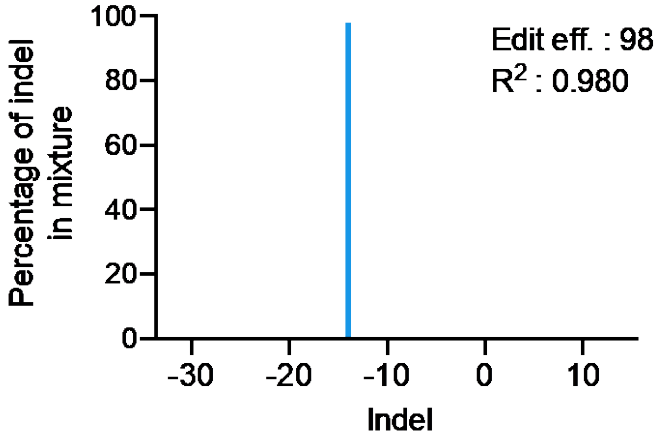

Supplementary Figure 3.1 Generation of AhR-KO LX-2 Cells

The percentage of insertion-deletion (INDEL) mutations in clone-2 was calculated using the Sanger ICE online tool. The X-axis represents the number of base pairs of addition or deletion. The Y-axis represents the percentage of INDEL mixtures. The editing efficiency refers to the percentage of INDEL mixtures.

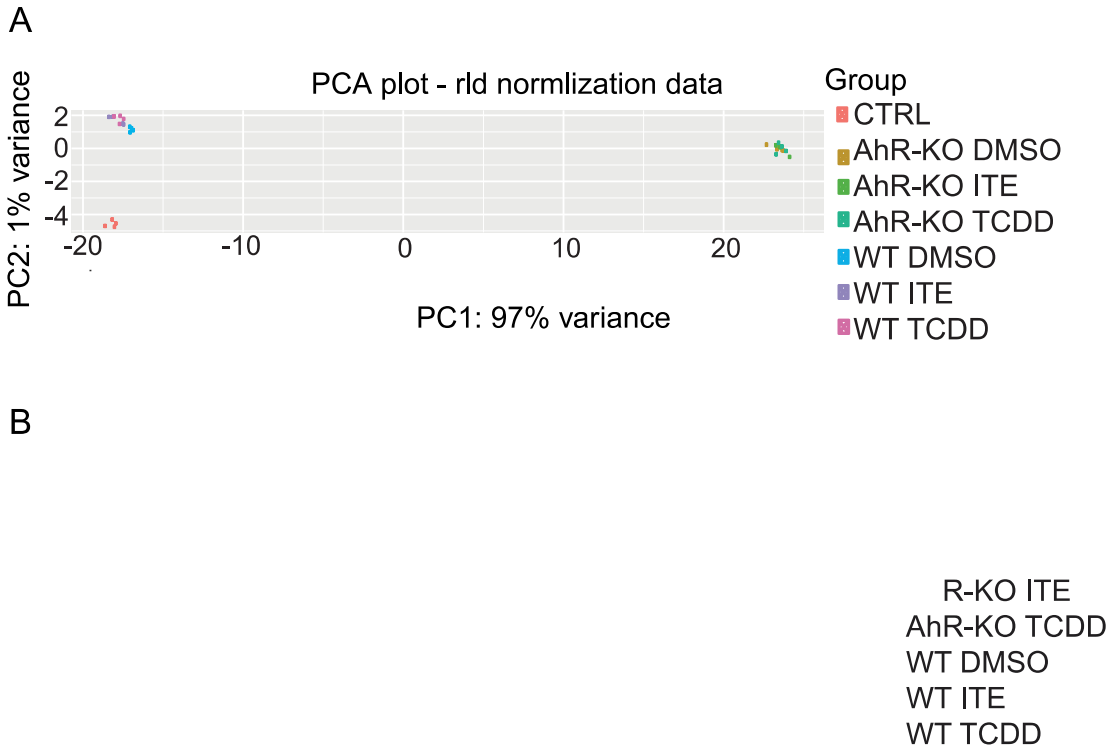

Supplementary Figure 3.2 Analysis of Gene Expression Variances Using Principal Component Analysis (PCA).

PCA analysis of gene expression across all treatments in wildtype and AhR-KO LX-2 cells. The components PC1 and PC2 define the x- and y-axis, respectively. The distance between any two points represents the variance in gene expression between them. (A) PCA plot was generated using the rlog transformation (rld) function of normalized count data. (B) PCA plot was generated using the variance stabilizing transformation (vst) function of normalized count data.

A

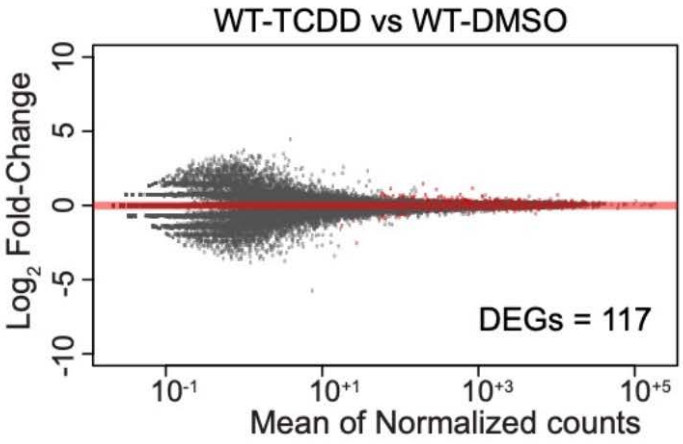
WT-TCDD vs WT-DMSO
Log2 Fold-Change
10
5
0
-5
-10
DEGs = 117
10-1
10+1
10+3
10+5
Mean of Normalized counts

B

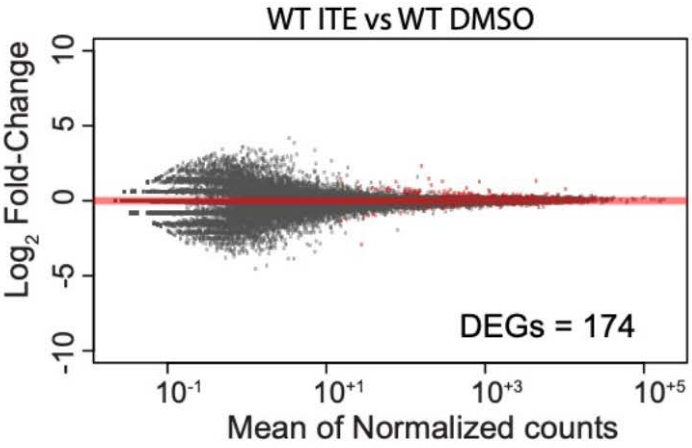
WT ITE vs WT DMSO
Log2 Fold-Change
10
5
0
-5
-10
DEGs = 174
10-1
10+1
10+3
10+5
Mean of Normalized counts

C

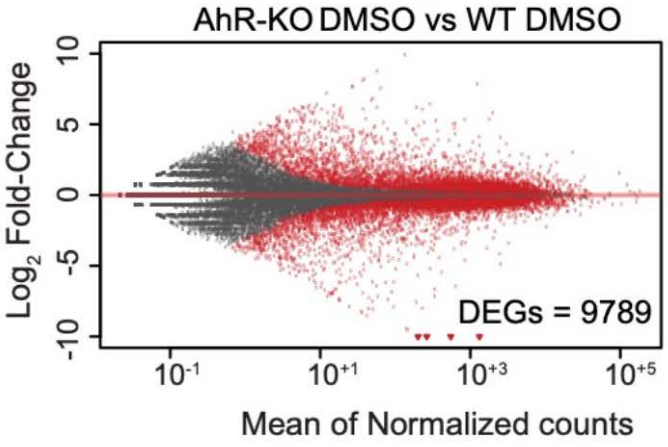
AhR-KO DMSO vs WT DMSO
Log2 Fold-Change
10
5
0
-5
-10
DEGs = 9789
10-1
10+1
10+3
10+5
Mean of Normalized counts

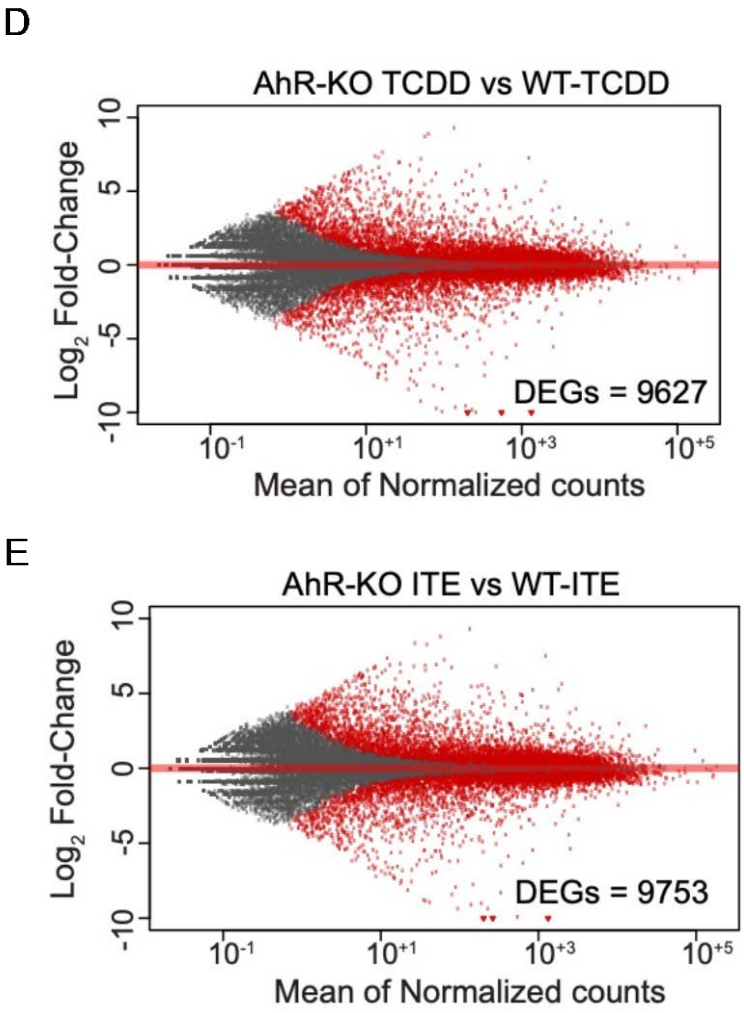

Supplementary Figure 3.3 'MA Plots' for Differentially Expressed Genes

(A-E) 'MA plots' for differentially expressed genes (red) enriched for the defined comparisons shown at the top of each figure.

References

Canbay, A. *et al.* (2003) 'Apoptotic body engulfment by a human stellate cell line is profibrogenic', *Laboratory Investigation*, 83(5), pp. 655–663.

Casini, A. *et al.* (1997) 'Neutrophil-derived superoxide anion induces lipid peroxidation and stimulates collagen synthesis in human hepatic stellate cells: role of nitric oxide', *Hepatology*, 25(2), pp. 361–367.

Cradick, T. J. *et al.* (2014) 'COSMID: A web-based tool for identifying and validating CRISPR/Cas off-target sites', *Molecular Therapy - Nucleic Acids*, 3(12), pp. 212–222.

Fernandez-Salguero, P. *et al.* (1996) 'Aryl-hydrocarbon receptor-deficient mice are resistant to 2,3,7,8-tetrachlorodibenzo-p-dioxin-induced toxicity', *Toxicology and Applied Pharmacology*, 140, pp. 173–179.

Han, M. *et al.* (2017) '2,3,7,8-Tetrachlorodibenzo-p-dioxin (TCDD) induces hepatic stellate cell (HSC) activation and liver fibrosis in C57BL6 mouse via activating Akt and NF-κB signaling pathways', *Toxicology Letters*, 273, pp. 10–19.

Harvey, W. A. *et al.* (2016) 'Exposure to 2,3,7,8-tetrachlorodibenzo-p-dioxin (TCDD) increases human hepatic stellate cell activation', *Toxicology*, 26(33), pp. 344–346.

Hazra, S. *et al.* (2004) 'Peroxisome proliferator-activated receptor γ induces a phenotypic switch from activated to quiescent hepatic stellate cells', *The Journal of Biological Chemistry*, 279(12), pp. 11392–11401.

Iwaisako, K. *et al.* (2014) 'Origin of myofibroblasts in the fibrotic liver in mice', *Proceedings of the National Academy of Sciences of the United States of America*, 111(32), pp. 3297–3305.

Kim, D., Langmead, B. and Salzberg, S. L. (2015) 'HISAT: a fast spliced aligner with low memory requirements', *Nature Methods*, 12(4), pp. 357–360.

Kisseleva, T. and Brenner, D. A. (2007) 'Role of hepatic stellate cells in fibrogenesis and the reversal of fibrosis', *Journal of Gastroenterology and Hepatology*, 22(1), pp. 73–78.

Kisseleva, T. and Brenner, D. A. (2008) ‘Mechanisms of fibrogenesis’, *Experimental Biology and Medicine*, 233(2), pp. 109–122.

Kong, B. *et al.* (2009) ‘Farnesoid x receptor deficiency induces nonalcoholic steatohepatitis in low-density lipoprotein receptor-knockout mice fed a high-fat diet’, *Journal of Pharmacology and Experimental Therapeutics*, 328(1), pp. 116–122.

Lamb, C. L. *et al.* (2016a) ‘2,3,7,8-Tetrachlorodibenzo-p-dioxin (TCDD) increases necroinflammation and hepatic stellate cell activation but does not exacerbate experimental liver fibrosis in mice’, *Toxicology and Applied Pharmacology*, 311, pp. 42–51.

Lamb, C. L. *et al.* (2016b) ‘Aryl hydrocarbon receptor activation by TCDD modulates expression of extracellular matrix remodeling genes during experimental liver fibrosis’, *BioMed Research International*, 2016, pp. 1–13.

Livak, K. J. and Schmittgen, T. D. (2001) ‘Analysis of relative gene expression data using real-time quantitative PCR and the 2(-Delta Delta C(T)) method’, *Methods*, 25(4), pp. 402–408.

Love, M. I., Huber, W. and Anders, S. (2014) ‘Moderated estimation of fold change and dispersion for RNA-seq data with DESeq2’, *Genome Biology*, 15(12), pp. 550–571.

Marra, F. *et al.* (1993) ‘Cultured human liver fat-storing cells produce monocyte chemotactic protein-1 regulation by proinflammatory cytokines’, *Journal of Clinical Investigation*, 92(4), pp. 1674–1680.

Marra, F. *et al.* (1999) ‘Monocyte chemotactic protein-1 as a chemoattractant for human hepatic stellate cells’, *Hepatology*, 29(1), pp. 140–148.

Maza, E. *et al.* (2013) ‘Comparison of normalization methods for differential gene expression analysis in RNA-Seq experiments: a matter of relative size of studied transcriptomes’, *Communicative and Integrative Biology*, 6(6), pp. 1–8.

Moreira, R. K. (2007) ‘Hepatic stellate cells and liver fibrosis’, *Archives of Pathology and Laboratory Medicine*, 131, pp. 1728–1733.

Naito, M. *et al.* (2004) 'Differentiation and function of kupffer cells', *Medical Electron Microscopy*, 37(1), pp. 16–28.

Nault, R. *et al.* (2016) 'Dose-dependent metabolic reprogramming and differential gene expression in TCDD-elicited hepatic fibrosis', *Toxicological Sciences*, 154(2), pp. 253–266.

Nebert, D. W. and Karp, C. L. (2009) 'Endogenous functions of the aryl hydrocarbon receptor (AHR): intersection of (CYP1)-metabolized eicosanoids', *The Journal of Biological Chemistry*, 283(52), pp. 36061–36065.

Nguyen, L. P. and Bradfield, C. A. (2008) 'The search for endogenous activators of the aryl hydrocarbon receptor', *Chemical Research in Toxicology*, 21, pp. 102–116.

Pierre, S. *et al.* (2014) 'Aryl hydrocarbon receptor-dependent induction of liver fibrosis by dioxin', *Toxicological Sciences*, 137(1), pp. 114–123.

Puga, A., Ma, C. and Marlowe, J. L. (2009) 'The aryl hydrocarbon receptor cross-talks with multiple signal transduction pathways', *Biochemical Pharmacology*, 77, pp. 713–722.

Thatcher, T. H. *et al.* (2015) 'Endogenous ligands of the aryl hydrocarbon receptor regulate lung dendritic cell function', *Immunology*, 147, pp. 41–53.

Tsukamoto, H. (1999) 'Cytokine regulation of hepatic stellate cells in liver fibrosis', *Alcoholism: Clinical and Experimental Research*, 23(5), pp. 911–916.

Walla, R. J. *et al.* (2012) 'Novel 2-amino-isoflavones exhibit aryl hydrocarbon receptor agonist or antagonist activity in a species/cell-specific context', *Toxicology*, 297(1), pp. 26–33.

Wynn, T. (2008) 'Cellular and molecular mechanisms of renal fibrosis', *Journal of Pathology*, 214(2), pp. 199–210.

Xu, L. *et al.* (2005) 'Human hepatic stellate cell lines, LX-1 and LX-2: new tools for analysis of hepatic fibrosis.', *Gut*, 54(1), pp. 142–151.

Yan, J. *et al.* (2019) ‘Aryl hydrocarbon receptor signaling prevents activation of hepatic stellate cells and liver fibrogenesis in mice’, *Gastroenterology*, 157(3), pp. 793–806.

Yoshida, T. *et al.* (2012) ‘Effects of AhR ligands on the production of immunoglobulins in purified mouse B cells’, *Biomedical Research*, 33(2), pp. 67–73.

CHAPTER FOUR: SUMMARY AND FUTURE DIRECTIONS

Summary

Several studies implicate a role for AhR signaling in the regulation of HSC activation and the development of liver fibrosis. However, little is known about AhR activation in this relatively small population of liver cells. Furthermore, in the absence of liver injury or inflammation, HSCs typically exist in a quiescent form. It is quite possible that short-term transient activation of the AhR with a potent agonist such as TCDD fails to elicit remarkable changes in quiescent HSCs. This could explain why previous studies failed to find any significant, reproducible effects of AhR activation on these cells. Given the involvement of multiple liver cell populations in the development of fibrosis, the endogenous role of the AhR may be unique among individual cell populations.

The first goal of this dissertation was to determine how AhR signaling in hepatocytes and in HSCs contributed to HSC activation and fibrogenesis in mice treated chronically with TCDD. One of the challenges of in vivo studies is presence of confounding variables, such as injury and inflammation, which also facilitate HSC activation. This makes it difficult to distinguish between AhR-mediated events in the HSCs and those events in hepatocytes and other cells, such as macrophages. The second goal of this dissertation was to determine the direct impact of AhR functionality during HSC activation, in the absence of secondary effects. To accomplish this AhR signaling was evaluated in LX-2 cells lacking AhR functionality. Furthermore, transcriptome

analysis was carried out for liver tissues from mice and LX-2 cells to identify AhR-modulated transcriptional changes.

Results from Chapter 2 indicate that TCDD increases HSC activation through a mechanism that requires AhR signaling in hepatocytes. Moreover, this possibly occurs through a steatosis-dependent mechanism that is independent of inflammation. Although less likely, we cannot completely exclude the possibility that TCDD directly activates HSCs, but maximal HSC activation in TCDD-treated mice is not achieved through AhR signaling in HSCs alone. We also found that AhR signaling in hepatocytes and HSCs was not an absolute requirement for hepatic inflammation.

Data presented in Chapter 3 describe the successful creation of the AhR-KO LX-2 cells, which were then used to investigate the impact of endogenous and exogenous AhR activity on HSC activation. Results support the notion that the AhR functions as an endogenous repressor of HSC activation. Furthermore, we found that removal of the AhR decreased LX-2 cell proliferation. It is possible that the reduction of proliferation in AhR-deficient cells occurs through the upregulation of p21Cip1, which is a negative regulator of cell cycle progression at the G1/S phase checkpoint. This AhR-deficient cell line could be used to investigate how alternative AhR ligands might be used therapeutically to modulate HSC proliferation and activation, both of which could influence the development and progression of liver disease.

Future Directions

The complex role AhR activity in liver fibrosis highlights the intriguing possibility that the AhR could play diverse, cell-specific roles during liver health and disease. A recent study reported that chronic exposure to TCDD modulated hepatocyte

gene expression to essentially reorganize glycogen, ascorbic acid, and amino acid metabolism in support of ECM remodeling (Nault *et al.*, 2016). However, the contribution of AhR to these individual metabolic pathways is largely unknown. For instance, transcriptome analysis of hepatic tissue from mice with AhR-deficient hepatocytes identified 570 genes that were differentially expressed in response to TCDD. In comparison, only 21 genes were differentially expressed in the liver of TCDD-treated mice with AhR-deficient HSCs, compared to their wild-type counterparts. It could be argued that, since hepatocytes make up about 80% of the liver cell population, and because my research shows that TCDD directly targets hepatocytes, one would expect to see a large number of differentially expressed genes. However, very few genes were found to be sigificantly repressed in both hepatocyte- and HSC-specific knockout mice. Hence, specific genes and pathways may be exclusively dependent on hepatocyte- and HSC-specific AhR signaling. A logical next step would be to validate these genes and pathways to understand their contributions to HSC activation and liver fibrosis. Eventually, this might shed light on how AhR signaling impacts liver fibrosis.

The physiological role of endogenous AhR activity likely depends on the tissue of consideration, and this is an emerging area of research. In LX-2 cells, AhR activation by TCDD or ITE produced 117 and 174 differentially expressed genes, respectively, when compared to untreated cells. It can be speculated that the difference in gene expression for 57 genes is probably due to endogenous AhR signaling, as ITE is a potent endogenous ligand of the AhR. It would be logical to further assess the molecular pathways that these 57 genes regulate to understand endogenous ligand-specific AhR activation. Furthermore, the transcriptome analysis of AhR-knockout LX-2 cells revealed 9789 differentially

expressed genes compared to wildtype LX-2 cells. This significant number raises the possibility of the interplay and crosstalk between the AhR and a wide variety of pathways and genes. Future studies could validate changes in enriched pathways and shed light on divergent and convergent AhR signaling pathways. Accomplishing these tasks will potentially provide a basis for additional studies to identify and test novel AhR ligands for therapeutic use as modulators of HSC activation.

References

Nault, R. *et al.* (2016) ‘Dose-dependent metabolic reprogramming and differential gene expression in TCDD-elicited hepatic fibrosis’, *Toxicological Sciences,* 154(2), pp. 253–266.

APPENDIX A

Generation of Mice With AhR-Deficient Hepatocytes and AhR-Deficient Hepatic Stellate Cells

Introduction

Experiments in this dissertation rely on the generation of mice with a liver cell-specific deletion of the aryl hydrocarbon receptor (AhR). To this end, a Cre-Lox system was used to selectively remove the AhR from either hepatocytes or hepatic stellate cells (HSCs).

Mice expressing floxed AhR gene ($Ahr^{tm3.1Bra}$/J, The Jackson Laboratory, Bar Harbor, ME), referred to as $AhR^{fl/fl}$, were crossbred with each other to produce male $AhR^{fl/fl}$. For hepatocyte-specific AhR knockout mice, referred to as $AhR^{\Delta Hep}$ mice, female albumin-Cre recombinase (Alb-Cre) transgenic mice (B6N.Cg-Speer6-ps1$^{Tg(Alb\text{-}cre)21Mgn}$/J, The Jackson Laboratory) were crossbred with male $AhR^{fl/fl}$ mice to produce $AhR^{fl;Alb\text{-}cre}$ females. $AhR^{fl;Alb\text{-}cre}$ females were then crossbred with $AhR^{fl/fl}$ males to generate mice homozygous for floxed AhR and hemizygous for Alb-Cre. Mice homozygous for floxed AhR were used as controls and referred to as $AhR^{fl/fl}$. Similarly, for HSC-specific AhR knockout mice, referred to as $AhR^{\Delta HSC}$ mice, female glial fibrillary acidic protein promoter-Cre recombinase (GFAP-Cre) transgenic mice (FVB-Tg(GFAP-cre)25Mes/J, The Jackson Laboratory, Bar Harbor, ME) were crossbred with male $AhR^{fl/fl}$ mice to produce $AhR^{fl;\,GFAP\text{-}cre}$ females. $AhR^{fl;\,GFAP\text{-}cre}$ females were crossbred with $AhR^{fl/fl}$ males to generate mice with homozygous for floxed AhR and heterozygous for GFAP-Cre. Several reports suggest that GFAP-Cre specifically targets HSCs (Kocabayoglu *et al.*, 2016; Ceni *et al.*, 2017; Alsamman *et al.*, 2018). mice were used as controls. All individuals were generated on a C57BL/6 background.

AhR Gene Alleles

Mice express one of four phenotypic alleles of the AhR gene: Ah^{b-1}, Ah^{b-2}, Ah^{b-3}, and Ah^{d} (Poland and Glover, 1990). The Ah^{b-1} allele encodes a protein of 805 amino acids (~95kDa), the Ah^{d} and Ah^{b-2} alleles encode a protein of 848 amino acids (~104kDa), and the Ah^{b-3} allele encodes a protein of 883 amino acids (~105kDa) (Poland, Glover and Taylor, 1987; Poland and Glover, 1990). These allelic variants of the AhR express different binding affinities for 2,3,7,8-tetrachlorodibenzo-p-dioxin (TCDD) (Chang and Puga, 1998). Ah^{b-1}, Ah^{b-2}, and Ah^{b-3} alleles encode an AhR protein with high ligand-binding affinity, whereas the Ah^{d} allele encodes a protein with low-binding affinity. These four alleles are distributed across strains of laboratory mice such that some strains of mice are sensitive to TCDD toxicity, whereas other strains are highly resistant. For example, C57Bl/6 mice carry the Ah^{b-1} allele that encodes an AhR that binds to TCDD with high affinity. As a result, these mice are sensitive to the toxic effects of TCDD, with an LD50 of ~ 114 µg/kg (Poland, Palen and Glover, 1994). Most studies of TCDD toxicity and AhR biology have been conducted in C57Bl/6 mice. In contrast, strains that express the d allele of the AhR, such as FVB-129 are highly resistant to TCDD toxicity, requiring doses of TCDD that are 10-20 times higher to produce lethality (LD50 of ~ 536 µg/kg) (Swanson and Bradfield, 1993). 129SvJ ES mice are widely used in the production of targeted mutations due to the availability of multiple embryonic stem cell lines derived from them. In fact, the $AhR^{fl/fl}$ used for initial breeding was on a 129SvJ ES background.

The change in affinity among alleles is attributed to structural changes associated with amino acid mutations. A study conducted by overlapping five fragments of AhR

coding sequence and PCR sequencing ten, 10-nucleotide differences between Ah^{b-1} and Ah^{d} alleles. Five of the differences were found to be silent. Among the remaining five, four of them replaced the leucine residue in Ah^{b-1} with a proline residue in Ah^{d}, which results in a potential break in the alpha-helix near the Q-rich region of the AhR. The one remaining change replaces the termination codon in Ah^{b-1} with an arginine residue in Ah^{d} at position 3330. This extends translation by 43 amino acids, which eventually results in a change in size from 95 kDa to 105 kDa (Chang *et al.*, 1993).

Because we used SV129 mice (Ah^{d} allele) and crossed them with C57Bl/6 mice (b allele), it was important to identify which AhR allele was expressed in the offspring, as this would be the main factor in selecting the dose of TCDD used for our experiments.

Materials and Methods

DNA Isolation

Tissue was collected by ear punch from founder mice and offspring. DNA was extracted using Extracta™ DNA Prep for PCR (Quanta Biosciences, Beverly MA) according to the manufacturer's protocol.

Primer Design

Primers were designed to flank exon 11 of the AhR, which has 12 nucleotides; the point mutation was expected to occur at the 10^{th} position. Forward primer (CGAAAGACTTAGCCATGAGC) and reverse primer (GAAGTTACTGAGCAGGGAACC) were designed to anneal to DNA 123 and 292 nucleotides from the expected point mutation.

PCR Amplification

Genomic DNA (100 ng) was amplified with the primers shown above using GoTaq G2 colorless master mix (Promega, Madison, WI). Samples were run in duplicate. The master mix containing genomic DNA and primers was preincubated at 95° C for 10 minutes followed by 40 cycles at the following protocol: denaturation at 95° C for 30 seconds, annealing at 57° C for 30 seconds, amplification at 72° C for 30 seconds for 40 cycles. After a final extension at 72° C for 10 minutes, PCR products were separated on a 2% agarose gel, and bands were visualized under UV light using ChemiDoc imaging systems (Biorad, Hercules, CA). The expected amplicon size was 516 base pairs.

Sanger Sequencing

Sanger sequencing was carried out at Idaho State University. In brief, the amplified products were cleaned using a PCR Cleanup kit (Thermo Scientific, Waltham, CA) and prepared for sequencing using the BigDye® Terminator v3.1 Cycle sequencing kit (Applied Biosystems, Foster City, CA). Sequencing was performed on Applied Biosystems 3130xl Genetic Analyzer with a 3130x*l*/3100 Genetic Analyzer 16-Capillary Array, 50 cm; sequencing base calls were determined by sequence analysis software v6.0 using the default analysis settings.

Results

$AhR^{fl/fl}$, $AhR^{\Delta Hep}$, and $AhR^{\Delta HSC}$ Mice Express the Ah^{d} Allele

To determine which AhR allele was expressed in the cell-specific knockout mice, we sequenced exon 11. The results in Figure A.1 show the sequencing data of exon 11 in C57BL/6, $AhR^{fl/fl}$, $AhR^{\Delta Hep}$, and $AhR^{\Delta HSC}$ mice. C57BL/6 was found to have thymine, and $AhR^{fl/fl}$, $AhR^{\Delta Hep,}$ and $AhR^{\Delta HSC}$ mice were found to have cytosine, at position 3330.

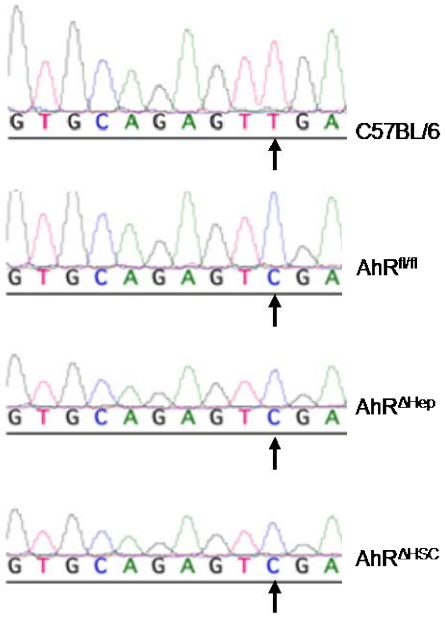

Figure A.1 Sanger Sequence Analysis of Amplified PCR Products

The nucleotide sequence at position 3330 (indicated by the black arrow) indicates whether the b or d AhR allele is expressd.

Discussion

In this study, we determined which allele was present in the mice used for the experiments described in Chapter 2. $AhR^{fl/fl}$, $AhR^{\Delta Hep}$, and $AhR^{\Delta HSC}$ mice were all found to have the 'd' allele, which encodes an AhR protein with relatively low ligand-binding affinity. This is due to the fact that conditional $AhR^{fl/fl}$ mice were originally generated from 129SvJ ES cells that carry the lower affinity Ah^{d} (Walisser *et al.*, 2005).

In Chapter 2, we used a 100-µg/kg dose of TCDD, which is 3-4 times higher than 25-30 µg/kg doses reportedly in other studies of TCDD-induced liver fibrosis in C57BL/6 mice that carry the b allele (Pierre *et al.*, 2014; Nault *et al.*, 2016). Other investigators have used the 100 ug/kg dose of TCDD to produce classic endpoints of TCDD toxicity in mice carrying the d allele (Walisser *et al.*, 2005). This dose was found to induce hepatomegaly, mild elevation in serum ALT levels, and increased expression of Cyp1a1. Furthermore, it did not produce any lethality. For this reason, we selected the 100 µg/kg dose of TCDD to use in the experiments described in Chapter 2.

References

Alsamman, M. *et al.* (2018) 'Endoglin in human liver disease and murine models of liver fibrosis-A protective factor against liver fibrosis', *Liver International*, 38(5), pp. 858–867.

Ceni, E. *et al.* (2017) 'The orphan nuclear receptor COUP-TFII coordinates hypoxia-independent proangiogenic responses in hepatic stellate cells', *Journal of Hepatology*, 66(4), pp. 754–764.

Chang, C.-Y. and Puga, A. (1998) 'Constitutive activation of the aromatic hydrocarbon receptor', *Molecular and Cellular Biology*, 18(1), pp. 525–535.

Chang, C. *et al.* (1993) 'Ten nucleotide differences, five of which cause amino acid changes, are associated with the Ah receptor locus polymorphism of C57BL/6 and DBA/2 mice', *Pharmacogenetics*, pp. 312–21.

Kocabayoglu, P. *et al.* (2016) 'Induction and contribution of β-PDGFR signaling by hepatic stellate cells to liver regeneration after partial hepatectomy in mice', *Liver International*, 36(6), pp. 874–882.

Nault, R. *et al.* (2016) 'Dose-dependent metabolic reprogramming and differential gene expression in TCDD-elicited hepatic fibrosis', *Toxicological Sciences*, 154(2), pp. 253–266.

Pierre, S. *et al.* (2014) 'Aryl hydrocarbon receptor-dependent induction of liver fibrosis by dioxin', *Toxicological Sciences*, 137(1), pp. 114–124.

Poland, A. and Glover, E. (1990) 'Characterization and strain distribution pattern of the murine Ah receptor specified by the Ah ' and Ahb3 Alleles', *Molecular Pharmacology*, 38, pp. 306–312.

Poland, A., Glover, E. and Taylor, B. A. (1987) 'The murine Ah locus: a new allele and mapping chromosome 12', *Molecular Pharmacology*, 32, pp. 471–478.

Poland, A., Palen, D. and Glover, E. (1994) 'Analysis of the four alleles of the murine aryl hydrocarbon receptor', *Molecular Pharmacology*, 46, pp. 915–921.

Swanson, H. I. and Bradfield, C. A. (1993) 'The AH-receptor: genetics, structure and function.', *Pharmacogenetics*, 3(5), pp. 213–230.

Walisser, J. A. *et al.* (2005) 'Aryl hydrocarbon receptor-dependent liver development and hepatotoxicity are mediated by different cell types', *Proceedings of the National Academy of Sciences of the United States of America*, 102(49), pp. 17858–17863.